Delft University of Technology

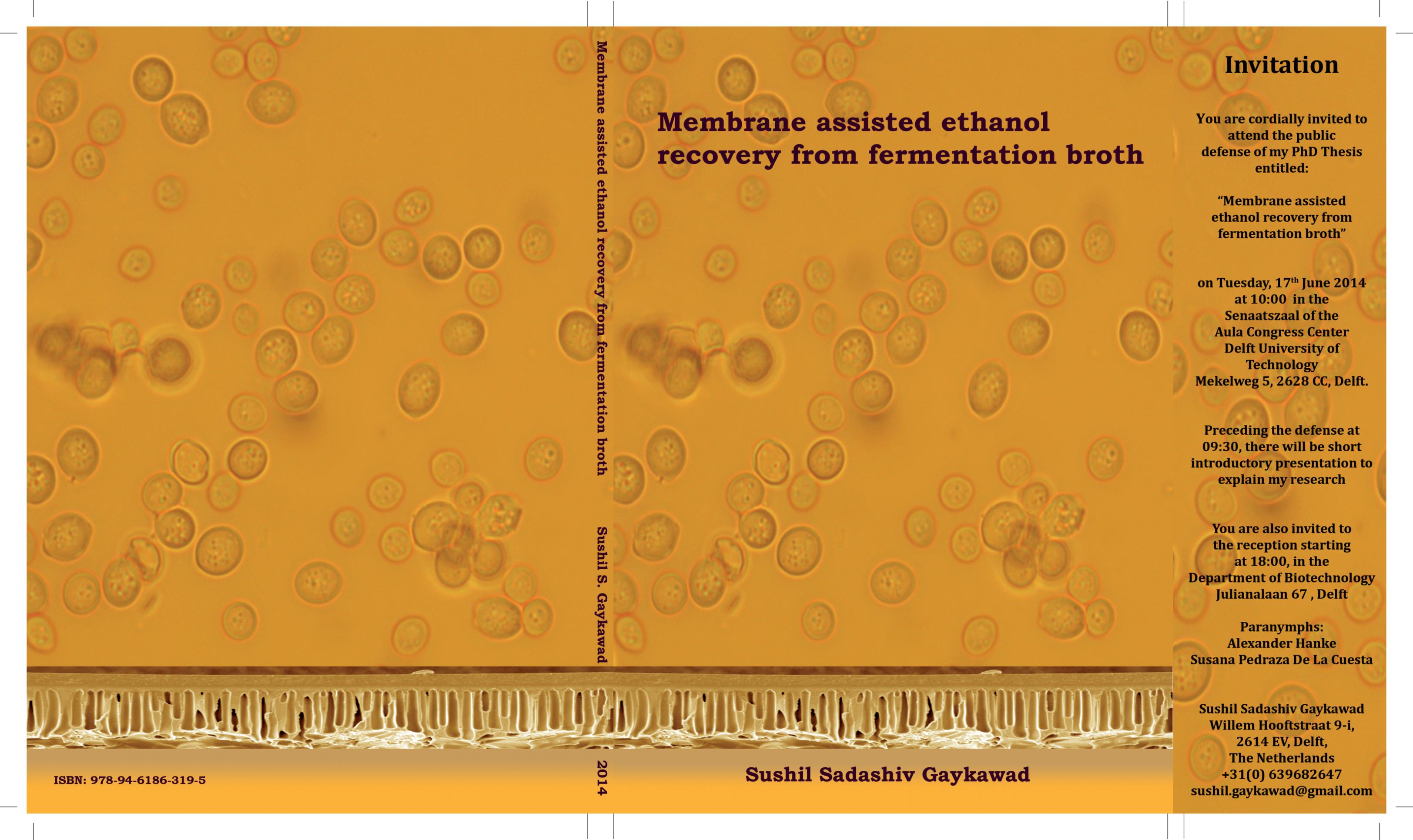Membrane assisted ethanol recovery from fermentation broth

Gaykawad, SS

Important note
To cite this publication, please use the final published version (if applicable).
Please check the document version above.

Membrane assisted ethanol recovery from fermentation broth

Sushil Sadashiv Gaykawad

Membrane assisted ethanol recovery from fermentation broth

Sushil S. Gaykawad

2014

Invitation

You are cordially invited to attend the public defense of my PhD Thesis entitled:

"Membrane assisted ethanol recovery from fermentation broth"

on Tuesday, 17th June 2014 at 10:00 in the Senaatszaal of the Aula Congress Center Delft University of Technology Mekelweg 5, 2628 CC, Delft.

Preceding the defense at 09:30, there will be short introductory presentation to explain my research

You are also invited to the reception starting at 18:00, in the Department of Biotechnology Julianalaan 67 , Delft

Paranymphs:
Alexander Hanke
Susana Pedraza De La Cuesta

Sushil Sadashiv Gaykawad
Willem Hooftstraat 9-i,
2614 EV, Delft,
The Netherlands
+31(0) 639682647
sushil.gaykawad@gmail.com

Propositions accompanying the PhD thesis
"Membrane assisted ethanol recovery from fermentation broth"
by Sushil Sadashiv Gaykawad

1. Pervaporation membrane fouling should be taken into account before designing a pervaporation based process.

2. Among the cellular components originating from yeast cell lysis, lipids irreversibly foul PDMS and POMS membranes. (*This thesis*)

3. The most effective way to reduce pervaporation membrane fouling is to minimize by–product formation in the hydrolysate and in broth. (*This thesis*)

4. A prerequisite for hydrophobic vapour permeation to be successful for ethanol recovery from ethanol-water vapour mixtures is the availability of suitable membranes. (*This thesis*)

5. Application of pervaporation, as a complementary separation process to mature technologies, can widen the industrial scope of pervaporation.

6. Comparison between two process options is like comparison between two individuals.

7. There is close resemblance between a research project and a chain reaction.

8. The desire of the common people to become economically prosperous is one of the reasons, besides the government's economic policies, to drive the economic growth of India.

9. The best way to integrate in any society or environment is to be born and brought-up in it.

10. Even though a message exchanged with gestures is one of the most primitive ways of human interaction, it is still widely used and a preferred way of communication in a modern world of advanced communication.

These propositions are considered opposable and defendable and have been approved as such by the promotor Prof.dr.ir. L.A.M. van der Wielen and co-promotor dr.ir. A.J.J. Straathof.

Stellingen behorende bij het proefschrift
"Membrane assisted ethanol recovery from fermentation broth"
door Sushil Sadashiv Gaykawad

1. Voordat een op pervaporatie gebaseerd proces ontworpen wordt moet rekening gehouden worden met pervaporatiemembraanvervuiling.

2. Onder de cellulaire componenten die bij cellysis van gist vrijkomen, vervuilen lipiden PDMS- en POMS-membranen irreversibel. (Dit proefschrift)

3. De effectiefste manier om pervaporatiemembraanvervuiling te verlagen is door het verminderen van bijproductvorming in het hydrolysaat en in het beslag. (Dit proefschrift)

4. De beschikbaarheid van geschikte membranen is een voorwaarde om met hydrofobe damppermeatie succesvol ethanol terug te winnen. (Dit proefschrift)

5. Pervaporatie als complementair scheidingsproces bij volwassen technologieën kan het industriële toepassingsgebied van pervaporatie verbreden.

6. Twee procesmogelijkheden vergelijken is net als twee individuen vergelijken.

7. Er is een grote overeenkomst tussen een onderzoeksproject en een kettingreactie.
8. Het verlangen van de gewone man om economisch welvarend te zijn is, naast het economisch beleid van de regering, een van de redenen die de economische groei van India aandrijft.

9. De beste manier om in een maatschappij of milieu te integreren is om er geboren en getogen te zijn.

10. Alhoewel een bericht dat overgebracht is met gebaren een van de meest primitieve manieren van menselijke interactie is, wordt dit toch veel gebruikt en is het een geprefereerde manier van communicatie in een moderne wereld van geavanceerde communicatie.

Deze stellingen worden opponeerbaar en verdedigbaar geacht en zijn als zodanig goedgekeurd door de promotor Prof.dr.ir. L.A.M. van der Wielen en copromotor dr.ir. A.J.J. Straathof.

Membrane assisted ethanol recovery from fermentation broth

Proefschrift

ter verkrijging van de graad van doctor
aan de Technische Universiteit Delft,
op gezag van de Rector Magnificus prof. ir. K.C.A.M Luyben,
voorzitter van het College voor Promoties,
in het openbaar te verdedigen op dinsdag 17 juni 2014 om 10:00 uur

door

Sushil Sadashiv GAYKAWAD
Master of Science in Chemical Engineering
Technische Universität Dortmund
geboren te Chalisgaon, India.

Dit proefschrift is goedgekeurd door de promotor:
Prof. dr. ir. L.A.M. van der Wielen
Copromotor: Dr. ir. A.J.J. Straathof

Samenstelling promotiecommissie:

Rector Magnificus	voorzitter.
Prof.dr.ir. L.A.M. van der Wielen	Technische Universiteit Delft, promotor.
Dr.ir. A.J.J. Straathof	Technische Universiteit Delft, copromotor.
Prof.dr.ir. H.J. Noorman	Technische Universiteit Delft.
Prof.Dr.-Ing. R. Wichmann	Technische Universität Dortmund.
Prof.dr.ir. P.J. Punt	Universiteit Leiden.
Prof.dr.ir. R.M. Boom	Wageningen Universiteit.
Dr. J.C. Jansen	ITM-CNR, Rende.
Prof.dr. P. Osseweijer	Technische Universiteit Delft, reservelid.

प्रिय आई आणि पपा यांस,

Dedicated to
my loving father and beloved late mom...

Summary/Samenvatting

Summary

Application of bioethanol as a fuel additive or alternative transportation fuel has increased its global consumption. However, up till now the cost of production is considerably higher for bioethanol than for gasoline. To increase the ethanol productivity and minimize the production cost, process modification and process integration was suggested and explored in this thesis. The proposed modified integrated process consists of continuous two-stage ethanol fermentation coupled with pervaporation. The aim of this research was to investigate the feasibility of hydrophobic pervaporation for ethanol recovery during fermentation.

An experimental evaluation of the proposed integrated process was carried out and the results achieved are presented in chapter 2. Consumption of glucose by *Saccharomyces cerevisiae* CEN.PK113–7D was complete, and concentrations of cells and ethanol were higher in fermenter 2 than in fermenter 1. Commercially available PDMS membrane was used in pervaporation during ethanol recovery from the 2nd fermenter and the results showed irreversible fouling of the membrane. Two process configurations namely, two fermenters coupled with pervaporation followed by microfiltration (configuration A) and two fermenters integrated with microfiltration followed by pervaporation (configuration B), were proposed and analyzed numerically. The aim was to find the potentially most suitable conditions for high ethanol productivity, yield, and concentration. The results showed that configuration A performs better than configuration B. The highest recovered yield, 0.419 g·g⁻¹, was achieved with configuration B at productivity of 0.128 g·g⁻¹·h⁻¹ and at $C_{e,2}$ (ethanol concentration in fermenter 2) value of 0.002 g·g⁻¹, but in configuration A the optimum performance was achieved at productivity of 0.041 g·g⁻¹·h⁻¹ and at $C_{e,2}$ value of 0.066 g·g⁻¹. The experimental results, however, suggest that configuration A may be more prone to membrane fouling than configuration B. Thus, the research focus of next study was to investigate the fouling of the membrane.

The potential membrane fouling components that might be present in the fermentation broth were identified as cellular polymers such as proteins, lipids, polysaccharides and nucleic acids (RNA and

DNA) released due to cell lysis. The effect of these polymers on the pervaporative membrane performance was investigated and the results obtained are discussed in chapter 3. Commercially available cellular polymers were examined and the types of representative bio–polymers selected were BSA and lysozyme (proteins), glyceryl trioleate (lipid), 1,2 dipalmitoyl–sn–glycero–3–phosphocholine (phospholipid), RNA from *Torula* yeast and glycogen from bovine liver (polysaccharides). POMS and commercial PDMS membranes were used in pervaporation. The results indicated irreversible fouling of PDMS and POMS membranes with flux decrease of 50% and 33% respectively, in the presence of lipids. In case of PDMS membrane, the total flux decreased with increasing BSA concentration whereas lysozyme, glycogen and RNA did not affect the membrane. The selectivity of PDMS membrane remained unchanged. All the cellular components decreased the water flux through the POMS membrane whereas the ethanol flux remained unaltered resulting in increased membrane selectivity.

In an effort to make bioethanol production cost effective, the use of lignocellulosic biomass as feedstock and pervaporation as ethanol recovery process was proposed. The application of pervaporation in ethanol recovery from lignocellulosic fermentation broth was investigated in chapter 4. Three types of fermentation broths were obtained from barley straw pretreated with concentrated acid (F–9) and mild alkaline method (F–13) and wood willow chips pretreated with mild alkaline method (F–12). The ethanol recovery from these fermentation broths was carried out by hydrophobic pervaporation employing commercial PDMS membrane. The results showed irreversible membrane fouling with total flux decrease by 17–20% as compared to a base case containing only 3 wt.% ethanol in water. To investigate the membrane fouling, pretreatment/hydrolysis by–products furanics and phenolics were studied here. Selected model components were HMF, furfural, 4–hydroxybenzaldehyde, vanillin, syringaldehyde and catechol. The pervaporation experiments using these components were carried out with 1 g·L^{-1} of individual components in 3 wt.% ethanol–water solution. Besides furfural, a total flux decrease of 12–15%, as compared to the base case, was observed for each component. Catechol was found to be most fouling component.

To avoid membrane fouling, vapour permeation, which uses vapour as feed, was proposed as an optional process to pervaporation for ethanol recovery. Vapour permeation using hydrophobic membrane for ethanol recovery from fermentation off–gas was proposed and techno–economic comparison was carried out against conventional absorption process in chapter 5. By recovering ethanol from fermentation off–gas, the bioethanol yield can be increased and the legal limit for ethanol emission from a bioethanol plant, which can be 40 t·year^{-1} for example, can be achieved. In the vapour permeation case, the ethanol concentration obtained in the recovered stream, by assumed PIM–1 membrane, was 66.08 mass% and this concentration was very high compared to the concentration in the absorber outlet (bottom) stream (1.94 mass%). The distillation energy cost needed for the absorber outlet stream and condensed permeate stream of vapour permeation to achieve 93 mass% ethanol was added and ethanol recovery cost was calculated for both process options. The ethanol recovery costs for base case absorption and for hydrophobic vapour permeation were calculated to be 0.217 and 1.366 US \$·kg^{-1}, respectively. Besides the membrane costs, vacuum costs dominate the overall costs in the membrane process.

In the Outlook, chapter 6, recommendations for performance improvement of integrated system are presented.

This thesis concludes that, for the pervaporation to be applied industrially for ethanol recovery, the membrane properties should be improved, membrane cost should be minimized and membrane fouling should be avoided.

Samenvatting

Het gebruik van bioethanol als bijmenging of als alternatieve transportbrandstof heeft ervoor gezorgd dat het wereldwijde verbruik ervan is toegenomen. Tot nu toe echter zijn de productiekosten van bioethanol aanmerkelijk hoger dan van benzine. Om de ethanolproductiviteit te verhogen en de productiekosten te verminderen wordt in dit proefschrift procesmodificatie en procesintegratie voorgesteld en onderzocht. Het voorgestelde gemodificeerde geïntegreerde proces bestaat uit een continue tweestaps ethanolfermentatie gekoppeld met pervaporatie. Het doel van dit onderzoek is de haalbaarheid te onderzoeken van hydrofobe pervaporatie voor ethanolterugwinning tijdens fermentatie.

Een experimentele evaluatie van het voorgestelde geïntegreerde proces is uitgevoerd en de behaalde resultaten worden gepresenteerd in hoofdstuk 2. Glucose is volledig geconsumeerd door *Saccharomyces cerevisiae* CEN.PK113–7D en concentraties cellen en ethanol zijn hoger in fermentor 1 dan in fermentor 2. Een commercieel verkrijgbaar PDMS-membraan is gebruikt bij pervaporatie tijdens ethanolterugwinning van de tweede fermentor en de resultaten laten irreversibele vervuiling van het membraan zien. Twee procesconfiguraties, configuratie A: twee fermentors gekoppeld met pervaporatie gevolgd door microfiltratie en configuratie B: twee fermentors geïntegreerd met microfiltratie gevolgd door pervaporatie zijn voorgesteld en numeriek geanalyseerd. Het doel is het vinden van de potentieel meest geschikte condities voor hoge ethanolproductie, opbrengst en concentratie. De resultaten laten zien dat configuratie A beter presteert dan configuratie B. De hoogste teruggewonnen opbrengst, 0.419 g·g⁻¹, is bereikt met configuratie B bij een productiviteit van 0.128 g·g⁻¹·h⁻¹ en bij een $C_{e,2}$ -waarde (ethanolconcentratie in fermentor 2) van 0.002 g·g⁻¹, maar in configuratie A is de optimale prestatie bereikt; dit was bij een productiviteit van 0.041 g·g⁻¹·h⁻¹ en bij een $C_{e,2}$ -waarde van 0.066 g·g⁻¹.

De experimentele resultaten wijzen er echter op dat configuratie A gevoeliger is voor membraanvervuiling dan configuratie B. Daarom is de aandacht van het volgende onderzoek gericht op de invloed van de vervuiling van het membraan.

De mogelijke membraanvervuilende componenten die aanwezig kunnen zijn in het fermentatiebeslag zijn geïdentificeerd als cellulaire polymeren zoals eiwitten, lipiden, polysacchariden en nucleïnezuren (RNA en DNA) die vrijkomen door cellyis. Het effect van deze polymeren op de pervaporatieve membraanprestaties is onderzocht en de resultaten zijn besproken in hoofdstuk 3. Uit de commercieel beschikbare cellulaire polymeren zijn representatieve biopolymeren geselecteerd: BSA en lysozym (eiwitten), glyceryl trioleaat (lipide), 1,2 dipalmitoyl–sn–glycero–3–phosphocholine (fosfolipide), RNA van *Torula*-gist en glycogeen uit runderlever (polysacchariden). POMS- en commerciële PDMS-membranen zijn gebruikt bij pervaporatie. De resultaten wezen op irreversibele vervuiling van de PDMS- en POMS-membranen in de aanwezigheid van lipiden met een fluxafname van respectievelijk 50% en 33%. Bij het PDMS-membraan nam de totale flux af bij toenemende BSA-concentratie, terwijl lysozym, glycogeen en RNA het membraan niet beïnvloedden. De selectiviteit van het PDMS-membraan bleef ongewijzigd. Alle cellulaire componenten verlaagden de waterflux door het POMS-membraan terwijl de ethanolflux niet veranderde zodat de membraanselectiviteit toenam.

In een poging bioethanolproductie rendabel te maken, is het gebruik van lignocellulose-bevattende biomassa als grondstof en pervaporatie als ethanol recovery proces voorgesteld. De toepassing van pervaporatie bij ethanolterugwinning uit lignocellulose-bevattend fermentatiebeslag werd onderzocht in hoofdstuk 4. Drie typen fermentatiebeslag waren verkregen: uit gerststro dat voorbehandeld was met 1) geconcentreerd zuur (F–9) , 2) via milde alkalische methode (F–13) en 3) wilgenspaanders voorbehandeld via milde alkalische methode (F–12). De ethanolterugwinning van deze fermentatiebeslagen vond plaats door hydrofobe pervaporatie met een commercieel verkrijgbaar PDMS-membraan. De resultaten toonden onomkeerbare membraanvervuiling met een fluxdaling van 17-20% vergeleken met een basisgeval dat slechts 3 gew.% ethanol in water bevat. Om de membraanvervuiling te onderzoeken werden de voorbehandeling-/hydrolyse- bijproducten furanen en fenolen bestudeerd. Geselecteerde modelcomponenten waren HMF, furfural, 4–hydroxybenzaldehyde, vanilline, syringaldehyde en catechol. De pervaporatie-experimenten met deze componenten werden uitgevoerd met 1 g·L^{-1} van de individuele

componenten in 3 gew.% ethanol–water-oplossing. Behalve bij furfural werd voor iedere component een totale fluxverlaging van 12–15% waargenomen vergeleken met het basisgeval. Catechol bleek de meest vervuilende component te zijn.

Om membraanvervuiling te vermijden werd voorgesteld damppermeatie te gebruiken, hierbij wordt damp gebruikt als toevoer, in plaats van pervaporatie voor ethanolterugwinning. Damppermeatie met gebruik van hydrofobe membranen voor ethanolterugwinning werd voorgesteld en een techno–economische vergelijking tegen het conventionele absorptieproces werd gemaakt in hoofdstuk 5. Door terugwinnen van ethanol uit het gas dat de fermentor verlaat kan de bioethanol-opbrengst worden verhoogd en binnen de juridische grenswaarde voor ethanolemissie die bijvoorbeeld 40 ton per jaar kan zijn, worden gebleven. In de damppermeatie-casus was de ethanolconcentratie in de teruggewonnen stroom bij verondersteld gebruik van een PIM–1 membraan 66.08 massa% en deze concentratie was zeer hoog vergeleken met de concentratie in de absorberuitlaat (onder) stroom (1.94 massa%). De distillatie-energiekosten die nodig waren voor de absorber-uitlaatstroom en de gecondenseerde permeaatstroom van damppermeatie om 93 massa% ethanol te bereiken was toegevoegd en de ethanolterugwinningskosten waren berekend voor beide proces-opties. De ethanolterugwinningskosten voor basisgeval absorptie en hydrofobe damppermeatie werden berekend op 0.217 and 1.366 US $·kg^{-1}, respectievelijk. Naast de membraankosten domineren de vacuümkosten de totale kosten van het membraanproces.

In de vooruitblik, hoofdstuk 6, worden aanbevelingen voor prestatieverbetering van geïntegreerde systemen gepresenteerd.

Dit proefschrift concludeert dat om pervaporatie industrieel toe te passen voor ethanolterugwinning de membraaneigenschappen moeten worden verbeterd, de membraankosten worden verlaagd en membraan-vervuiling moet worden vermeden.

Table of content

Chapter 1

General Introduction

The present day energy sector is dominated by fossil fuels. Almost 81% of the world's energy is derived from fossil fuels such as coal, oil and natural gas. These fossil fuels, due to their abundance in nature and the efficient technologies developed for their application, will remain the main feedstock for energy generation in the near future.

Among these fossil fuels, crude–oil is widely used as transportation fuel. The global transportation sector is almost entirely dependent on petroleum–based fuels and accounts for 77% of the world transport oil demand (IEA, 2011). But, the burning of these fossil fuels leads to some serious environmental threats such as emission of hazardous gases (NO_x, CO), greenhouse gas (CO_2) and particulate matter (lead). The transportation sector alone contributes for 22% to global CO_2 (2010) and more than 70% to global CO emissions. With more modernization, there is increasing energy demand. Being non–renewable resources, the fossil fuel reserves are finite and with increased consumption their depletion is occurring much faster than previously predicted. This necessitates the search for sustainable energy sources.

Fuels obtained from biomass, commonly known as biofuels, are renewable and environmentally friendly and exhibit many advantages over petroleum based fuels. Thus, they are considered as the next generation energy source. Biofuels include bioethanol, biobutanol, biomethanol, vegetable oils, biodiesel, biogas, biosynthetic gas (bio–syngas), bio–oil, bio–char, Fischer–Tropsch liquids, and biohydrogen. But the term biofuels is generally practiced for liquid biofuels used in the transportation sector (Balat, 2011).

The biofuels, which have gained more importance recently, in fact are not new to the scientific world. They have been widely used as energy source and transportation fuel in the 18th century. In 1900, at the World Exhibition in Paris, France, Rudolf Diesel demonstrated his engine by running it on vegetable (peanut) oil. The early prototype of internal combustion engines (by Samuel Morey in 1826 and Henry Ford in 1903) were running on ethanol, a corn product. Bioethanol has been used as fuel in Brazil since 1925. The heavy tax on alcohol during American civil war (2 US $ per gallon) and the influx of cheap, efficient gasoline overlooked the application of alcohols as a fuel till the 1970s. The clean environment act that passed in the USA and the increase in

gasoline prices due to the Arab oil crisis in the 1970s, led to the quest of alternative fuels. The increasing concern regarding environmental impact (greenhouse gas emissions) caused by fossil fuels and realization of their premature depletion raised the necessity for cleaner and renewable fuel.

1.1. Bioethanol as fuel

Being renewable, environmentally friendly and historically applied as transportation fuel, bioethanol has emerged as promising alternative to gasoline. Bioethanol has many advantages over gasoline as transportation fuel (das Neves et al., 2007; Zaldivar et al., 2001) and can be used as fuel in two forms. It can be either blended with gasoline as fuel oxygenate or can be directly applied as transportation fuel. The concentration of bioethanol added to the gasoline ranges from 5% (E5) to 85% (E85) and varies from country to country. Hydrous bioethanol (96% bioethanol + 4% water) can be used as neat fuel instead of gasoline. The flexi–fuel vehicle (FFV) can use bioethanol as fuel in both forms (Balat, 2011; Balat and Balat, 2009; Cheng and Timilsina, 2011). Due to this application the demand for bioethanol is increasing, which is reflected in the increase by global ethanol production and it is estimated that it will keep increasing in the near future (Figure 1.1).

The feedstock used for bioethanol production can be divided broadly into sugar crops (e.g. sugar cane, sugar beet, sweet sorghum and fruits), starchy crops (e.g. corn, milo, wheat, rice, potato, cassava, sweet potato and barley) and lignocellulosic biomass (e.g. wood, straw, and grasses) (Balat and Balat, 2009; Lin and Tanaka, 2006). The bioethanol produced using sugars and starches as a raw material is known as 1st generation bioethanol. Competition with the food market due to usage of sugar cane and corn for 1st generation bioethanol has led to a research focus on lignocellulosic biomass, which includes agriculture waste, forest waste food waste, and is abundant in nature. The bioethanol produced from this cellulosic biomass is called 2nd generation bioethanol. Bioethanol produced by using microalgae is called 3rd generation of bioethanol (Nigam and Singh, 2011). Currently, bioethanol is mainly produced from sugar cane in Brazil, from corn in the USA and from sugar beet in the EU. In this study we focus on 1st and 2nd generation bioethanol production processes.
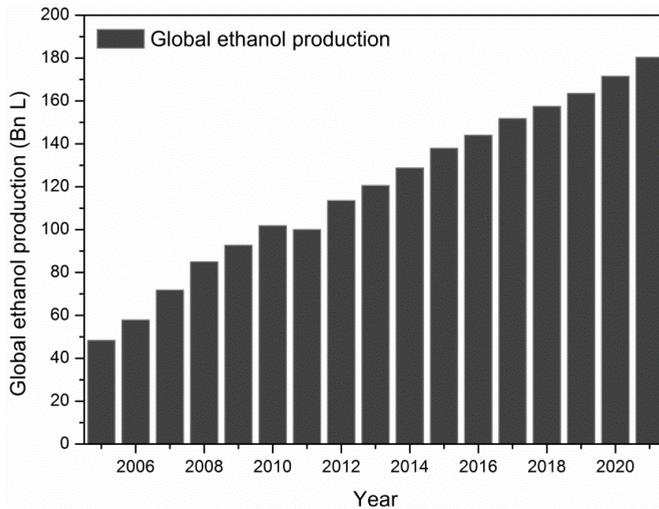
Figure 1.1. Global ethanol production (OECD–FAO agriculture outlook (2012)).

1.2. Bioethanol production process

Bioethanol production process can be broadly divided into four steps, namely conversion of raw material into fermentable sugars, production of ethanol by fermentation of sugars, separation and purification, and waste treatment. For all kind of feedstocks, the processes required to obtain fermentable sugars from raw material differ whereas the remaining steps in the process remain the same. The steps included in the bioethanol process based on the feedstock used are described by Mussatto and co–workers (2010) and are shown in Figure 1.2.

Using sugar cane (Brazilian process) as raw material, the extraction of sugars, in the form of sugarcane juice, is carried out by milling. In case of starchy materials such as corn (US process), saccharification is necessary to obtained fermentable sugars. In this process, hydrolysis of milled corn is carried out using alpha–amylase and glucoamylase enzymes (Kwiatkowski et al., 2006) followed by fermentation of obtained sugars. The ethanol production process from corn can be either dry–grind process or wet–grind process.

The conversion of lignocellulosic material into sugars is carried out by pretreatment and cellulose hydrolysis. The pretreatment involves the breakdown of lignocellulosic matrix to separate cellulose and hemicellulose from lignin, reduce their crystallinity degree and increase

the amorphous portion so as to make them more suitable for hydrolysis. Pretreatment of lignocellulosic biomass can be done by using physical (milling, grinding), physio–chemical (steam explosion, hydrothermolysis, wet oxidation), chemical (alkali, dilute acid, oxidizing agents, and organic solvents) and biological processes (Balat, 2011; Cardona Alzate and Sánchez Toro, 2006; Cheng and Timilsina, 2011). Pretreated lignocellulosic biomass is converted into fermentable sugars during hydrolysis. The most common methods applied for hydrolysis are chemical hydrolysis (dilute and concentrated acid) and enzymatic hydrolysis. The fermentable sugars obtained using sugar cane and corn are hexoses (6 carbon) whereas lignocellulosic biomass yields hexoses and pentoses (5 carbon).

Different bacteria, yeasts and fungi have been used for ethanol production. Traditionally, *Saccharomyces cerevisiae*, baker's yeast, has been the most commonly used microbe converting glucose into ethanol. Pentose fermenting yeasts, such as *Candida shehatae* or *Pichia stipitis*, are used to convert pentose sugars generated from lignocellulosic biomass to ethanol (Kuhad et al., 2011). Also, bacteria such as *Zymomonas mobilis*, *Escheria coli* and *Klebsiella oxytoca* have been reported to be applied for ethanol fermentation. Among these, *Zymomonas mobilis*, a Gram–negative bacterium, can utilize glucose, fructose and sucrose for ethanol production and showed higher ethanol yield and higher specific ethanol productivity than *S. cerevisiae*. But due to its robustness, *S. cerevisiae* is most widely used for industrial ethanol production. Various anaerobic thermophilic bacteria with optimal growth temperature above 60 °C can also be used for bioethanol production but due to their low ethanol tolerance their application is limited (Bai et al., 2008; Balat, 2011; Chang and Yao, 2011; Lin and Tanaka, 2006; Sprenger, 1996).

The recovery of ethanol from fermentation broth is widely carried out in two steps. The ethanol recovery up to its azeotropic concentration (95.6 wt.% ethanol) by using distillation is followed by ethanol dehydration by adsorption. In US based ethanol process, in the first distillation column, also known as beer column, the ethanol concentration up to 37% in distillate is achieved and the bottom product containing all the solids and water is called stillage. The top product from beer column is further purified using a rectification

column to get the azeotropic concentration. The removal of water from the bottom stream of the rectification column is done using a stripping column and the bioethanol concentrated stream thus obtained is combined with the feed of the rectifier. The anhydrous ethanol (99.6 wt.%) is achieved by adsorption of water from the distillate of the rectifier using molecular sieves (Balat, 2011; Huang et al., 2008; Kwiatkowski et al., 2006).
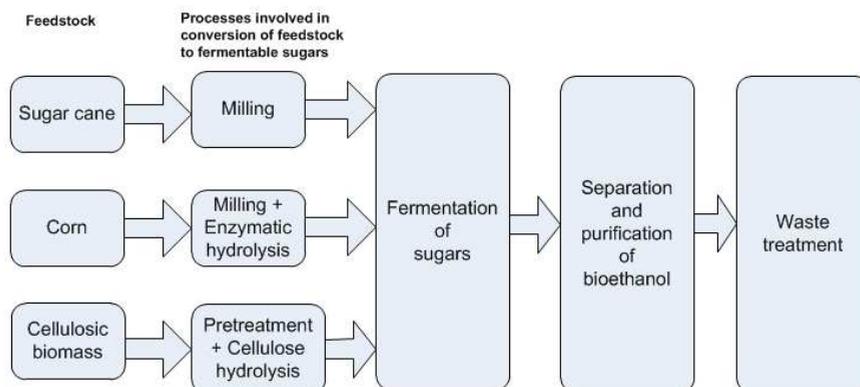
Figure 1.2. Schematic diagram for steps involved in 1st and 2nd generation bioethanol production (modified from Mussatto and co-workers (2010)).

The wastes generated during the bioethanol production are mainly the waste water from the bottom of the stripping column and stillage. The recovery and purification of water is carried out and it is recycled into the process. The water from the stillage is recovered and recycled to process. The stillage solid fraction is either treated further to produce co–product such as distiller's dried grains with solubles (DDGS), in case of corn as feedstock, or burned for cogeneration of process steam and electricity when cellulosic biomass is used as feedstock. The various current and potential added–value co–products that can be obtained during bioethanol production process are described by Cardona and Sánchez (2007b).

1.3. Challenges in bioethanol production

Bioethanol production, requiring numerous process steps varying with different feedstocks, is a complex process. Though the ethanol production process based on sugarcane and corn is mature, the

production process using cellulosic biomass is still developing. Thus, it has significant potential for improvements and some of the challenges involved in the process are discussed here.

1.3.1 Ethanol fermentation

Commercially, fed–batch ethanol fermentation is the most common process for ethanol production (Amorim et al., 2011). However, high ethanol concentration and accumulation of by–products during fed–batch process inhibit the cell growth. When using lignocellulosic feedstock, the challenges faced include very expensive biomass hydrolysis using cellulose hydrolysing enzymes, high cost pretreatment of cellulosic biomass (around 0.08 US$.L^{-1} of bioethanol produced) (Balat, 2011) and low ethanol yield due to microbial limitation for complete utilization of different sugars; like glucose and xylose (Cheng and Timilsina, 2011; Gnansounou and Dauriat, 2010; Lin and Tanaka, 2006).

1.3.2 Ethanol recovery by distillation

The concentration of ethanol in the fermentation broth usually ranges between 5 and 12 wt.%. But using cellulosic feedstock, the ethanol concentration in broth is found to be below 5 wt.% (Olsson and Hahn-Hägerdal, 1996). Commercial recovery of ethanol from broth is carried out by distillation. However, for decreasing ethanol concentrations (< 5 wt.%) the energy requirement for bioethanol separation by distillation increases exponentially (Madson and Lococo, 2000). This makes the distillation step cost–intensive, thereby increasing the ethanol production cost.

1.3.3 Bioethanol production cost

The bioethanol production cost has been regulated and subsidised by supporting policies in different countries to encourage its production and application. However, up till now the cost of bioethanol production is considerably higher than gasoline and varies significantly depending on many factors such as feedstock used and its cost, by–products revenue, process energy cost, plant size, etc. (Balat, 2011; Gnansounou and Dauriat, 2010). The current and estimated costs of bioethanol production from different feedstock have been reported in literature

(Balat, 2011; Cheng and Timilsina, 2011; Gnansounou and Dauriat, 2010). The ethanol production by sugar cane in Brazil is more competitive and economical (0.23–0.29 US $\$\cdot L^{-1}$) than production processes using corn in US (0.53 US $\$\cdot L^{-1}$) and using sugar beet in EU (0.29 US $\$\cdot L^{-1}$). The bioethanol production cost using lignocellulosic biomass is still too high (0.80–1.10 US $\$\cdot L^{-1}$) due to its process complexity (Balat, 2011). It is estimated that till 2030 the bioethanol production will be competitive compared to gasoline considering the development of innovative technologies for conversion of cheaper cellulosic biomass and waste material into bioethanol (Walker, 2011).

1.4. Ways to overcome these challenges

The challenges to be dealt with during bioethanol production, mentioned in the previous section, can be minimized and overcome by applying cell and process engineering tools. The current research focus and potential solutions to make the bioethanol process more efficient and cost effective are discussed here.

1.4.1 Fermentation process development

The first step to improve the bioethanol process is the availability and usage of cheaper feedstock, as it represents 60–75% of the total bioethanol production cost (Balat and Balat, 2009). Recently, cheaper and abundantly available cellulosic biomass has been identified as feedstock and has a potential to reduce feedstock contribution in bioethanol cost to 50–55% (Gnansounou and Dauriat, 2010). New technologies are being developed for bioethanol production based on lignocellulosic biomass to make the overall process more economical.

The fermentable sugars generated from cellulosic biomass are hexoses and pentoses. To increase the fermentation yield and to make the ethanol production cost effective, complete utilization of these sugars by microorganisms is necessary. Also, it is necessary to minimize the inhibition of microorganisms by high ethanol concentration and by inhibitory compounds generated during pretreatment of cellulosic biomass. Efficient conversion of hexoses to ethanol can be carried out using *S. cerevisiae*, but the fermentation of pentoses to ethanol has been challenging (Lin and Tanaka, 2006). By applying genetic engineering tools, new improved strains have been

developed for efficient utilization of pentose sugars (Kuhad et al., 2011). Similar tools have also been applied to produce new strains having high tolerance to inhibitory compounds and capable of co–fermenting glucose and xylose to ethanol (Lin and Tanaka, 2006).

To make the bioethanol process more cost competitive, continuous fermentation process can be applied instead of more widespread batch and fed–batch process. Continuous processes have the advantages of high volume–specific productivity, low inhibitory component concentration and reduced investment costs.

1.4.2 Process engineering tool to improve process

In addition to strain development and cheaper feedstock utilization, process engineering is essential to establish highly efficient bioethanol production processes (Cardona and Sánchez, 2007b; Mussatto et al., 2010). It includes the design of innovative process configurations, process integration, process analysis and optimization. Process design involves the formulation and assessment of possible process configurations and the selection of the ones having improved performance parameters, whereas process integration incorporates combination of different operations in a single unit. Process integration has the potential advantages of increasing the product yield, decreasing the size and number of process units and intensifying fermentation and downstream processes. The application of process engineering tools to bioethanol production process has been discussed in detail by Cardona and Sánchez (2007b). The different technological flowsheets proposed for bioethanol production from cellulosic biomass and their assessment presented in literature have also been summarized in their review.

In bioethanol production process, the process integration options suggested by Cardona and Sánchez (2007b) are mainly based on combining reaction–reaction, reaction–separation and separation–separation steps. Reaction–reaction integration corresponds to the coupling of different biological transformations taking place during ethanol production. It involves co–fermentation of lignocellulosic hydrolysates, simultaneous saccharification and fermentation (SSF), simultaneous saccharification and co–fermentation (SSCF) and consolidated bioprocessing (CBP). Reaction–separation integration involves the integration between fermentation and various separation

operations whereas separation–separation integration includes the combination of different separation processes.

Energy integration, in the form of heat integration using pinch technology approach, can also be applied in bioethanol process. This minimizes the consumption of external energy sources such as fossils fuels, electricity and thereby reduces the ethanol cost (Cardona and Sánchez, 2007b).

1.4.3 Co–product production and cogeneration

Generation of valuable products during bioethanol formation and of the corresponding revenue could make the overall process more profitable. The type of co–product produced during the process mainly includes yeast, bagasse, corn gluten meal, corn gluten feed and DDGS depending on the feedstock used (Cardona and Sánchez, 2007b).

Cogeneration of steam and electricity is possible by thermal conversion of non–fermentable residue, such as lignin in case of cellulosic biomass as feed, obtained during process. This can satisfy the energy needed during the ethanol production and is the crucial step to make the process more economical.

1.5. Process modification and integration

Bioethanol produced from different feedstocks is often still more expensive than gasoline. Hence, the main focus of bioethanol related research is to increase the ethanol productivity and minimize the ethanol price. The process engineering approach, already mentioned in the previous section, was explored to achieve this goal. It involves the designing of modified integrated process configurations for bioethanol production. Several modified integrated processes are discussed here.

1.5.1 Process modification

The conversion of fermentable sugars into bioethanol is commonly performed in a single stage fermenter using batch or fed–batch mode. However, inhibition of the cells due to high concentration of accumulated ethanol and toxic components leading to lower cell growth is the main drawback of these processes. A continuous fermentation system coupled with cell retention process has the potential of increasing the productivity. Groot et al. (1992b) achieved the ethanol

productivity of 55 g·L^{-1}·h^{-1} with continuous fermentation integrated with microfiltration unit.

1.5.1.1 Two stage fermentation

A two–stage continuous fermentation process, capable of improving ethanol production rate, has been suggested and studied (Lee et al., 1988; Nishiwaki and Dunn, 1998). The first stage in this process is dedicated to growth of the cells whereas ethanol production takes place in the second fermenter.

Two–stage fermentation system coupled with cell retention has been investigated by Ben Chaabane et al., (2006) and Nishiwaki and Dunn (1998). These configurations achieve high cell densities in fermenter by cell recycle and complete substrate conversion. A numerical analysis of continuous two–stage ethanol fermentation with cell separation after each stage by Nishiwaki and Dunn (1998) showed that this system was more efficient than a conventional recycle chemostat and a recycle two–stage fermenter with a separator after the final stage. The successful experimental performance of a two–stage continuous fermenter with cell recycle using ultrafiltration has been demonstrated by Ben Chaabane et al., (2006). The high cell density (157 g·CDW^{-1}), high ethanol concentration (65 g·L^{-1}) and complete conversion of substrate in the second stage was achieved at an ethanol productivity of 41 g·L^{-1}·h^{-1} for this system (Ben Chaabane et al., 2006).

On the basis of these numerical and experimental studies, the continuous two–stage ethanol fermentation system, capable of giving high ethanol productivity was selected as modified fermentation process for our study.

1.5.1.2 Ethanol recovery from broth

Industrial recovery of ethanol from fermentation broth is carried out by distillation. As a result of the high energy requirement alternative energetically efficient recovery processes were investigated and these include gas or steam stripping (Ennis et al., 1986), liquid–liquid extraction (Roffler et al., 1987), adsorption (Groot et al., 1992c) and pervaporation (Fadeev et al., 2003; García et al., 2009b; Mulder et al., 1983). These separation technologies have been reviewed comprehensively in literature (Huang et al., 2008; Vane, 2005a).

Among these processes, pervaporation emerges as potentially viable process due to the possibility to remove ethanol in–situ, without introducing an auxiliary phase. Because of the ongoing developments in the membrane production (Adymkanov et al., 2008), the pervaporation technique was considered for ethanol separation in this study.

1.5.1.3 Pervaporation as separation process

Pervaporation, a term literally derived from the combination of permeation and evaporation, is a membrane separation process in which the liquid mixture to be separated (feed) is placed in contact with one side of a membrane and the permeated product (permeate) is removed in vapour phase on the other side of the membrane. The permeate vapour, rich in the desired product, is then condensed and collected (Figure 1.3).
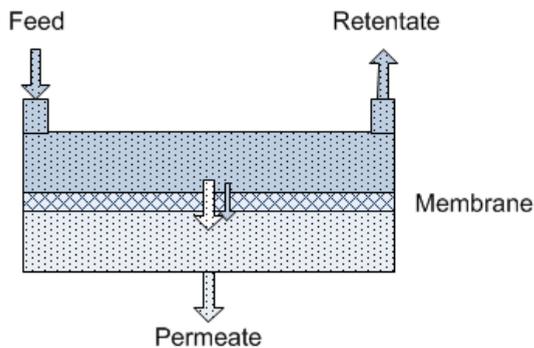
Figure 1.3. Schematic diagram of pervaporation.

The separation of different species in the feed mixture is due their different affinities for the membrane and different diffusion rates through the membrane. The widely accepted mechanism for separation by pervaporation is the solution–diffusion mechanism where the feed molecules sorb into/onto the membrane, diffuse through the membrane and evaporate into the vapour phase on the permeate side. The driving force for the mass transport through membrane is the chemical potential gradient across the membrane based on partial pressure difference. The lower partial pressure on the permeate side can be achieved by applying vacuum or by using sweep gas (Feng and Huang, 1997; Lipnizki et al., 2000b; Vane, 2005a). The performance of the

pervaporation process is measured in terms of flux through the membrane and membrane selectivity (See chapter 2 for equations definition).

The membranes used in the pervaporation play an important role in the separation and are broadly divided into organic/polymeric membranes, inorganic membranes and composite membranes (Wee et al., 2008). The hydrophilic and hydrophobic membranes used for separation in pervaporation are discussed by Huang and co–workers (2008). Based on the membrane placement, the pervaporation module could be a flat sheet, hollow fibre or spiral wound (Dutta et al., 1996). The spiral wound and hollow fibre modules are commonly used due their ability to provide a large membrane surface area to volume ratio but the selection of the module mainly depends on the composition of the feed stream.

Applications of pervaporation involve the dehydration of organic solvents (hydrophilic pervaporation), removal of organic compounds from aqueous solutions, and separation of anhydrous organic solvents (hydrophobic pervaporation).

Commercially, pervaporation is widely applied for dehydration of alcohols and other organic solvents due to development of hydrophilic membranes with advanced performance parameters. In the bioethanol production process, coupling of distillation with pervaporation for the production of anhydrous ethanol has been reported. A pilot plant study of such hybrid process indicated energy savings whereas simulation results showed that this system is more economical than azeotropic distillation (Cardona and Sánchez, 2007b; Kunnakorn et al., 2013). The variety of pervaporation membranes used for alcohol dehydration is discussed extensively in literature (Chapman et al., 2008; Shao and Huang, 2007).

The other applications of pervaporation (organic–water and organic–organic separation) are still at the research scale because of unavailability of membranes with efficient performance parameters and their poor stability in harsh organic solvents. The numerical evaluation and comparison between two processes namely, azeotropic distillation using benzene and pervaporation using multiple membrane modules to achieve the same ethanol production rate and concentration (99.8 wt.%) was performed. The simulation results obtained showed that the

operating costs for pervaporation, with membrane life of 2–4 years, are approximately 1/3 to 1/4 of those of azeotropic distillation (Cardona and Sánchez, 2007b). Thus pervaporation has the potential to replace distillation to make bioethanol production more economical, but the availability of membranes with high performance parameters is the prerequisite. However, with currently available membranes, pervaporation can be employed to concentrate fermentation outlet stream before feeding it to distillation thereby reducing the energy load on distillation.

Thus, in the bioethanol production process, pervaporation can either be used for dehydration of ethanol to achieve fuel grade ethanol or to concentrate the feed stream from fermentation before sending it to distillation (Chapter 4; Figure 4.1).

1.5.2 Process integration

The integration of single stage fermentation with pervaporation for bioethanol production has been investigated by many researchers (Groot et al., 1992b; Nakao et al., 1987b; O'Brien and Craig Jr, 1996b; Shabtai et al., 1991b). This integrated system facilitates continuous operation with in–situ ethanol recovery. This allows to maintain the ethanol concentration below inhibitory levels in fermentation and enables cell recycling resulting in increase in productivity. The economic analysis indicated that with modest improvements in membrane properties and membrane cost, such a system can be economically more attractive and can replace the beer column in bioethanol production (Di Luccio et al., 2002; O'Brien et al., 2000a).

Similarly, the integration of continuous two–stage fermentation and pervaporation was proposed here for ethanol production so as to have the combined benefits of individual systems to achieve high productivity and minimize the production cost. The two–stage fermentation coupled with pervaporation for continuous butanol production has been studied before by Van Hecke and co–workers (Van Hecke et al., 2012), however to our knowledge, such integrated system has not been studied so far for ethanol production. In this process, pervaporation can perform dual functions of cell retention system and of in–situ ethanol recovery step.

1.6. Aim and outline of the thesis

The new modified integrated process consisting of continuous two–stage ethanol fermentation coupled with pervaporation having potential of increasing ethanol productivity and minimizing the ethanol cost was proposed. The aim of this research was to investigate the feasibility of hydrophobic pervaporation for ethanol recovery during fermentation.

In line with the aim of thesis, **Chapter 2** deals with the experimental analysis of the model integrated system consisting of continuous two fermenters and pervaporation (explained in detailed in chapter 2; Figure 2.1). Two process options consisting of different combinations of two–stage fermenters, microfiltration and pervaporation are suggested and are analysed numerically based on performance parameters.

During the integrated experiment of chapter 2, membrane fouling occurred. The fermentation broth may contain, besides the excreted by–products, cellular components released by cell lysis. The effect of these cellular polymers on pervaporation membrane performance is shown in **Chapter 3**.

The effects of real lignocellulosic fermentation broth and its by–products on ethanol recovery by pervaporation are investigated in the **Chapter 4**. The experimental evaluation of effects of lignocellulosic biomass and pretreatment method used on ethanol concentration in the hydrolysate and on ethanol recovery by pervaporation are presented.

To overcome the membrane fouling observed in pervaporation during integrated experiment, vapour permeation is suggested as an alternative process option. The feasibility of vapour permeation for ethanol recovery from fermentation off–gas is analysed in **Chapter 5,** which includes techno–economic evaluation of this system.

Finally, in **Chapter 6** the outlook of this thesis and recommendations for future work are given.

References:

1. Adymkanov, S.V., Yampol'skii, Y.P., Polyakov, A.M., Budd, P.M., Reynolds, K.J., McKeown, N.B., Msayib, K.J., 2008. Pervaporation of alcohols through highly permeable PIM-1 polymer films. Polym Sci Ser A. 50, 444-450.

2. Amorim, H., Lopes, M., Castro Oliveira, J., Buckeridge, M., Goldman, G., 2011. Scientific challenges of bioethanol production in Brazil. Appl. Microbiol. Biotechnol. 91, 1267-1275.

3. Bai, F.W., Anderson, W.A., Moo-Young, M., 2008. Ethanol fermentation technologies from sugar and starch feedstocks. Biotechnol. Adv. 26, 89-105.

4. Balat, M., 2011. Production of bioethanol from lignocellulosic materialsvia the biochemical pathway: A review. Energy Convers. Manage. 52, 858-875.

5. Balat, M., Balat, H., 2009. Recent trends in global production and utilization of bio-ethanol fuel. Appl. Energ. 86, 2273-2282.

6. Ben Chaabane, F., Aldiguier, A.S., Alfenore, S., Cameleyre, X., Blanc, P., Bideaux, C., Guillouet, S.E., Roux, G., Molina-Jouve, C., 2006. Very high ethanol productivity in an innovative continuous two-stage bioreactor with cell recycle. Bioprocess Biosystems Eng. 29, 49-57.

7. Cardona Alzate, C.A., Sánchez Toro, O.J., 2006. Energy consumption analysis of integrated flowsheets for production of fuel ethanol from lignocellulosic biomass. Energy. 31, 2447-2459.

8. Cardona, C.A., Sánchez, Ó.J., 2007. Fuel ethanol production: Process design trends and integration opportunities. Bioresour. Technol. 98, 2415-2457.

9. Chang, T., Yao, S., 2011. Thermophilic, lignocellulolytic bacteria for ethanol production: current state and perspectives. Appl. Microbiol. Biotechnol. 92, 13-27.

10. Chapman, P.D., Oliveira, T., Livingston, A.G., Li, K., 2008. Membranes for the dehydration of solvents by pervaporation. J Membr Sci. 318, 5-37.

11. Cheng, J.J., Timilsina, G.R., 2011. Status and barriers of advanced biofuel technologies: A review. Renewable Energy. 36, 3541-3549.

12. das Neves, M.A., Kimura, T., Shimizu, N., Nakajima, M., 2007. State of the art and future trends of bioethanol production. Dynamic Biochemistry, Process Biotechnology and Molecular Biology. 1, 1-14.

13. Di Luccio, M., Borges, C.P., Alves, T.L.M., 2002. Economic analysis of ethanol and fructose production by selective fermentation coupled to pervaporation: effect of membrane costs on process economics. Desalination. 147, 161-166.

14. Dutta, B.K., Ji, W., Sikdar, S.K., 1996. Pervaporation: Principles and Applications. Separation & Purification Reviews. 25, 131-224.

15. Ennis, B.M., Marshall, C.T., Maddox, I.S., Paterson, A.H.J., 1986. Continuous product recovery by in-situ gas stripping/condensation during solvent production from whey permeate usingClostridium acetobutylicum. Biotechnol. Lett. 8, 725-730.

16. Fadeev, A.G., Kelley, S.S., McMillan, J.D., Selinskaya, Y.A., Khotimsky, V.S., Volkov, V.V., 2003. Effect of yeast fermentation by-products on poly[1-(trimethylsilyl)-1-propyne] pervaporative performance. J Membr Sci. 214, 229-238.

17. Feng, X., Huang, R.Y.M., 1997. Liquid Separation by Membrane Pervaporation: A Review. Ind. Eng. Chem. Res. 36, 1048-1066.

18. García, M., Sanz, M.T., Beltrán, S., 2009. Separation by pervaporation of ethanol from aqueous solutions and effect of other components present in fermentation broths. J. Chem. Technol. Biotechnol. 84, 1873-1882.

19. Gnansounou, E., Dauriat, A., 2010. Techno-economic analysis of lignocellulosic ethanol: A review. Bioresour. Technol. 101, 4980-4991.

20. Groot, W.J., Kraayenbrink, M.R., Waldram, R.H., van der Lans, R.G.J.M., Luyben, K.C.A.M., 1992a. Ethanol production in an integrated process of fermentation and ethanol recovery by pervaporation. Bioprocess Biosystems Eng. 8, 99-111.

21. Groot, W.J., van der Lans, R.G.J.M., Luyben, K.C.A.M., 1992b. Technologies for butanol recovery integrated with fermentations. Process Biochem. 27, 61-75.

22. Huang, H.-J., Ramaswamy, S., Tschirner, U.W., Ramarao, B.V., 2008. A review of separation technologies in current and future biorefineries. Sep. Purif. Technol. 62, 1-21.

23. IEA, I.E.A., 2011. World Energy Outlook. available on www.worldenergyoutlook.org.

24. Kuhad, R.C., Gupta, R., Khasa, Y.P., Singh, A., Zhang, Y.H.P., 2011. Bioethanol production from pentose sugars: Current status and future prospects. Renewable and Sustainable Energy Reviews. 15, 4950-4962.

25. Kunnakorn, D., Rirksomboon, T., Siemanond, K., Aungkavattana, P., Kuanchertchoo, N., Chuntanalerg, P., Hemra, K., Kulprathipanja, S., James, R.B., Wongkasemjit, S., 2013. Techno-economic comparison of energy usage between azeotropic distillation and hybrid system for water–ethanol separation. Renewable Energy. 51, 310-316.

26. Kwiatkowski, J.R., McAloon, A.J., Taylor, F., Johnston, D.B., 2006. Modeling the process and costs of fuel ethanol production by the corn dry-grind process. Ind Crop Prod. 23, 288-296.

27. Lee, S.B., Ryu, D.D.Y., Seigel, R., Park, S.H., 1988. Performance of recombinant fermentation and evaluation of gene expression efficiency for gene product in two-stage continuous culture system. Biotechnol. Bioeng. 31, 805-820.

28. Lin, Y., Tanaka, S., 2006. Ethanol fermentation from biomass resources: current state and prospects. Appl. Microbiol. Biotechnol. 69, 627-642.

29. Lipnizki, F., Hausmanns, S., Laufenberg, G., Field, R., Kunz, B., 2000. Use of Pervaporation-Bioreactor Hybrid Processes in Biotechnology. Chemical Engineering & Technology. 23, 569-577.

30. Madson, P., Lococo, D., 2000. Recovery of volatile products from dilute high-fouling process streams. Appl. Biochem. Biotechnol. 84-86, 1049-1061.

31. Mulder, M.H.V., Hendrickman, J.O., Hegeman, H., Smolders, C.A., 1983. Ethanol—water separation by pervaporation. J Membr Sci. 16, 269-284.

32. Mussatto, S.I., Dragone, G., Guimarães, P.M.R., Silva, J.P.A., Carneiro, L.M., Roberto, I.C., Vicente, A., Domingues, L., Teixeira, J.A., 2010. Technological trends, global market, and challenges of bio-ethanol production. Biotechnol. Adv. 28, 817-830.

33. Nakao, S.-i., Saitoh, F., Asakura, T., Toda, K., Kimura, S., 1987. Continuous ethanol extraction by pervaporation from a membrane bioreactor. J Membr Sci. 30, 273-287.

34. Nigam, P.S., Singh, A., 2011. Production of liquid biofuels from renewable resources. Prog. Energy Combust. Sci. 37, 52-68.

35. Nishiwaki, A., Dunn, I.J., 1998. Analysis of a two-stage fermentor with recycle for continuous ethanol production. Chem. Eng. Commun. 168, 207-227.

36. O'Brien, D.J., Craig Jr, J.C., 1996. Ethanol production in a continuous fermentation/membrane pervaporation system. Appl. Microbiol. Biotechnol. 44, 699-704.

37. O'Brien, D.J., Roth, L.H., McAloon, A.J., 2000. Ethanol production by continuous fermentation–pervaporation: a preliminary economic analysis. J Membr Sci. 166, 105-111.

38. OECD-FAO Agriculture Outlook, 2012. Biofuels. available on http://dx.doi.org/10.1787/888932639. Chapter 3.

39. Olsson, L., Hahn-Hägerdal, B., 1996. Fermentation of lignocellulosic hydrolysates for ethanol production. Enzyme Microb. Technol. 18, 312-331.

40. Roffler, S.R., Blanch, H.W., Wilke, C.R., 1987. In-situ recovery of butanol during fermentation. Bioprocess Eng. 2, 1-12.

41. Shabtai, Y., Chaimovitz, S., Freeman, A., Katchalski-Katzir, E., Linder, C., Nemas, M., Perry, M., Kedem, O., 1991. Continuous ethanol production by immobilized yeast reactor coupled with membrane pervaporation unit. Biotechnol. Bioeng. 38, 869-876.

42. Shao, P., Huang, R.Y.M., 2007. Polymeric membrane pervaporation. J Membr Sci. 287, 162-179.

43. Sprenger, G.A., 1996. Carbohydrate metabolism in *Zymomonas mobilis*: a catabolic highway with some scenic routes. FEMS Microbiol. Lett. 145, 301-307.

44. Van Hecke, W., Vandezande, P., Claes, S., Vangeel, S., Beckers, H., Diels, L., De Wever, H., 2012. Integrated bioprocess for long-term continuous cultivation of *Clostridium acetobutylicum* coupled to pervaporation with PDMS composite membranes. Bioresour. Technol. 111, 368-377.

45. Vane, L.M., 2005. A review of pervaporation for product recovery from biomass fermentation processes. J. Chem. Technol. Biotechnol. 80, 603-629.

46. Walker, G.M., 2011. 125th Anniversary Review: Fuel Alcohol: Current Production and Future Challenges. Journal of the Institute of Brewing. 117, 3-22.

47. Wee, S.-L., Tye, C.-T., Bhatia, S., 2008. Membrane separation process—Pervaporation through zeolite membrane. Sep. Purif. Technol. 63, 500-516.

48. Zaldivar, J., Nielsen, J., Olsson, L., 2001. Fuel ethanol production from lignocellulose: a challenge for metabolic engineering and process integration. Appl. Microbiol. Biotechnol. 56, 17-34.

Chapter 2

Experimental and theoretical analysis of two-stage ethanol fermentation coupled with pervaporation

Abstract

A process configuration consisting of continuous two–stage ethanol fermentation integrated with ethanol pervaporation, was proposed and experimentally tested. Complete conversion of glucose by *Saccharomyces cerevisiae* took place in the system. Ethanol and cell concentrations obtained in the 2nd fermenter were higher than in the 1st. Irreversible fouling of the pervaporative membrane was observed.

To achieve highly efficient fermentations, cell retention should be incorporated in this system. Therefore, two process configurations having different combination of two–stage fermenters, microfiltration and pervaporation were proposed. They were analyzed numerically with the aim to find the potentially most suitable conditions for high ethanol productivity, yield, and concentration.

A configuration consisting of two fermenters performs better when it is coupled with pervaporation which is followed by microfiltration (configuration A) than when microfiltration is followed by pervaporation (configuration B). The simulation results showed that the productivity in configuration A decreases with increasing $C_{e,2}$ whereas, the productivity in configuration B first increases with increasing ethanol mass fraction till $C_{e,2}$ = 0.045 g·g^{-1} and then decreases at higher values of $C_{e,2}$. The highest recovered yield, 0.419 g·g^{-1}, was achieved with configuration B at a productivity of 0.128 g·g^{-1}·h^{-1} and at a $C_{e,2}$ value of 0.002 g·g^{-1}, but in configuration A the optimum performance was obtained at productivity of 0.041 g·g^{-1}·h^{-1} and at a $C_{e,2}$ value of 0.066 g·g^{-1}. In the model calculations, the size of the 1st fermenter and the required recycle flow from 2nd to 1st fermenter vary significantly with the input conditions. At optimum conditions they are small but significant, so including a 1st fermenter and a recycle flow to it are supposed to be favorable. The experimental results, however, suggest that configuration A may be more prone to membrane fouling than configuration B.

Keywords: Two–stage fermenter, ethanol fermentation, pervaporation, membrane fouling, modeling and simulation.

2.1. Introduction

Application of bioethanol as renewable fuel or fuel additive has increased its global consumption. To meet this increasing demand, great efforts are being undertaken to explore ways to improve the ethanol productivity and minimize the production cost. Modifying the process configuration and performing process integration are means to do so.

Modified ethanol fermentation process configurations consisting of multistage fermenters with continuous and multistage feeding techniques are described in literature (Bai et al., 2004; Nishiwaki and Dunn, 1998). A continuous two–stage fermentation system has been explored due to its potential to maximize ethanol productivity ($g \cdot L^{-1} \cdot h^{-1}$) and substrate utilization (Ben Chaabane et al., 2006; Nishiwaki and Dunn, 1998). The first fermenter in such a system is dedicated to growth of cells whereas the product formation takes place in second fermenter. This separation of growth and product synthesis minimizes the cell degeneration (Heijnen et al., 1992) and improves the cell viability due to better vitamin assimilation at low ethanol concentration (Ben Chaabane et al., 2006).

Integration options in the ethanol process such as reaction–reaction, reaction–separation and separation–separation have been extensively described by Cardona and Sánchez (2007b). As major costs in process industry are generated in the separation step, the reaction–separation integration plays a very important role in the production of fuel ethanol. Proposed integrated schemes of this type include the coupling of fermentation with separation unit operations such as gas stripping, liquid–liquid extraction, pervaporation and adsorption (Cardona and Sánchez, 2007b). High cell densities and product concentrations can be obtained by coupling the fermenter with a cell retention system. Mostly ultra– or microfiltration systems are used for cell retention and retained cells are sent back to the fermenter.

A numerical study of continuous two–stage fermentation with cell retention at each stage was performed by Nishiwaki and Dunn (1998; 1999). Their work showed that such a system was more efficient than single stage fermentation or two–stage fermentation with cell retention after the final stage. An experimental demonstration of a two–stage fermentation with cell retention by ultrafiltration after the final stage

was done by Ben Chaabane et al. (2006). Their configuration includes a recycle loop from the second stage to the first and separation of growth from product formation. The outcome of this research showed that such integrated system is capable of providing a high ethanol productivity at industrially relevant ethanol titers. One of the challenges in this system was to deal with high ethanol concentrations in the second fermenter leading to the product inhibition. To overcome this problem, we studied a modified configuration (Figure 2.1) replacing ultrafiltration with pervaporation. Here, the pervaporation might function as cell retention and ethanol recovery system thereby providing high cell density and ethanol concentration well below the inhibitory levels in the second fermenter. Van Hecke and co–workers (2012) have successfully demonstrated experimental validation of a similar process configuration for the ABE fermentation. The optimization of such system led to superior solvent productivity and greater carbohydrate utilization (Van Hecke et al., 2013). To our knowledge, the experimental validation of two–stage fermentation coupled with pervaporation for ethanol production has not been reported.

Thus, the aim of this study was the test of the proposed integrated system. On the basis of the experimental results, two modified integrated process options consisting of different combination of microfiltration (MF) and pervaporation (PV) coupled with two–stage fermenters were proposed and were analyzed numerically. The comparison of these process options was carried out based on three process performance parameters: recovered ethanol yield, achieved ethanol concentration and overall ethanol productivity. The effect of different process settings (dilution rate, mass ratio of the two fermenters, necessity of recycle from stage 2 to stage 1, etc.) on the performance of the systems was evaluated in this study.

2.1.1 Experimental configuration

The schematic diagram for the integrated system with all streams is shown in Figure 2.1. A glucose fermentation carried out with *Saccharomyces cerevisiae* was considered as model system. The first fermenter was run aerobically and hence was associated with the cell growth whereas the ethanol formation should take place in the microaerated second fermenter. The pervaporation integrated with

fermentation performs a dual function of cell retention and ethanol separation. The pervaporation uses a hydrophobic membrane to separate ethanol from the fermentation broth. The retentate containing the cells and other by–products was sent back to fermenter 2. Glucose and medium components were fed continuously to reactor 1 only. A bleed stream (Q_b) was taken out from reactor 2 to avoid the accumulation of water and inhibitory components. A constant mass was maintained in both fermenters by regulating Q_{12} and Q_b.
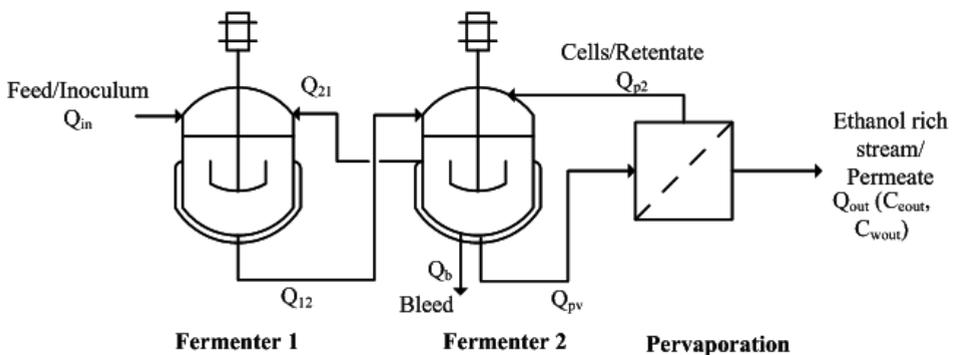
Figure 2.1. Schematic diagram of integrated system used for experimental validation.

2.1.2 Simulated process configurations

Several possible process integration options for single stage fermentation and pervaporation have been reported in literature (Groot et al., 1993; Lipnizki et al., 2000b). Here we propose two process options consisting of different combination of two–stage fermenters, microfiltration (MF) and pervaporation (PV) with the aim to maximize ethanol productivity and minimize ethanol loss through the bleed.

The first option (Figure 2.2A) is an extension of the proposed experimental system with addition of MF after the PV unit. The permeate stream size and permeate ethanol concentration in pervaporation will depend on the membrane properties. The pervaporation retentate stream is then fed to MF where further separation of ethanol from cells is performed. The retentate from MF is sent back to the second fermenter. The size of this recycle stream can be regulated by the cut–rate in MF. The bleed is taken out from this

recycle stream which should contain a high cell concentration and a low ethanol concentration. This minimizes the ethanol loss through the bleed but the loss of cells will depend on the size of bleed stream. A high risk of membrane fouling in both PV and MF can be anticipated in this process option. The permeate flows from PV and MF can be treated further based on their ethanol composition. This process option has never been explored before in the literature.

In the second process option (Figure 2.2B), the MF is directly coupled with the 2nd fermenter and performs as cell retention system. The retentate from MF is sent back to the 2nd fermenter and the bleed is taken out from this stream. The bleed stream here might have a high ethanol concentration leading to larger ethanol loss compared to configuration A. The permeate from MF is fed to PV where the further separation of ethanol takes place. The cell free feed to PV potentially reduces the fouling of the membrane. A comparable process configuration has been proposed by Groot et al. (1993), but with a single fermenter, with cell bleed taken directly from the fermenter and with a medium bleed from the PV retentate stream. Cell bleed from the fermenter can lead to relatively high loss of viable cells, product and medium components resulting in productivity loss. A comparable process option has also been shown by Lipnizki et. al. (2000b), with bleed from the PV retentate stream. Here they avoid the product loss but have no cell bleed which can result in accumulation non–viable cells in the fermenter leading to lower productivity. With our process option (Figure 2.2B), these issues can be minimized.

A.
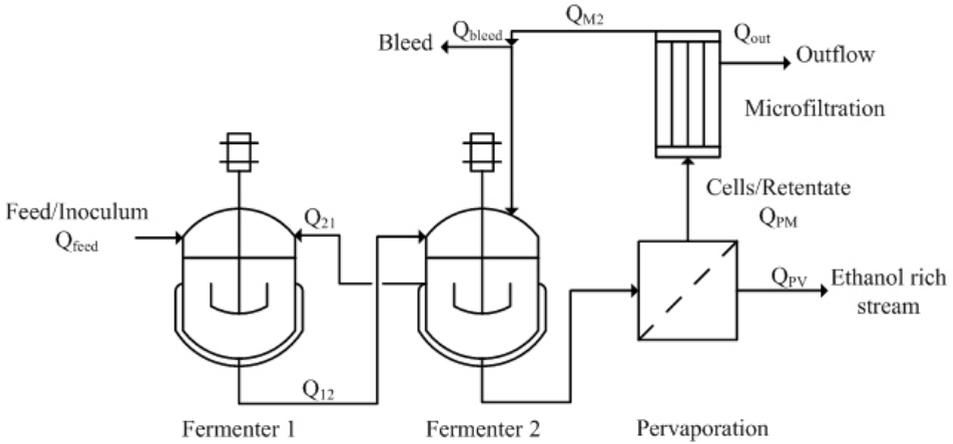
B.
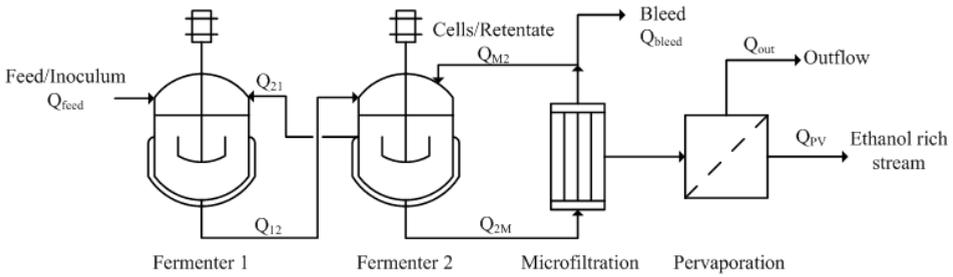
Figure 2.2. Proposed process configurations.

2.2. Materials and Methods

2.2.1 Strain and Media

Saccharomyces cerevisiae CEN.PK113–7D was used. The pre–culture medium contained 5.0 g·L^{-1} (NH$_4$)$_2$SO$_4$, 3.0 g·L^{-1} KH$_2$PO$_4$, 0.5 g·L^{-1} MgSO$_4$.7H$_2$O, 15 g·L^{-1} glucose and 1.0 mL·L^{-1} of a trace element solution and 1.0 mL·L^{-1} of a vitamin solution. The compositions of the trace element and vitamin solutions are described by Verduyn et al. (1990). The batch medium contained 3.5 g·L^{-1} (NH$_4$)$_2$SO$_4$, 3.0 g·L^{-1} NH$_4$H$_2$PO$_4$, 4.0 g·L^{-1} KH$_2$PO$_4$, 0.8 g·L^{-1} MgSO$_4$.7H$_2$O, 50 g·L^{-1} glucose, 7.0 mL·L^{-1} of trace element solution and 1.5 mL·L^{-1} of vitamin solution. The medium used for the chemostat cultivation was composed of 0.3 g·L^{-1} (NH$_4$)$_2$SO$_4$, 3.0 g·L^{-1} NH$_4$H$_2$PO$_4$, 4.0 g·L^{-1} KH$_2$PO$_4$, 0.7 g·L^{-1} MgSO$_4$.7H$_2$O,

100 g·L^{-1} glucose, 7.0 mL·L^{-1} of trace element solution and 1.5 mL·L^{-1} of vitamin solution.

The pre–culture medium was filter sterilized by using PVDF membrane with 0.2 µm pore diameter (Millipore, Massachusetts, USA) whereas batch and chemostat culture media with trace elements and vitamin solutions were filter sterilized via a 0.2 µm pore diameter PES membrane (Sartorius Stedim Biotech, Germany). Heat sterilized 20 wt.% Struktol (Schill and Seilacher AG, Hamburg, Germany) solution (1.5 mL·L^{-1}) was used as antifoam.

2.2.2 Chemostat cultivation

The set–up used for the integrated experiment is schematically illustrated in Figure 2.1.

Shake flasks containing 100 g of a pre–culture medium were inoculated with 1 mL of working cell stock. Pre–culturing was performed for 12 h at 30 °C and 200 rpm on a gyratory shaker. The whole pre–culture was used to inoculate batch fermentation.

A batch phase was started by inoculation at t = 0 in two 2.0 L fermenters (Applikon, Schiedam, The Netherlands) at the same time with the same operational conditions. The fermenters were aerated at 0.5 L·min^{-1} and 30 ˚C at 1.5 kg of initial liquid mass. The fermentation medium was stirred at 800 rpm and the pH of the broth was maintained at 5.0 by addition of 2.5% (v·v^{-1}) NH$_4$OH solution.

When the off–gas CO$_2$ concentration dropped to zero in both fermenters, the batch phase was considered to be finished. After the completion of batch phase, chemostat medium feeding to fermenter 1 was set at 0.3 L·h^{-1}. The air flow in the second fermenter was reduced to 0.1 L·min^{-1} and the recycle from fermenter 2 to fermenter 1 was set at 0.15 L·h^{-1}. The liquid flow from fermenter 1 to fermenter 2 and the outlet flow from fermenter 2 were controlled with electrical level controllers so as to have constant mass of 1.5 kg in both the fermenters. The amount of effluent was monitored with a balance during the entire experiment.

The broth pH, temperature, dissolved oxygen, stirring speed were controlled and monitored using Biostat Bplus controller (Sartorius BBI Systems, Melsungen, Germany). The air flow rates to the fermenter were maintained by means of mass flow controllers (Brooks 5850 TR,

Hatfield, PA, USA). The circulation of the medium and fermentation broth was carried out using a peristaltic pump (Masterflex console drive).

Samples (5 g in duplicate for each fermenter) were taken periodically to measure the concentration of yeast and extracellular metabolites. The exhaust gas was cooled with a condenser connected to a cryostat set at 5 °C and dried with a Permapure dryer (Inacom Instruments, Overberg, The Netherlands) before online analysis of the CO_2 and O_2 volume fractions by a Rosemount NGA 2000 gas analyzer (Minnesota, USA). When the fermentation system was in steady–state, (after 10 residence times: 50 h since starting of the chemostat), the pervaporation unit was integrated with fermenter 2 and ethanol recovery was attained.

2.2.3 Pervaporation

A custom made flat–sheet pervaporation unit was used with an effective membrane cross–sectional area of 50 cm². Pervaporation experiments were performed using commercially available PDMS (polydimethylsiloxane) membrane obtained from Pervatech BV (Enter, The Netherlands). The fermentation broth from fermenter 2 was circulated over the membrane through Norprene® tubing (Masterflex 06404–18, Saint Gobain, France) at a flow rate of 605 g·min⁻¹ by using a peristaltic pump (Masterflex console drive) so as to have a Reynolds No. of 4025 (turbulent flow). A constant vacuum of 10 mbar on the permeate side was maintained by a vacuum pump (SC920, KNF, Germany) and permeate was collected alternatively in two parallel glass flasks kept in cryostats at -14 °C (RMS 6, LAUDA, Germany) and -20 °C (RE 307, LAUDA, Germany).

Before integrating pervaporation with the fermentation, the membrane was equilibrated by circulating 5 wt.% aqueous ethanol for at least 12 h. After membrane equilibration, the pervaporation system was sterilized by circulating 70% (v·v⁻¹) aqueous ethanol through the system for 30 min followed by removal of excess ethanol from the system by circulating sterilized water over the membrane for 1 h.

After the first integration experiment, the pervaporation system was emptied and the membrane was cleaned with hot (37°C) sterile demineralized water (O'Brien and Craig Jr, 1996b) for at least 3 h. Then

the membrane was again equilibrated overnight with 5 wt.% aqueous ethanol. The next pervaporation experiment was carried out with the cleaned/used membrane after equilibration and sterilization steps.

Permeate samples were collected every 60 min and the mass amount of total permeate W^p was determined by weighing the flasks. The total flux through the membrane J_{Total} was calculated using Equation (2.1):

$$J_{Total} = \frac{W^p}{A_m \cdot t}$$
(2.1)

where A_m represents the effective membrane area (m²) and t indicates the permeate collection time (h). Samples were collected till the total flux through the membrane was less than 100 g·m⁻²·h⁻¹.

The mass fraction of water C_i^p in permeate was calculated from the mass fraction of ethanol in permeate. The partial fluxes of individual components J_i were evaluated using Equation (2.2):

$$J_i = J_{Total} \cdot C_i^p$$
(2.2)

The separation performances of the membranes were compared on the basis of the selectivity α_{EtOH,H_2O}. As feed and retentate compositions will be virtually identical at our conditions, we can apply Equation (2.3) to calculate membrane selectivity.

$$\alpha_{EtOH,H_2O} = \frac{(C_{EtOH}/C_{H_2O})^p}{(C_{EtOH}/C_{H_2O})^f}$$
(2.3)

where C_{EtOH} and C_{H_2O} represent the mass fractions of ethanol and water, and superscripts p and f denote the permeate and feed side, respectively.

2.2.4 Analysis

5 mL of fermentation broth was filtered using dried and pre–weighed 0.45 µm pore diameter filter paper (Supor®–450, Pall Life Sciences, Michigan, USA). The filter with cell mass was washed with deionized water, dried at 70 °C for 24 h, and weighed to yield cell dry weight.

The filtrate obtained from the broth filtration was used to determine extracellular metabolites (ethanol, acetate, succinate and glycerol) and residual substrate concentration. The residual amounts of glucose, as well as the concentrations of ethanol (in fermentation broth and in pervaporation permeate), glycerol and acetate, were determined by high–performance liquid chromatography analysis with a Bio–Rad Aminex HPX–87H column at 59 °C. The column was eluted with 5 mmol·L^{-1} phosphoric acid at a flow rate of 0.6 mL·min^{-1}. Acetate and succinate were detected using a Waters 2489 dual–wavelength absorbance detector at 210 nm. Glucose, ethanol, and glycerol were detected with a Waters 2414 refractive index detector.

2.3. Results

2.3.1 Experimental results

After the completion of the batch phase (feed glucose concentration = 50 g·L^{-1}) in both fermenters, chemostat cultivation was started at t = 12 h by continuous feeding of medium (feed glucose conc. = 100 g·L^{-1}) to fermenter 1 only. Due to this higher feed glucose concentration, an increase in concentrations of products and by–products was observed at the beginning of the chemostat in both fermenters. The concentration profiles obtained in both the fermenters during the integrated experiment are shown in Figure 2.3A and 2.3B.
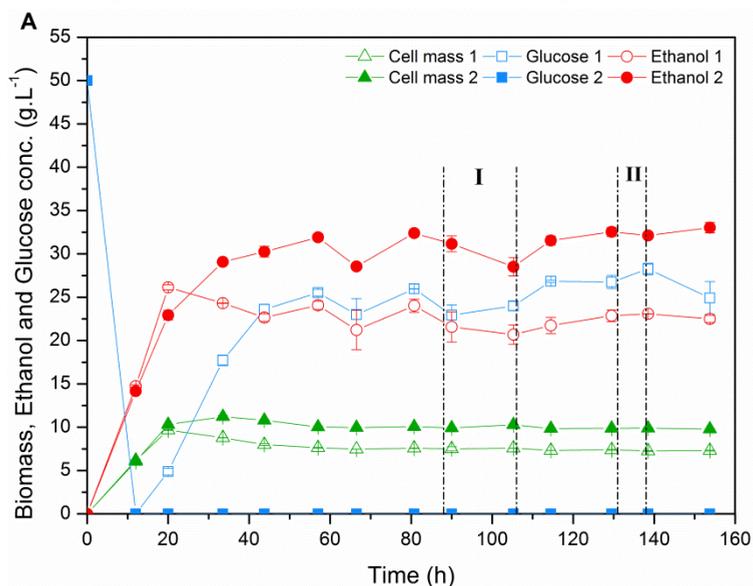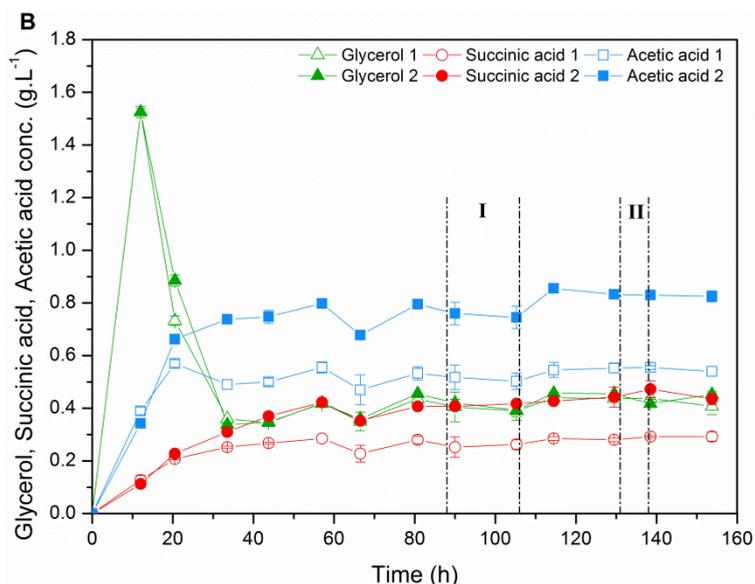
Figure 2.3. Concentration profiles for cell mass, ethanol and glucose (A) and by–products (B) in continuous two–stage fermentation coupled with pervaporation.

> I = Integrated experiment with fresh PDMS membrane.
> II = Integrated experiment with cleaned membrane from I.

Due to a high glucose concentration in fermenter 1 (aerobic), ethanol production takes place according to the Crabtree effect (De Deken, 1966). Complete conversion of leftover glucose from fermenter 1 (around 25 g·L^{-1}) takes place in fermenter 2. Except for glycerol, the concentration of other components was found to be higher in the 2nd fermenter than in the 1st. A high glycerol concentration was obtained in both fermenters after the completion of the batch phase but eventually it decreased during the chemostat cultivation. Steady state ethanol concentrations, ethanol yield and productivity achieved in 1st and 2nd fermenter are listed in Table 2.1.

Table 2.1. Steady state ethanol concentration, ethanol yield and ethanol productivity obtained during integrated experiment. Ethanol yield was calculated from $\left(\dfrac{q_{e,i}}{q_{s,i}}\right)$ and ethanol productivity from $q_{e,i}.C_{x,i}$, after using mass balances to determine q–values.

	Ethanol concentration (g·L^{-1})	Ethanol yield (g·g^{-1})	Ethanol Productivity (g·L^{-1}·h^{-1})
Fermenter 1	22.4	0.290	3.61
Fermenter 2	31.2	0.348	2.63
Overall (process)	31.2	0.312	6.24

When the fermentation system reached steady state, the pervaporation unit was coupled to the 2nd fermenter. The total flux through the membrane and the membrane ethanol selectivity achieved from integration carried out using fresh membrane (PV experiment 1) are shown in Figure 2.4A. The results obtained indicated that the total flux and the membrane selectivity decreased with time. This decrease was very fast and within 16 h after starting the integrated experiment, the membrane selectivity was below 1.

A new integration experiment (experiment 2) was performed with cleaned membrane keeping the other operating conditions the same as in integrated experiment 1. The total flux and selectivity obtained are given in Figure 2.4B.

The results showed a similar trend as in the first experiment. However, the initial selectivity of the membrane (4.4) in first experiment was not gained back in the second experiment (after cleaning). Also, the membrane selectivity was below 1 within 6 h after starting the experiment, which was much faster than that in the first experiment. This rapid decrease in the membrane performance was a clear indication of membrane fouling.
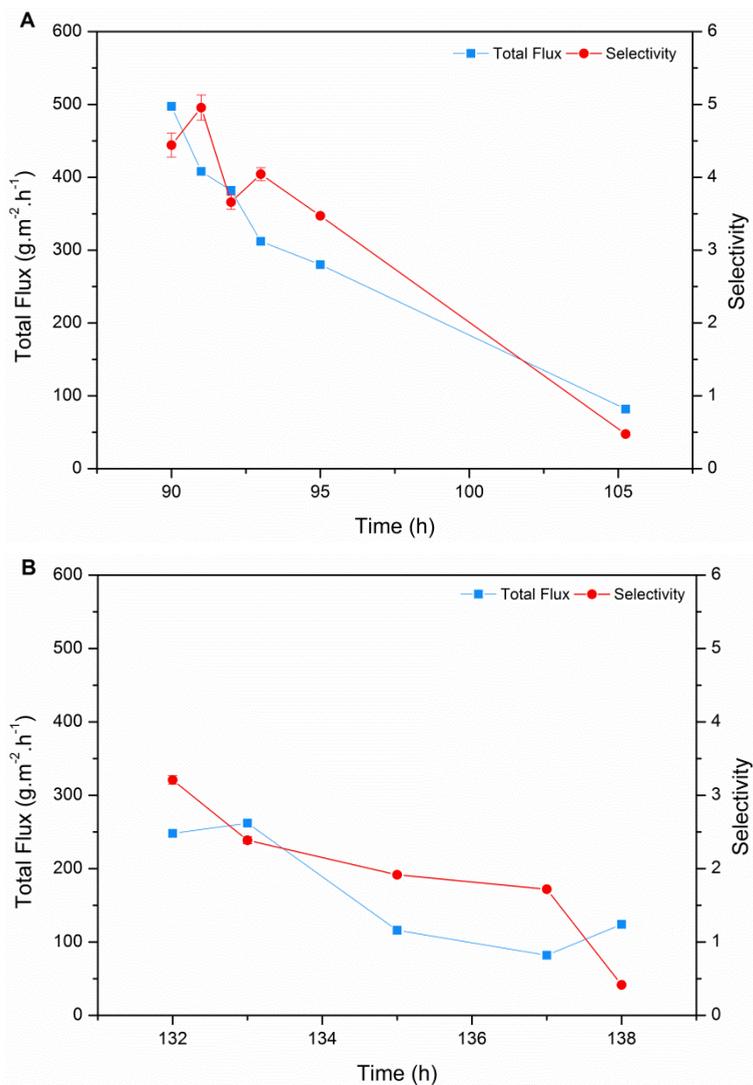
Figure 2.4. Total flux through the membrane and membrane ethanol selectivity obtained during the integrated experiment. A = integration experiment with fresh membrane (experiment 1); B = integration experiment with cleaned/washed membrane (experiment 2).

2.3.2 Simulation results

The proposed configurations (Figure 2.2A and 2.2B) were numerically evaluated to compare their potential performance. Kinetic models for fermentations were formulated for aerobic and anaerobic conditions based on literature data (Groot et al., 1992b; Herwig and von Stockar, 2002). In addition to mass balances for glucose, ethanol, O_2 and cell mass, an overall mass balance was used to account for NH_3, H_2O, CO_2 and by–products. Formation of ethanol in fermenter 1 was assumed to be negligible because of sufficient aeration, whereas growth was minimized in anaerobic fermenter 2. To be able to find the best fermentation conditions, perfect pervaporation was assumed. Thus, it was assumed that complete recovery of ethanol from the feed stream at infinite selectivity was achieved by pervaporation. The steady state mass balances were then formulated and kinetic models were included. The kinetic model and its parameters are approximations, but should capture the main characteristics of the system. The complete model for the proposed configurations, see Appendix, was solved with different input parameters so as to achieve high volumetric productivity (Equation 2.4), high yield on glucose (Equation 2.5) and high ethanol mass fraction in fermenter 2, using M_1 and M_2 as the mass contents of the fermenters.

$$\text{Productivity } (P) = \frac{Q_{PV}}{M_1 + M_2} \tag{2.4}$$

$$\text{Recovered yield on glucose } (y) = \frac{Q_{pv}}{Q_{feed}.C_{s,0}} \tag{2.5}$$

The calculations for configuration A (Figure 2.2A) and configuration B (Figure 2.2B) were carried out by setting $C_{e,bleed} = 0$ and $C_{e,bleed} = C_{e,2}$, respectively. The feed glucose mass fraction ($C_{s,0}$) was assumed to be 300 g·kg^{-1}. Also, the achievable maximum cell mass fraction in fermenter 2 ($C_{x,2}$) and in the bleed ($C_{x,bleed}$) were assumed to be 100 and 200 g·kg^{-1} respectively, because these were assumed the maximum values that could be stirred and pumped. The effect of ethanol concentration in 2nd fermenter ($C_{e,2}$) on mass–specific productivity at different recovered yield was evaluated for both systems

and the steady states that were calculated to be feasible are shown in Figure 2.5. To avoid inconsistencies in the model, concentrations and productivities are expressed per kg solution rather than per liter solution.

The results in Figure 2.5 show for $C_{e,2}$ values less than $C_{e\max}$ = 0.096 g·g^{-1} because the model assumes that glucose uptake stops at this maximum ethanol concentration. The results achieved for both configurations A and B, indicate that productivity increases with increase in recovered yield and higher productivity, at all considered recovered yield values, obtained at lower $C_{e,2}$ values.

The productivity in configuration A, at all values of recovered yield, decreases with increasing $C_{e,2}$. With configuration B, the productivity first increases with increasing ethanol mass fraction till $C_{e,2}$ = 0.045 g·g^{-1} and then decreases at higher values of $C_{e,2}$. In configuration B, the realistic values for productivity were obtained at $C_{e,2}$ less than 0.03 g·g^{-1}·h^{-1} and for recovered yield higher than 0.405 g·g^{-1}. At these conditions, a sharp increase in productivity was observed with increase in recovered yield.

For obtaining a high $C_{e,2}$ at high yield, configuration A gives a better productivity than configuration B. Higher productivities, at any recovered yield and irrespective of $C_{e,2}$, were obtained at configuration B compared to configuration A. The highest productivity, 0.128 g·g^{-1}·h^{-1}, was achieved with configuration B at a recovered yield of 0.419 g·g^{-1} and at a $C_{e,2}$ value of 0.002 g·g^{-1}.

The concentrations of components in the two fermenters and the flow rates for the two configurations calculated for recovered yields resulting in highest productivity (P_1 = 0.1105 g·g^{-1}·h^{-1} and P_2 = 0.1276 g·g^{-1}·h^{-1}) and lowest productivity (P_1 = 0.0414 g·g^{-1}·h^{-1} and P_2 = 0.0369 g·g^{-1}·h^{-1}) are given in Table 2.2.

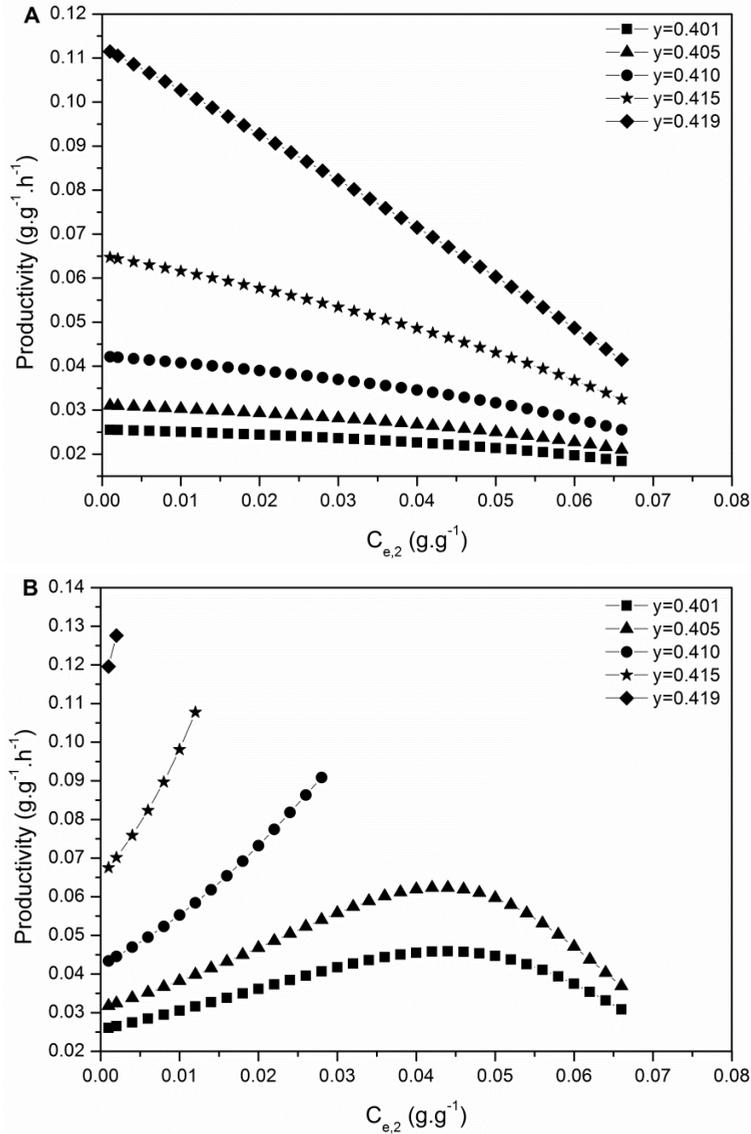**Figure 2.5.** Effect of ethanol mass fraction in 2nd fermenter ($C_{e,2}$) on productivity at different recovered yields for both process options. y = recovered yield; A= configuration A (Figure 2.2A; $C_{e,bleed} = 0$), B = configuration B (Figure 2.2B; $C_{e,bleed} = C_{e,2}$).

At higher recovered yield ($y_1 = y_2 = 0.419$ g·g⁻¹), for both configurations, all the flow rates and other parameters were similar

except for the mass in fermenter 1. The mass in fermenter 1 (M_1) obtained was negligible compared to mass in fermenter 2 (M_2) for configuration B. At lower recovered yield (y_1 = 0.419, y_2 = 0.405), the lowest productivity was obtained at higher ethanol mass fraction in fermenter 2 ($C_{e,2}$ = 0.066 g·g^{-1}) for both configurations. The unconverted glucose in fermenter 2 was also higher in both configurations. The higher flow rates and fermenter masses ($M_1 + M_2$) were observed in configuration B compared to configuration A. The recycle flow rate Q_{21} calculated at lowest recovered yield condition is almost similar to that obtained at highest recovered yield condition. Also, the mass in fermenter 1 and 2 (M_1 and M_2) differs considerably with change in recovered yield conditions for both configurations. The necessity of fermenter 1 in the proposed configurations and of the recycle flow to fermenter 1 depends on the desired performance. But fermenter 1 is important for growth of the cells and might also be helpful for maintaining the viability of the cells.

For both process configurations, the model calculations were also performed at feed glucose mass fraction ($C_{s,0}$) of 200 g·kg^{-1} and 400 g·kg^{-1}. The results (not shown) show similar trends as presented in Figure 2.5. At lower feed mass fraction additional steady states become feasible, but these are at low productivities and low yields.

2.4. Discussion

During the experiment with integrated pervaporation (Figure 2.1), the glucose was continuously fed to fermenter 1 (aerobic) and also the fermenter 2 was partially aerated. Due to these operating conditions it was postulated that ethanol formation in fermenter 1 by the Crabtree effect and cell growth in fermenter 2 due to partial aeration took place. Growth in fermenter 2 is observed in the concentration profiles shown in Figure 2.3. The steady state ethanol concentration in fermenter 1 calculated based merely on the experimental steady state concentration in fermenter 2 and flows to and from fermenter 1 was found to be lower (around 10.4 g·L^{-1}) than the experimentally recorded ethanol

concentration (22.4 g·L^{-1}) which indicates the formation of ethanol in fermenter 1 by the Crabtree effect.

During the experimentation, the integrated system (Figure 2.1) performed poorly mainly due to the large bleed stream from fermenter 2 as compared to the pervaporation permeate flow and the decrease in membrane performance due to fouling. This indicated that the process configuration needed to be adapted. Hence, the integrated processes were proposed with a aim to minimize the membrane fouling, reduce the losses through the bleed and to increase the productivity by incorporating a microfiltration unit.

It was also observed during experimental evaluation that many process parameters affect the process performance and need to be optimized. These parameters are: fermenter masses, ethanol concentration in fermenter 2, different flow sizes, feed glucose concentration, recycle flow from fermenter 2 to fermenter 1, bleed through the fermenter 2, aeration in fermenter 2, membrane area, membrane selectivity, etc. The experimental optimization of integrated process based on five independent variables (feed glucose concentration, dilution rate, fermenter masses (M_1 and M_2), membrane area) and at three different values of each variable (maximum, minimum and in between) will result into 243 experiments per configuration for using a factorial design method; 3^5 = 243. To avoid such an extensive and time consuming experimental analysis of the integrated process, a numerical evaluation of the integrated process was opted.

In the model it is not attempted to simulate the performed experiment but to analyze the proposed configurations. The Crabtree is difficult to model, and therefore conditions were chosen at which ethanol formation in fermenter 1 was assumed to be absent. However, in the model calculations a positive, though very low, ethanol concentration in fermenter 1 was obtained due to the recycle flow from fermenter 2 to fermenter 1 (Q_{21}). The necessity of incorporating flow Q_{21} to maintain the viability of the cells in fermenter 2 was illustrated by Ben Chaabane (2006), but for simplicity this phenomenon was not included in the model. Our model calculations, for both configurations,

show a low but considerable recycle flow Q_{21} at lowest and highest productivity conditions.

The numerical results obtained with process options A and B differ widely (Figure 2.5). This is due to difference in ethanol and cell loss via bleed in both process options. The extent of ethanol loss changes the masses in the two fermenters. The change in productivity in configuration B is due to change in M_1/M_2 ratio. The productivity increases, with increase in $C_{e,2}$, when this ratio is larger than 1, and productivity decreases when this ratio becomes less than 1. This might be due to the fact that when the formed ethanol disappears with the bleed, more ethanol needs to be produced to achieve the yield. This requires larger M_2, also causing more growth in fermenter 2. Due to this less feed is available for growth in fermenter 1, and M_1 will have to be smaller. This affects productivity as M_1+M_2 may either increase or decrease. This effect is clearly seen in Table 2.2. In addition to the change in fermenter masses, a difference in recycle flow from fermenter 2 to fermenter 1 (Q_{21}) for both process options was also observed. In option B, Q_{21} increases with increase in $C_{e,2}$ whereas it remains unchanged in option A. This results in increase in ethanol mass fraction in fermenter 1 in option B.

At lower productivity (P_1 = 0.0414 g·g^{-1}·h^{-1} and P_2 = 0.0369 g·g^{-1}·h^{-1}) in both configurations, the higher glucose concentration in fermenter 2 ($C_{s,2}$) caused due to slow cell growth (μ_2) might be due to high $C_{e,2}$, which is closer to ethanol inhibition concentration ($C_{e\max,x}$). This also results in lower $q_{s,2}$ and $q_{e,2}$.

During the integrated experiment, irreversible membrane fouling was observed and membrane selectivity below 1 was obtained. This might be due to adsorption of fermentation broth components on the membrane surface making it more hydrophilic resulting in lower ethanol concentration in the permeate and membrane selectivity below 1.

The effect of pervaporation membrane properties on the ethanol concentration in the permeate was neglected in the model calculations and complete separation of ethanol was considered. Based on these assumptions, configuration A performs better in the simulations at high recovered yield and high $C_{e,2}$ but exposes the pervaporation membrane to the cells, which leads to severe membrane fouling according to the experiments. In this regard, configuration B might be more suitable than configuration A, and also gives better productivity at any yield when $C_{e,2}$ does not matter.

In practice, based on the available membranes, complete separation of ethanol is not possible with pervaporation. Thus, the performance parameters obtained with the model are overestimated. Also, the irreversible membrane fouling observed during pervaporation should be included in the detailed modeling.

Configuration A was not experimentally implemented at the optimized settings as membrane fouling was observed during pervaporation, and further studies are focused on investigation of membrane fouling (Gaykawad et al., 2012; 2013).

Table 2.2. The process parameters for process options A ($C_{e,bleed}$ = 0) and B ($C_{e,bleed} = C_{e,2}$) at different productivities.

Process configuration	A	B	A	B
Productivity (g·g⁻¹·h⁻¹)	0.1105	0.1276	0.0414	0.0369
Yield (y)[†] (g·g⁻¹)	0.419	0.419	0.419	0.405
$C_{e,2}$ [#] (g·g⁻¹)	0.002	0.002	0.066	0.066
$C_{x,1}$ (g·g⁻¹)	6.25×10^{-3}	6.25×10^{-3}	6.25×10^{-3}	6.25×10^{-3}
$C_{s,1}$ (g·g⁻¹)	0.2814	0.2813	0.2815	0.2817
$C_{e,1}$ (g·g⁻¹)	1.19×10^{-4}	1.24×10^{-4}	3.93×10^{-3}	3.67×10^{-3}
$C_{x,2}$ [†] (g·g⁻¹)	0.100	0.100	0.100	0.100
$C_{s,2}$ (g·g⁻¹)	4.85×10^{-3}	4.85×10^{-3}	1.14×10^{-1}	1.14×10^{-1}
$C_{e,bleed}$ [#] (g·g⁻¹)	0	0.002	0	0.066
Q_{feed} [#] (kg·h⁻¹)	7.955	7.955	7.955	8.2304
Q_{12} (kg·h⁻¹)	8.459	8.480	8.459	8.716
Q_{21} (kg·h⁻¹)	0.526	0.548	0.526	0.490
Q_{pv} [*] (kg·h⁻¹)	1.0	1.0	1.0	1.0
Q_{bleed} (kg·h⁻¹)	0.919	0.912	0.444	0.475
Q_{out} (kg·h⁻¹)	6.036	6.044	6.511	6.755
μ_1 (h⁻¹)	0.2497	0.2497	0.2398	0.2404
μ_2 (h⁻¹)	0.2436	0.2436	0.0385	0.0385
M_1 (kg)	1.601	0.378	1.668	3.964
M_2 (kg)	7.45	7.46	22.45	23.15
$q_{s,1}$ (g·g⁻¹·h⁻¹)	-0.568	-0.567	-0.545	-0.546
$q_{s,2}$ (g·g⁻¹·h⁻¹)	-3.197	-3.197	-1.061	-1.061
$q_{e,2}$ (g·g⁻¹·h⁻¹)	1.343	1.343	0.445	0.445
$Y_{sx,2}$ (g·g⁻¹)	0.0762	0.0762	0.0363	0.0363
$Y_{se,2}$ [†] (g·g⁻¹)	0.42	0.42	0.42	0.42

[*] = Fixed parameter.

[#] = Input parameters.

[†] = Assumed parameters.

2.5. Conclusions

Continuous two–stage fermentation was coupled with pervaporation, but irreversible fouling of the pervaporative membrane was observed during the experiment with integrated pervaporation. Optimization of such an integrated process requires a modeling approach.

Concerning the proposed process options consisting of different combination of two–stage fermenters, MF and pervaporation, at all values of recovered yield, the productivity in configuration A was calculated to decrease with increasing ethanol mass fraction in fermenter 2 ($C_{e,2}$). The productivity in configuration B first increases with increasing ethanol concentration till $C_{e,2}$ = 0.045 g·g^{-1} and then decreases at higher values of ethanol mass fraction in fermenter 2. Configuration A gives better productivity than configuration B at high ethanol mass fraction in fermenter 2 and at high yield. Higher productivities, at any recovered yield and irrespective of ethanol mass fraction in fermenter 2, were obtained at configuration B compared to configuration A. The highest productivity, 0.128 g·g^{-1}·h^{-1} was achieved with configuration B at recovered yield of 0.419 g·g^{-1} and at a $C_{e,2}$ value of 0.002 g·g^{-1}.

The flow from fermenter 2 to fermenter 1 (Q_{21}) required according to model calculations was low but considerable for the lowest and highest productivity conditions and its significance in maintaining cell viability should be investigated experimentally. The size of first fermenter to obtain the highest productivity condition (configuration B, Recovered yield y = 0.419 g·g^{-1}) was found to be small but not zero.

Notations and symbols:

A_m =   effective membrane area (m^2).

$C_{e,bleed}$ =   Ethanol mass fraction in bleed (kg·kg^{-1}).

C_e, $C_{e,i}$ =   Ethanol mass fraction (kg·kg^{-1}).

C_{H_2O} =   Mass fraction of water (kg·kg^{-1}).

C_i^p =   Mass fraction of component i in the permeate (kg·kg^{-1}).

$C_{s,i}$ =   Substrate mass fraction (kg·kg^{-1}).

$C_{x,bleed}$ =   Cell mass fraction in bleed (kg·kg^{-1}).

$C_{x,i}$ =   Cell mass fraction in i (kg·kg^{-1}).

J_i =   Partial flux of component i through the membrane (kg·m^{-2}·h^{-1}).

J_{Total} =   Total flux through the membrane (kg·m^{-2}·h^{-1}).

K_s =   Saturation constant (kg·kg^{-1}).

$m_{s,i}$ =   Maintenance coefficient of cells in i (kg·kg^{-1}·h^{-1}).

M_i =   Mass in fermenter i (kg).

OTR_{max} =   Maximum oxygen transfer rate (kg·kg^{-1}·h^{-1}).

P =   Productivity (kg-EtOH·(kg-Fermentation broth)$^{-1}$·h^{-1}).

Q_{bleed} =   Bleed stream flow rate (kg·h^{-1}).

Q_{feed} =   Feed stream flow rate (kg·h^{-1}).

Q_{out} =   Flow rate of outlet stream (kg·h^{-1}).

Q_{pv} =   Pervaporation permeate stream flow rate (kg·h^{-1}).

Q_{12} =   Flow rate of stream from reactor 1 to reactor 2 (kg·h^{-1}).

Q_{21} =   Flow rate of stream from reactor 2 to reactor 1 (kg·h^{-1}).

q =   Yeast–mass specific uptake rate (kg·kg^{-1}·h^{-1}).

t =   Permeate collection time (h).

W^p =   Mass amount of total permeate (kg).

$Y_{Ox\,max}$ =   Maximum yield of biomass on oxygen (kg·kg^{-1}).

$Y_{se,i}$ =   Ethanol yield on substrate in i (kg·kg^{-1}).

$Y_{sx,i}$ =   Biomass yield on substrate in i (kg·kg^{-1}).

y =   Recovered ethanol yield (kg-EtOH·kg-glucose^{-1}).

μ_i =   Cell growth rate in i (h^{-1}).

Subscript:

$1 =$	in fermenter 1.
$2 =$	in fermenter 2.
$i =$	in fermenter i.
$e =$	for ethanol.
$max =$	maximum.
$O_2 =$	for oxygen.
$s =$	for glucose.
$x =$	for yeast (per mole C).

Superscript:

$f =$	feed.
$p =$	permeate.

References:

1. Bai, F.W., Chen, L.J., Anderson, W.A., Moo-Young, M., 2004. Parameter oscillations in a very high gravity medium continuous ethanol fermentation and their attenuation on a multistage packed column bioreactor system. Biotechnol. Bioeng. 88, 558-566.
2. Ben Chaabane, F., Aldiguier, A.S., Alfenore, S., Cameleyre, X., Blanc, P., Bideaux, C., Guillouet, S.E., Roux, G., Molina-Jouve, C., 2006. Very high ethanol productivity in an innovative continuous two-stage bioreactor with cell recycle. Bioprocess Biosystems Eng. 29, 49-57.
3. Boender, L.G.M., de Hulster, E.A.F., van Maris, A.J.A., Daran-Lapujade, P.A.S., Pronk, J.T., 2009. Quantitative Physiology of Saccharomyces cerevisiae at Near-Zero Specific Growth Rates. Appl. Environ. Microbiol. 75, 5607-5614.
4. Cardona, C.A., Sánchez, Ó.J., 2007. Fuel ethanol production: Process design trends and integration opportunities. Bioresour. Technol. 98, 2415-2457.
5. De Deken, R.H., 1966. The Crabtree Effect: A Regulatory System in Yeast. J. Gen. Microbiol. 44, 149-156.
6. Gaykawad, S.S., van der Wielen, L.A.M., Straathof, A.J.J., 2012. Effects of yeast-originating polymeric compounds on ethanol pervaporation. Bioresour. Technol. 116, 9-14.
7. Gaykawad, S.S., Zha, Y., Punt, P.J., van Groenestijn, J.W., van der Wielen, L.A.M., Straathof, A.J.J., 2013. Pervaporation of ethanol from lignocellulosic fermentation broth. Bioresour. Technol. 129, 469-476.
8. Groot, W.J., Kraayenbrink, M.R., van der Lans, R.G.J.M., Luyben, K.C.A.M., 1993. Ethanol production in an integrated fermentation/membrane system. Process simulations and economics. Bioprocess Eng. 8, 189-201.
9. Groot, W.J., Kraayenbrink, M.R., Waldram, R.H., van der Lans, R.G.J.M., Luyben, K.C.A.M., 1992. Ethanol production in an integrated process of fermentation and ethanol recovery by pervaporation. Bioprocess Biosystems Eng. 8, 99-111.
10. Heijnen, J.J., Terwisscha van Scheltinga, A.H., Straathof, A.J., 1992. Fundamental bottlenecks in the application of continuous bioprocesses. J. Biotechnol. 22, 3-20.
11. Herwig, C., von Stockar, U., 2002. Quantitative analysis of the oxidative metabolism in HXK2- and REG1-deletion mutants of Saccharomyces cerevisiae. Enzyme Microb. Technol. 31, 698-710.
12. Lipnizki, F., Hausmanns, S., Laufenberg, G., Field, R., Kunz, B., 2000. Use of Pervaporation-Bioreactor Hybrid Processes in Biotechnology. Chemical Engineering & Technology. 23, 569-577.
13. Nishiwaki, A., Dunn, I.J., 1998. Analysis of a two-stage fermentor with recycle for continuous ethanol production. Chem. Eng. Commun. 168, 207-227.

14. Nishiwaki, A., Dunn, I.J., 1999. Analysis of the performance of a two-stage fermentor with cell recycle for continuous ethanol production using different kinetic models. Biochem. Eng. J. 4, 37-44.

15. O'Brien, D.J., Craig Jr, J.C., 1996. Ethanol production in a continuous fermentation/membrane pervaporation system. Appl. Microbiol. Biotechnol. 44, 699-704.

16. van't Riet, K., Tramper, J., 1991. Basic bioreactor design. Marcel Dekker, Inc.

17. Van Hecke, W., Hofmann, T., De Wever, H., 2013. Pervaporative recovery of ABE during continuous cultivation: Enhancement of performance. Bioresour. Technol. 129, 421-429.

18. Van Hecke, W., Vandezande, P., Claes, S., Vangeel, S., Beckers, H., Diels, L., De Wever, H., 2012. Integrated bioprocess for long-term continuous cultivation of *Clostridium acetobutylicum* coupled to pervaporation with PDMS composite membranes. Bioresour. Technol. 111, 368-377.

19. Verduyn, C., Postma, E., Scheffers, W.A., van Dijken, J.P., 1990. Physiology of *Saccharomyces Cerevisiae* in Anaerobic Glucose-Limited Chemostat Culturesx. J. Gen. Microbiol. 136, 395-403.

Appendix: Mathematical model

The aim of the model is to predict the relation between recovered ethanol yield (y), productivity (P) and $C_{e,2}$ for realistic parameter settings.

Assumptions:

1. Order of MF and PV not fixed yet.

2. MF model: The feed is simply split in permeate with $C_x = 0$ and retentate with $C_x = C_{x,bleed}$.

3. PV model: The feed is simply split in permeate with $C_e = 1$ g.g^{-1} and retentate with $C_e = 0$.

4. Liquid flows leaving fermenter 1 contain virtually no O$_2$.

5. No ethanol formation or consumption in fermenter 1.

6. No maintenance in fermenter 1.

7. Negligible residual glucose in fermenter 2.

8. Negligible ethanol evaporation from fermenters and steady state operation.

9. No broth mass change because of reactions (i.e. gas phase is not considered).

10. Yeast molar composition per carbon: $CH_{1.8}N_{0.2}O_{0.5}$.

Balance equations:

Fermenter1 (liquid):

Yeast balance: Production + In = Out

$$\mu_1.C_{x,1}.M_1 + Q_{21}.C_{x,2} = Q_{12}.C_{x,1} \qquad \text{...(A1)}$$

Ethanol balance (if ethanol is not produced and consumed in fermenter 1):

$$Q_{21}.C_{e,2} = Q_{12}.C_{e,1} \qquad \text{...(A2)}$$

Glucose balance (assuming no glucose in Q_{21}):

$$Q_{feed}.C_{s,0} + q_{s,1}.C_{x,1}.M_1 = Q_{12}.C_{s,1} \qquad \text{...(A3)}$$

O$_2$ balance in liquid phase (assuming liquid flows contain virtually no O$_2$):

$$OTR.M_1 = -q_{O_2}.C_{x,1}.M_1 \qquad \text{...(A4)}$$

48

Total mass balance:

$$Q_{feed} + Q_{21} = Q_{12} \qquad \qquad ...(A5)$$

Fermenter 2 (including retentate liquid):

Glucose balance (assuming complete conversion of glucose in fermenter 2):

$$Q_{12}.C_{s,1} = -q_{s,2}.C_{x,2}.M_2 \qquad \qquad ...(A6)$$

Yeast balance:

$$Q_{12}.C_{x,1} + \mu_2.C_{x,2}.M_2 = Q_{21}.C_{x,2} + Q_{bleed}.C_{x,bleed} \qquad ...(A7)$$

Ethanol balance (amount of ethanol entering and leaving with

Q_{12} and Q_{21} cancel each other due to assumption of no ethanol

production in fermenter1):

$$q_{e,2}.C_{x,2}.M_2 = Q_{PV} + Q_{bleed}.C_{e,bleed} \qquad \qquad ...(A8)$$

Total mass balance:

$$Q_{12} = Q_{21} + Q_{pv} + Q_{out} + Q_{bleed} \qquad \qquad ...(A9)$$

Besides equation A1 to A9 we can have additional equations as:

$$\mu_1 = Y_{sx\max,1}.(-q_{s,1}) \qquad \qquad ...(A10)$$

$$q_{s,1} = q_{s\max,1}\left(1 - \frac{C_{e,1}}{C_{e\max}}\right) \qquad \qquad ...(A11)$$

$$-q_{s,2} = \frac{\mu_2}{Y_{sx\max,2}} + m_{s,2} \qquad \qquad ...(A12)$$

$$q_{s,2} = \frac{q_{s\max,2}.C_{s,2}}{C_{s,2} + K_s}.\left(1 - \frac{C_{e,2}}{C_{e\max}}\right) \qquad \qquad ...(A13)$$

$$Y_{se,2} = \frac{q_{e,2}}{-q_{s,2}} \qquad \qquad ...(A14)$$

$$\mu_2 = \mu_{\max,1}.\left(1 - \frac{C_{e,2}}{C_{e\max,x}}\right) \qquad \qquad ...(A15)$$

We have 15 independent equations with 18 unknown parameters. There are 10 unknown parameters that are scale-independent (μ_1, μ_2,

$q_{s,1}$, $q_{s,2}$, $q_{e,2}$, $C_{x,1}$, $C_{e,1}$, $C_{e,2}$, $C_{s,1}$, $C_{s,2}$) and 8 unknown parameters that are scale dependent (M_1, M_2, Q_{feed}, Q_{12}, Q_{pv}, Q_{21}, Q_{bleed}, Q_{out}). By fixing one of the latter, the scale is fixed. We choose Q_{pv} = 1 kg·h⁻¹.

The system of equations was solved algebraically using symbolic software. The resulting solutions are given in Figure 2.5 and Table 2.2, where $C_{e,2}$ and recovered yield were the degrees of freedom. Since there are two more unknown parameters than equations, there are two degrees of freedom.

Parameter used:

Table 2.3. Parameters used in the model.

Parameters	Values	Unit	Source
OTR_{max}	0.0016	kg·kg⁻¹·h⁻¹	(van'tRiet and Tramper, 1991)
$m_{s,2}$	0.66	kg·kg⁻¹·h⁻¹	(Boender et al., 2009b)
$q_{s\,max,2}$	-3.4	kg·kg⁻¹·h⁻¹	(Groot et al., 1992b)
K_s	0.0002	kg·kg⁻¹	(Groot et al., 1992b)
$C_{e\,max}$	0.096	kg·kg⁻¹	(Groot et al., 1992b)
$q_{O_2\,max}$	-0.256	kg·kg⁻¹·h⁻¹	(Herwig and von Stockar, 2002)
$Y_{se,2}$	0.42	kg·kg⁻¹	(Groot et al., 1992b)
$Y_{sx\,max,1}$	0.44	kg·kg⁻¹	(Herwig and von Stockar, 2002)
$\mu_{max,1}$	0.25	h⁻¹	(Herwig and von Stockar, 2002)
$Y_{sx\,max,2}$	0.096	kg·kg⁻¹	(Groot et al., 1992b)
$C_{e\,max,x}$	0.078	kg·kg⁻¹	(Groot et al., 1992b)
$C_{s,0}$	0.3	kg·kg⁻¹	Fermenter setting
$C_{x,2}$	0.1	kg·kg⁻¹	Fermenter setting
$C_{x,bleed}$	0.2	kg·kg⁻¹	Fermenter setting
Q_{pv}	1	kg	Fermenter setting
$q_{s\,max,1}$	-0.5682	kg·kg⁻¹·h⁻¹	Calculated

Chapter 3

Effects of yeast–originating polymeric compounds on ethanol pervaporation

Abstract

During ethanol fermentation with in–situ pervaporation, membrane fouling might occur due to polymers originating from yeast cell lysis. The aim of this study was to evaluate the influence of yeast cellular polymers on pervaporative membrane performance. Lipids were identified as the most detrimental component among these cellular polymers causing 50% and 33% flux decrease in polydimethylsiloxane (PDMS) and polyoctylmethylsiloxane (POMS) membranes, respectively. This fouling was irreversible and might be due to hydrophobic interactions between lipids and membranes resulting in high lipid adsorption on membrane surface. The relatively hydrophobic model protein BSA also contributed to flux decrease in PDMS membrane but RNA and the model polysaccharide glycogen did not. The PDMS membrane selectivity for ethanol/water remained ~4.5 in all cases. All the cellular components decreased the water flux through the POMS membrane. However, the ethanol flux through the membrane was not altered very much, resulting in increased membrane selectivity.

Keywords: Cellular polymers (bio–polymers), membrane fouling, membrane flux, selectivity, pervaporation.

3.1. Introduction

Among the different biofuels, bioethanol is widely used as a fuel oxygenates and is believed to be an alternative renewable fuel to gasoline (Cardona and Sánchez, 2007a; Vane, 2005b). The concentration of bioethanol blended into gasoline ranges from 5% to 85% (v.v^{-1}) and varies from country to country (Mustafa, 2011). This application of bioethanol as a transportation fuel leads to a worldwide increase in its production. Great efforts are being undertaken to improve ethanol productivity and minimize the overall production cost. To do so, different possibilities are explained in literature (Cardona and Sánchez, 2007a; Vane, 2005b). One of the ways to achieve these goals is to modify the process configuration and perform process integration.

Commercially, the recovery of ethanol from fermentation broth is dominated by distillation. For low ethanol feed concentrations (<5 wt.%) and small production scale, however, distillation is not economical and energy efficient (O'Brien et al., 2000b; Vane, 2005b). Alternative recovery processes are listed in the literature. Among these processes, pervaporation is suggested as viable option due to its potentially lower energy consumption and simplicity of operation requiring no additional chemicals (Chovau et al., 2011b; O'Brien et al., 2000b). Pervaporation may also be applied to the separation of other volatile organic compounds such as biobutanol (Claes et al., 2012; Dobrak et al., 2010; Fadeev et al., 2000; Yen et al., 2012). Industrial applicability of pervaporation (hydrophilic and hydrophobic) in bioethanol production is discussed in the literature (Jonquières et al., 2002; Vane, 2008).

Coupling ethanol fermentation and pervaporation has been explored by many researchers (Groot et al., 1992a; O'Brien and Craig Jr, 1996a; Shabtai et al., 1991a). This integration enables continuous operation while maintaining an ethanol concentration in the fermentation broth below inhibitory levels but still achieving an ethanol rich outlet stream (Lipnizki et al., 2000a). However, industrial applicability of pervaporation coupled directly with fermentation is limited by fouling of the membranes.

The common ethanol fermentation is performed by *Saccharomyces cerevisiae*. Most of the fouling studies done so far address the effects of unconverted sugars and excreted metabolites such as acetic acid, succinic acid, glycerol on membrane performance during pervaporation

(Aroujalian et al., 2006; Chovau et al., 2011b; García et al., 2009a; Nomura et al., 2002). For fermentation integrated with pervaporation, viability of the cells decreases with time due to the accumulation of non–volatile by–products and cell aging (Nakao et al., 1987a). This cell lysis causes release of cellular components in the fermentation broth. Detailed studies of lysis of *S. cerevisiae* have been performed using retentostat cultures where the cell viability decreased by 13% after 22 days resulting in an increase in extracellular proteins (Boender et al., 2009a). In Clostridial fermentation coupled with pervaporation, FT–IR analysis of fouled membrane demonstrated the presence of carbohydrates, proteins and amino acids on the membrane (Liu et al., 2011). Hence from these studies we can conclude that, in an integrated system, potential candidates for fouling, present in fermentation broth are cellular polymers such as proteins, lipids, polysaccharides and nucleic acids (RNA and DNA).

The influence of fatty acids on membrane performance has been reported by some researchers (Fadeev et al., 2000; Offeman and Ludvik, 2011), but a systematic study determining the effect of cellular polymeric components on pervaporative membrane performance is still missing.

Hence, the objective of this research is to evaluate the effects of these cellular polymers on the membrane performance. Identification of the biopolymers responsible for membrane fouling and quantifying their effects will indicate how to avoid this fouling. Also, this study will be useful when the suitability is evaluated of a pervaporation as cell retention method in addition to its use as ethanol recovery method.

3.2. Materials and Methods

3.2.1 Membranes

Commercially available membranes were investigated. PDMS (polydimethylsiloxane) was obtained from Pervatech BV (Enter, The Netherlands), and POMS (polyoctylmethylsiloxane) was supplied by GKSS (Germany).

3.2.2 Cellular polymers

As actual cellular polymers present in *S. cerevisiae* cells are laborious to extract and purify, commercially available cellular polymers

were examined during this research. The types of representative bio–polymers analyzed here are given in Table 3.1 and all of them were of analytical grade purity.

Table 3.1. Types of representative synthetic cellular polymers investigated.

Cellular polymer	Represented by	Product code#
Proteins	BSA	A2153
	Lysozyme	L6876
Lipids (triglyceride)	Glyceryl trioleate	T7140
Phospholipid	1,2 dipalmitoyl–sn–glycero–3–phosphocholine	P0763
RNA	RNA from *Torula* yeast	R6625
Polysaccharides	Glycogen from bovine liver	G0885

= Supplier: Sigma–Aldrich Chemie BV.

3.2.3 Water contact angle measurement

The change in hydrophobicity of the membranes was examined by measuring the water contact angles of unused and of fouled membranes. The membrane samples were dried at 70 °C for 24 h. A water drop was put on the active surface of the membrane and the contact angle was measured by using FM40 Easy Drop goniometer (Krüss GmbH, Germany) at room temperature with droplet size controlled using a Gilmont syringe. At least five measurements were done per membrane sample.

3.2.4 Ethanol concentration analysis

Ethanol concentrations in the feed and in permeate were determined using a refractometer (CONVEX, CETI, Belgium). Calibration at 21 °C gave a linear relation between refractive index and ethanol concentration in the range of 2.5–30 wt.%. The amount of ethanol added to the feed was used in selectivity and flux calculations. Some of these feed and permeate samples were analyzed by gas chromatography (Interscience; HP-INNOWAX column 30 m × 0.25 mm, column at 70 °C; injection temp. 200 °C; detector temp. 250 °C, detector: FID, carrier gas: Helium, and injection volume: 0.5 µL) to confirm the ethanol concentrations derived from refractometer, and then used for calculations. The ethanol concentrations obtained from

refractometer were within the error range (6%) of that derived from gas chromatography.

3.2.5 Pervaporation

A custom made flat–sheet pervaporation unit was used with an effective membrane cross–sectional area of 50 cm². Feed solution (1 kg) was prepared in a 1 L glass bottle and maintained at 30 °C. The feed was circulated over the membrane through Norprene® tubing (Masterflex 06404–18, Norprene®, Saint Gobain, France) at a flow rate of 905 g·min⁻¹ using a peristaltic pump (Masterflex console drive) so as to obtain a Reynolds No. of 5700 (turbulent flow). A constant vacuum of 10 mbar on the permeate side was maintained by a vacuum pump (SC920, KNF, Germany) and permeate was collected alternatively in two parallel glass flasks kept in cryostats at -14 °C (RMS 6, LAUDA, Germany) and -20 °C (RE 307, LAUDA, Germany).

The base case experiments were carried out using pure ethanol-water solution with either 3 or 5 wt.% of ethanol. As the proteins are sensitive to salts present in the solution and pH, the base case and regular experiments with proteins were carried out by mimicking a fermentation medium and maintaining the pH of the solution at 5 by addition of 2 mol·L⁻¹ KOH. The mimicked fermentation medium also contained $(NH_4)_2SO_4$ (0.3 g·L⁻¹), $NH_4H_2PO_4$ (3 g·L⁻¹), KH_2PO_4 (4 g·L⁻¹) and $MgSO_4·7H_2O$ (0.7 g·L⁻¹).

RNA from Torula yeast is not soluble in water at room temperature. To dissolve this RNA, the measured quantity of water was heated at 70–75 °C. The required ethanol was added to the mixture after cooling down to room temperature, and before starting experiments a make–up amount for evaporated water was added. Similarly, the lipids were first dissolved in the required quantity of ethanol (5 or 3 wt.%) and then added to the water.

The permeate samples were collected after each 60–120 min and the mass amount of total permeate W_p was determined by weighing the flasks. The total flux through the membrane J_{Total} was calculated using Equation (3.1):

$$J_{Total} = \frac{W_p}{A_m \cdot t} \qquad (3.1)$$

where A_m represents the effective membrane area (m²) and t indicates the permeate collection time (h).

The mass fractions of ethanol and water w_i^p in permeate were calculated on the basis of the ethanol concentration in the permeate, and the partial fluxes of the individual components J_i were evaluated using Equation (3.2):

$$J_i = J_{Total} \cdot w_i^p \qquad (3.2)$$

The separation performances of the membranes were compared on the basis of the selectivity α_{EtOH, H_2O} as defined by Equation (3.3):

$$\alpha_{EtOH, H_2O} = \frac{(w_{EtOH} / w_{H_2O})^p}{(w_{EtOH} / w_{H_2O})^f} \qquad (3.3)$$

w_{EtOH} and w_{H_2O} represent the mass fractions of ethanol and water, and superscripts *p* and *f* denote the permeate and feed side, respectively.

3.3. Results and discussion

3.3.1 Base case pervaporation experiments

Base case experiments were performed, three for PDMS and two for POMS membrane, differing in the feed ethanol concentration and presence of medium components. These base case experiments were considered as a reference for experiments with added polymers.

With PDMS membrane, solutions with 5 wt.% of ethanol were used as base case for RNA and polysaccharide and 3 wt.% for lipids. A solution containing 3 wt.% of ethanol including medium components was treated as base case for protein. Similarly, for POMS membrane, solutions of 5 wt.% of ethanol with and without medium components were the base case. Also, it was checked that the feed ethanol concentrations did not change in the course of experiments. The performance of the membranes for base cases is summarized in Table 3.2 and was comparable to literature data (Chovau et al., 2011b; Lee et al., 2012).

Table 3.2. Membrane performance in pervaporation for the base cases; temperature 30 °C.

		Ethanol conc.	Total flux	Partial fluxes		Selectivity
				EtOH	Water	
		wt.%	$g·m^{-2}·h^{-1}$	$g·m^{-2}·h^{-1}$	$g·m^{-2}·h^{-1}$	
PDMS	Base case	5	747 ± 24	143 ± 7	604 ± 19	4.5 ± 0.1
	Base case	3	689 ± 7	82 ± 1	607 ± 7	4.4 ± 0.1
	Base case – Medium	3	633 ± 16	76 ± 2	557 ± 14	4.4 ± 0.0
POMS	Base case	5	235 ± 13	55 ± 5	180 ± 8	5.7 ± 0.2
	Base case – Medium	5	220 ± 2	53 ± 2	168 ± 4	5.9 ± 0.3

Using PDMS membrane, the total flux dropped with decrease in feed ethanol concentration from 5 to 3 wt.%. The effect of reduction in ethanol concentration by 40% was seen on ethanol flux which declined by 40% whereas water flux and ethanol/water selectivity remained unchanged. Similar results have been reported by Favre et al. (1996), who claimed that for dilute aqueous solution (0–10 wt.% alcohol concentration) the water flux remained constant whereas the alcohol flux increased linearly with increasing alcohol concentration.

The effect of salts on the membrane flux was clearly visible for PDMS membrane, resulting in further decrease in the flux. As the percentage decrease in partial fluxes was the same as that of the total flux, the selectivity was unaffected, and it can be concluded that no salting out effect occurs. Plausible reasons for flux decrease might be partial pore blocking of the membrane, penetration of salts into the membrane or concentration polarization at the membrane surface caused by high concentration of hydrates formed as stated in literature (Lipnizki et al., 2004). Even though the effect of individual salts on membrane performance has been studied before (Favre et al., 1996; Lipnizki et al., 2004), the combined effect of these salts on the membrane is still unexplored. So, it is not possible to decide what the exact mechanism is for flux reduction by salts.

For the POMS membrane, the decrease due to medium components was lower for the ethanol flux (3%) than for the water flux (7%), but the resulting increase in selectivity was not very high and was within the standard deviation.

3.3.2 Influence of cellular polymers (bio–polymers) on membrane performance

The types and quantities of the bio-polymers used in this study were determined on the basis of the measured average mass fraction of cellular composition for *S. cerevisiae* CEN.PK 113–7D (Lange and Heijnen, 2001), a cell dry weight concentration of 10 g·L^{-1} obtained in a fermentation with this strain integrated with pervaporation (results not shown), and the 20% cell non–viability observed for the same strain at comparable conditions in retentostat cultures (Boender et al., 2009a). The final concentrations used during experiments were rounded off for the ease of measurements and are listed in Table 3.3.

Table 3.3. Mass fraction of cellular polymers present in the yeast cells and concentrations used in this study. (Mass fractions calculated here were mass of cellular polymer per cell dry mass).

Cellular polymer	Mass fraction %	Average %	For 2 g yeast g·L^{-1}	Typical conc. used g·L^{-1}
Proteins	40 – 46	42.2	0.8 – 0.92	0.75
Lipids	7 – 10	8.6	0.14 – 0.2	0.25
RNA	4 – 8	4.5 – 8	0.08 – 0.16	0.25
Polysaccharide	30 – 45	39	0.6 – 0.9	0.75
DNA	0.5	0.5	0.01	Not considered

The cellular polymers listed in Table 3.1 were selected on the basis of premises made for composition of *S. cerevisiae* in literature (Lange and Heijnen, 2001) except for the proteins. The range of proteins present in this yeast varies widely. To reduce the complexity of experiments, some standard proteins commonly applied in biotechnology (BSA and lysozyme) were considered here. The polysaccharide present in yeast mainly consists of glycogen, mannan, chitin and insoluble glucans. Out of these polysaccharides, glycogen, which acts as a storage material in yeast, was studied (Trevelyan and Harrison, 1956).

3.3.2.1 Proteins

The PDMS membrane performance was tested against BSA, using concentrations of 0.5 and 0.9 g·L^{-1}, and 0.5 g·L^{-1} of lysozyme. The average pervaporation fluxes are shown in Table 3.4. They slightly decrease with increasing BSA concentration. For lysozyme, the fluxes slightly increased from the base case but not significantly. Furthermore, it was observed that the selectivity of the membrane was not affected by any of these proteins and was the same as for the base case (Table 3.4).

In case of the POMS membrane, BSA and lysozyme slightly decreased the average total fluxes (Table 3.4). Surprisingly, it was observed that in the presence of BSA the ethanol flux increased by 7 %. This resulted in a higher membrane selectivity. On the contrary, using lysozyme, the total and partial fluxes decreased by the same percentage causing no change in membrane selectivity compared to the base case.

The fouling of microfiltration and ultrafiltration membranes by different proteins including BSA and lysozyme has been investigated in many studies (Güell et al., 1999; Huisman et al., 2000; Kelly and Zydney, 1997; Marshall et al., 1993). The mechanisms responsible for membrane fouling by proteins suggested in this literature include van der Waals forces, electrostatic interactions, hydrophobic interactions, and hydrogen bonding. Here, the probable explanation for flux decline might be due to adsorption of BSA on membrane surface by hydrophobic interaction. The average hydrophobicity (Unit: cal·res.$^{-1}$), calculated from its amino acid sequence, was found to be much higher for BSA (1120) than for lysozyme (970) (Bigelow, 1967). The net charge on BSA and lysozyme at the experimental condition (pH = 5), obtained from titration curves (Nfor et al., 2010), was found to be almost the same. Thus, the inherent hydrophobicity plays an important role in adsorption of these proteins.

Table 3.4. Performance parameters obtained for pervaporation with cellular polymers using different membranes: temperature 30 °C. The fluxes listed are the average values and errors shown here are the standard deviations, both calculated over the period of the experiment. The values given are rounded off to next significant number.

		Polymer conc. $g\cdot L^{-1}$	Ethanol conc. wt.%	Total flux $g\cdot m^{-2}\cdot h^{-1}$	Partial fluxes EtOH flux $g\cdot m^{-2}\cdot h^{-1}$	Water flux $g\cdot m^{-2}\cdot h^{-1}$	Selectivity
PDMS	Base case	0	5	747 ± 24	143 ± 7	604 ± 19	4.5 ± 0.1
	RNA	0.25	5	730 ± 9	134 ± 4	596 ± 8	4.3 ± 0.1
	Polysaccharide	0.75	5	712 ± 11	136 ± 2	576 ± 11	4.5 ± 0.1
	Base case	0	3	689 ± 7	82 ± 1	607 ± 7	4.4 ± 0.1
	Glyceryl	0.1	3	535 ± 29	58 ± 4	477 ± 26	4.0 ± 0.2
	trioleate	0.265	3	355 ± 53	43 ± 7	312 ± 47	4.5 ± 0.3
	Phospholipid	0.05	3	617 ± 20	72 ± 5	545 ± 20	4.3 ± 0.3
	Base case – Medium	0	3	633 ± 16	76 ± 2	557 ± 14	4.4 ± 0.0
	BSA	0.5	3	595 ± 27	74 ± 6	521 ± 21	4.6 ± 0.3
		0.9	3	589 ± 13	72 ± 1	517 ± 13	4.5 ± 0.1
	Lysozyme	0.5	3	655 ± 15	80 ± 3	574 ± 18	4.5 ± 0.3
POMS	Base case	0	5	235 ± 13	55 ± 5	180 ± 8	5.7 ± 0.2
	RNA	0.25	5	186 ± 6	47 ± 5	139 ± 2	6.4 ± 0.7
	Polysaccharide	0.75	5	192 ± 6	49 ± 6	143 ± 0	6.5 ± 0.8
	Glyceryl trioleate	0.25	5	157 ± 6	40 ± 3	117 ± 3	6.5 ± 0.4
	Base case – Medium	0	5	220 ± 2	53 ± 2	167 ± 4	6.0 ± 0.3
	BSA	0.75	5	205 ± 6	57 ± 0	148 ± 6	7.3 ± 0.3
	Lysozyme	0.75	5	208 ± 2	48 ± 4	160 ± 3	5.7 ± 0.6

Another possibility might be the deposition of large protein aggregates on membrane followed by chemical attachment of native proteins on growing deposit through intermolecular disulphide linkages as experienced by Kelly and Zydney (1997) for microfiltration. The formation of large protein aggregates depends on the presence of free thiol (–SH) and disulphide (S–S) groups in proteins which participate in thiol oxidation and thiol–disulphide interchange reactions resulting in formation of intermolecular disulphide linkage. BSA contains one –SH and 17 S–S groups, thus forming large aggregate structures which might be responsible for the fouling of the PDMS and POMS membranes. The possibility of such aggregate formation in lysozyme is very small as it contains four S–S groups and has no –SH group (Kelly and Zydney, 1997). Indeed, membrane fouling effects by lysozyme were less severe using either membrane type. Additional research will be required to determine the exact mechanism of pervaporative membrane fouling by proteins.

3.3.2.2 Polysaccharide

Glycogen affected the performance of both membrane types, although the extent of flux decrease was different. The total flux decreased by 4% when using PDMS membrane and by 18% when using POMS (Table 3.4). The partial flux and total flux decreased by the same percentage so the selectivity remained the same when using PDMS. But using POMS membrane, glycogen affected the water flux thereby increasing the ethanol concentration in the permeate. This increased ethanol concentration led to a higher selectivity but the standard deviation was also high.

Initial properties of POMS membrane were restored after overnight washing of the membrane with water at 30 °C. So, the probable reason for flux decrease might be weak adsorption of the glycogen on the membrane surface.

3.3.2.3 RNA

The reduction in the total flux caused by RNA was very small when using PDMS membrane (Table 3.4), that is within the standard deviation of base case, and it can be neglected. Consequently, the selectivity hardly varied. However, RNA caused a total flux decrease of

20% for POMS membrane. Here also, as observed with glycogen, the water flux suffered more than the ethanol flux. This led to a higher selectivity than in the base case but standard deviations were also high.

3.3.2.4 Lipids

The performance of PDMS membrane has been tested for two categories of lipids, namely triglyceride (glyceryl trioleate), and a phospholipid from the choline family, whereas POMS membrane was checked only against triglyceride. From the results achieved (Table 3.4), it was evident that both the triglyceride and phospholipids foul the PDMS membrane. Almost 50% of the initial flux decrease was observed using only 0.265 g·L^{-1} of glyceryl trioleate. The adsorption of lipids resulting from strong hydrophobic interaction between lipids and membranes was the probable cause for this huge flux decline. After the experiments, regeneration of the membrane was tried by washing with 70% (v·v^{-1}) ethanol but the initial properties were not regained. Comparable results were found by Fadeev et al., (2000) who tested Na–palmitate and Na–stearate against a PTMSP membrane causing more than 90% flux decline. They were also unable to regenerate the membrane after several washings with deionized water (Fadeev et al., 2000). Similar performance reduction in PDMS membrane was found using 8% oleic acid (Offeman and Ludvik, 2011). However, we have no indication of the occurrence of such concentrations of free fatty acids or their salts during ethanol fermentation (Lange and Heijnen, 2001).

For the POMS membrane tested here, the flux reduction was about 33% using 0.25 g·L^{-1} of trioleate (Table 3.4). Surprisingly, despite this decrease in the flux, the selectivity increased, which might be due to increased hydrophobicity of membrane caused by lipid adsorption on the membrane, resulting in a lower water flux through the membrane.

3.3.2.5 Combined effect of all cellular components on PDMS membrane

The combined effects of all cellular polymers on PDMS membrane was evaluated by sequential addition of individual components to an ethanol–water–medium mixture. Total fluxes and selectivities achieved using these components are mentioned in Figure 3.1. The time axis

indicates time elapsed starting with the base case (5 wt. % ethanol) experiment, but the experiment was not running continuously.
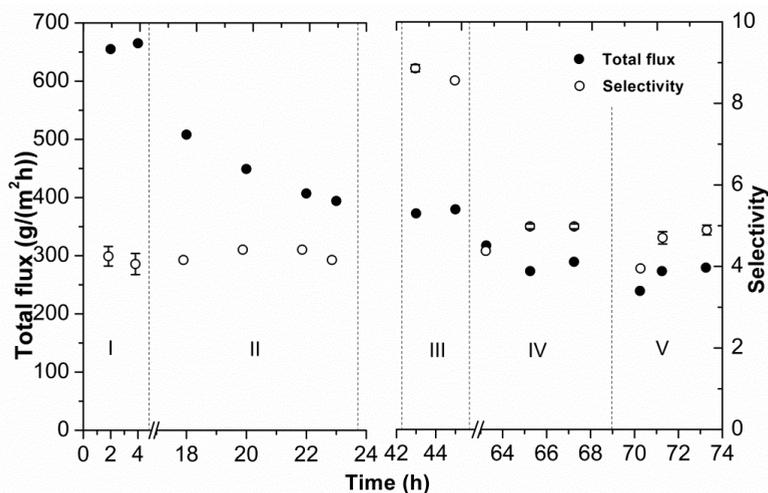
Figure 3.1. Total flux and selectivity resulting from the combined effect of all cellular polymers on PDMS membrane. I: Pervaporation (PV) carried out with base case (5 wt.% ethanol and medium components); II: PV of base case mixture with lipid and RNA; III: PV of base case after cleaning the membrane with 70% (v·v-1) ethanol; IV: PV of base case with lipid, RNA and BSA; V: PV of base case with lipid, RNA, BSA and glycogen.

The cellular polymers tested at the beginning were glyceryl trioleate and RNA (section II) due to their specific solubility requirements (mentioned Section 3.2.5). An initial drop in flux was observed which increased further with time. A 40% flux decrease relative to the base case (section I) was found, which is comparable to the results obtained using trioleate alone (Table 3.4). The medium components present in the feed might also contribute to this flux decrease, but it is assumed that the flux reduction is mainly due to trioleate and that RNA does not play any role. After finishing this part of the experiment, regeneration of the membrane was tried by overnight washing of the membrane with 5 wt.% ethanol–water mixture followed by circulating 70% (v·v-1) ethanol over the feed side of the membrane. After this membrane cleaning, the base case experiment (5 wt.% ethanol) was repeated but the results show (section III) that the total flux was not recovered and was the same as that obtained at the end of

experiment with lipid and RNA. This indicates that the membrane fouling caused by trioleate was not reversed.

The fluxes obtained after regeneration were considered as reference for further experiments. A make–up amount for pervaporated ethanol was added to ensure 5 wt.% of ethanol concentration in the feed solution. BSA was the next component added to this mixture containing lipid and RNA, which further decreased the flux (section IV). The flux reduction at the end of this experiment was about 24%, which is larger than in the experiment with BSA alone. This might be due to protein-protein and protein–lipid interactions. The formation of large protein aggregates (by the mechanism explained above) and hydrophobic interactions between adsorbed lipids and proteins might result in increased adsorption of protein leading to huge fouling. Furthermore, glycogen was added to the mixture containing lipid+RNA+BSA and a make–up amount for the pervaporated ethanol was added again. No further reduction in the flux was observed (section V). Hence glycogen did not foul the membrane even in presence of the other cellular components.

The membrane selectivity remained constant during the lipid+RNA experiment (section II), which indicates that ethanol and water fluxes decreased by the same extent. However, after the washing (section III) selectivity almost doubled as compared to the base case. This might be the consequence of membrane swelling due to washing with 70% $(v \cdot v^{-1})$ ethanol and removal of this ethanol, trapped inside the membrane. Hence, these higher selectivities observed after washing (section III) can be considered to be an artefact. This behaviour diminished when the experiment was further performed with BSA. The selectivity obtained with BSA (section IV) was slightly higher than in the base case. This indicates that BSA in the presence of lipid and RNA decrease the water flux through the membrane resulting in increased selectivity. The selectivity remained the same, as that obtained with BSA, in the presence of glycogen (section V).

The water contact angle, which is an indicator of hydrophobicity, was measured for membranes used with different cellular polymers and is listed in Table 3.5. The contact angle for membranes used in experiments with trioleate, phospholipids and all cellular polymers was not higher than that of fresh membrane even though these compounds

are hydrophobic. A significant change in water contact angle was observed with the membrane used for BSA whereas for the membranes used for other polymers, the contact angle was within the standard deviation of that for the fresh membrane. Hence, in this case the water contact angle is not representative of change in surface properties of the membranes and cannot be correlated to decrease in the flux.

Table 3.5. Water contact angle determined for pervaporation carried out using PDMS and POMS membranes for various conditions.

Membrane	Conditions	Water contact angle (º)
PDMS	Fresh	113 ± 5
	Used for PV with BSA	104 ± 0
	Used for PV with trioleate	114 ± 3
	Used for PV with phospholipid	107 ± 2
	All cellular polymers	111 ± 3
POMS	Fresh	115 ± 2
	Used for PV with trioleate	113 ± 2

To prevent this membrane fouling, several possibilities have been proposed in literature, in particular the use of a pre–pervaporation solid–liquid separation device, the selection of module design and operation conditions, and the immobilization of cells (Lipnizki et al., 2000a; Vane, 2005b). Additional options to minimize the membrane fouling include adsorption of fouling components using cheap and easily regenerable hydrophobic adsorbent before pervaporation; membrane surface modification or pre–coating of membrane with some functional groups that can adsorb the fouling components while maintaining the membrane properties intact; and developing efficient membrane cleaning methods. However, the most important option is to minimise the concentration of cellular polymers in the fermentation broth by reducing the cell lysis. This can be achieved by reducing the shear stress on cells, by strain selection or by fermentation medium engineering. Detailed investigation is necessary to address this issue.

Irreversible fouling of the PDMS membrane was also observed in an integrated fermentation–pervaporation experiment. The question is if living yeast cells contribute to fouling. Living yeast cells do not excrete cellular polymers except for some glycosylated enzymes such as invertase. These will be hydrophilic. The outer cell wall of yeast consists

of polysaccharide-protein complex (Moradas-Ferreira et al., 1994). The cell surface hydrophobicity is influenced by process parameters such as pH, medium composition and cell growth phase, and might result in flocculation of the cells (Kamada and Murata, 1984). If the yeast cell surface would be hydrophobic, adsorption of cells on the membrane might occur.

But during the integration experiment, such yeast cell flocculation and adsorption on membrane surface was not observed. The effects of living yeast cells, their surface hydrophobicity and flocculation properties on the membrane performance in pervaporation needs more detailed research and is out of the scope of this study.

The membranes tested need to be hydrophobic in order to be selective for the target product (ethanol) as compared to water, but consequently they are susceptible to fouling by hydrophobic components such as lipids.

3.4. Conclusions

The fluxes in PDMS and POMS membranes dropped severely in the presence of lipids. Hydrophobic interaction between membrane and lipids resulting in higher adsorption of lipids might cause fouling.

Proteins were observed to be the next most important fouling component for PDMS. The total flux in PDMS decreased with increasing BSA concentration whereas lysozyme did not affect the membrane. Also, the effects of glycogen and RNA on PDMS membrane were insignificant. The selectivity of PDMS membrane remained unchanged.

POMS membranes, being more hydrophobic than PDMS, were found to be more susceptible to fouling by all bio–polymers.

Acknowledgement

References:

1. Aroujalian, A., Belkacemi, K., Davids, S.J., Turcotte, G., Pouliot, Y., 2006. Effect of residual sugars in fermentation broth on pervaporation flux and selectivity for ethanol. Desalination. 193, 103-108.

2. Bigelow, C.C., 1967. On the average hydrophobicity of proteins and the relation between it and protein structure. J. Theor. Biol. 16, 187-211.

3. Boender, L.G.M., de Hulster, E.A.F., van Maris, A.J.A., Daran-Lapujade, P.A.S., Pronk, J.T., 2009. Quantitative Physiology of *Saccharomyces cerevisiae* at Near-Zero Specific Growth Rates. App. Environm. Microbiol. 75, 5607-5614.

4. Cardona, C.A., Sánchez, Ó.J., 2007. Fuel ethanol production: Process design trends and integration opportunities. Bioresour. Technol. 98, 2415-2457.

5. Chovau, S., Gaykawad, S., Straathof, A.J.J., Van der Bruggen, B., 2011. Influence of fermentation by-products on the purification of ethanol from water using pervaporation. Bioresour. Technol. 102, 1669-1674.

6. Claes, S., Vandezande, P., Mullens, S., De Sitter, K., Peeters, R., Van Bael, M.K., 2012. Preparation and benchmarking of thin film supported PTMSP-silica pervaporation membranes. J. Membr. Sci. 389, 265-271.

7. Dobrak, A., Figoli, A., Chovau, S., Galiano, F., Simone, S., Vankelecom, I.F.J., Drioli, E., Van der Bruggen, B., 2010. Performance of PDMS membranes in pervaporation: Effect of silicalite fillers and comparison with SBS membranes. Journal of Colloid and Interface Science. 346, 254-264.

8. Fadeev, A.G., Meagher, M.M., Kelley, S.S., Volkov, V.V., 2000. Fouling of poly[-1-(trimethylsilyl)-1-propyne] membranes in pervaporative recovery of butanol from aqueous solutions and ABE fermentation broth. J. Membr. Sci. 173, 133-144.

9. Favre, E., Nguyen, Q.T., Bruneau, S., 1996. Extraction of 1-butanol from aqueous solutions by pervaporation. J. Chem. Technol. Biotechnol. 65, 221-228.

10. García, M., Sanz, M.T., Beltrán, S., 2009. Separation by pervaporation of ethanol from aqueous solutions and effect of other components present in fermentation broths. J. Chem. Technol. Biotechnol. 84, 1873-1882.

11. Groot, W.J., Kraayenbrink, M.R., Waldram, R.H., Lans, R.G.J.M., Luyben, K.C.H.A.M., 1992. Ethanol production in an integrated process of fermentation and ethanol recovery by pervaporation. Bioproc. Biosys. Eng. 8, 99-111.

12. Güell, C., Czekaj, P., Davis, R.H., 1999. Microfiltration of protein mixtures and the effects of yeast on membrane fouling. J. Membr. Sci. 155, 113-122.

13. Huisman, I.H., Prádanos, P., Hernández, A., 2000. The effect of protein–protein and protein–membrane interactions on membrane fouling in ultrafiltration. J. Membr. Sci. 179, 79-90.

14. Jonquières, A., Clément, R., Lochon, P., Néel, J., Dresch, M., Chrétien, B., 2002. Industrial state-of-the-art of pervaporation and vapour permeation in the western countries. J. Membr. Sci. 206, 87-117.

15. Kamada, K., Murata, M., 1984. On the mechanism of brewer's yeast flocculation. Agric. Biol. Chem. 48, 2423-2433.

16. Kelly, S.T., Zydney, A.L., 1997. Protein fouling during microfiltration: Comparative behavior of different model proteins. Biotechnol. Bioeng. 55, 91-100.

17. Lange, H.C., Heijnen, J.J., 2001. Statistical reconciliation of the elemental and molecular biomass composition of *Saccharomyces cerevisiae*. Biotechnol. Bioeng. 75, 334-344.

18. Lee, H.-J., Cho, E.J., Kim, Y.-G., Choi, I.S., Bae, H.-J., 2012. Pervaporative separation of bioethanol using a polydimethylsiloxane/polyetherimide composite hollow-fiber membrane. Bioresour. Technol. 109, 110-115.

19. Lipnizki, F., Hausmanns, S., Field, R.W., 2004. Influence of impermeable components on the permeation of aqueous 1-propanol mixtures in hydrophobic pervaporation. J. Membr. Sci. 228, 129-138.

20. Lipnizki, F., Hausmanns, S., Laufenberg, G., Field, R., Kunz, B., 2000. Use of Pervaporation-Bioreactor Hybrid Processes in Biotechnology. Chem. Eng. Technol. 23, 569-577.

21. Liu, G., Wei, W., Wu, H., Dong, X., Jiang, M., Jin, W., 2011. Pervaporation performance of PDMS/ceramic composite membrane in acetone butanol ethanol (ABE) fermentation–PV coupled process. J. Membr. Sci. 373, 121-129.

22. Marshall, A.D., Munro, P.A., Trägårdh, G., 1993. The effect of protein fouling in microfiltration and ultrafiltration on permeate flux, protein retention and selectivity: A literature review. Desalination. 91, 65-108.

23. Moradas-Ferreira, P., Fernandes, P.A., Costa, M.J., 1994. Yeast flocculation—the role of cell wall proteins. Colloids Surf. B. Biointerfaces. 2, 159-164.

24. Mustafa, B., 2011. Production of bioethanol from lignocellulosic materials via the biochemical pathway: A review. Energy Convers. Managem. 52, 858-875.

25. Nakao, S.-i., Saitoh, F., Asakura, T., Toda, K., Kimura, S., 1987. Continuous ethanol extraction by pervaporation from a membrane bioreactor. J. Membr. Sci. 30, 273-287.

26. Nfor, B.K., Noverraz, M., Chilamkurthi, S., Verhaert, P.D.E.M., van der Wielen, L.A.M., Ottens, M., 2010. High-throughput isotherm determination and thermodynamic modeling of protein adsorption on mixed mode adsorbents. J. Chromatogr. A. 1217, 6829-6850.

27. Nomura, M., Bin, T., Nakao, S.-i., 2002. Selective ethanol extraction from fermentation broth using a silicalite membrane. Sep. Purif. Technol. 27, 59-66.

28. O'Brien, D.J., Craig Jr, J.C., 1996. Ethanol production in a continuous fermentation/membrane pervaporation system. Appl. Microbiol. Biotechnol. 44, 699-704.

29. O'Brien, D.J., Roth, L.H., McAloon, A.J., 2000. Ethanol production by continuous fermentation–pervaporation: a preliminary economic analysis. J. Membr. Sci. 166, 105-111.

30. Offeman, R.D., Ludvik, C.N., 2011. Poisoning of mixed matrix membranes by fermentation components in pervaporation of ethanol. J. Membr. Sci. 367, 288-295.

31. Shabtai, Y., Chaimovitz, S., Freeman, A., Katchalski-Katzir, E., Linder, C., Nemas, M., Perry, M., Kedem, O., 1991. Continuous ethanol production by immobilized yeast reactor coupled with membrane pervaporation unit. Biotechnol. Bioeng. 38, 869-876.

32. Vane, L.M., 2005. A review of pervaporation for product recovery from biomass fermentation processes. J. Chem. Technol. Biotechnol. 80, 603-629.

33. Vane, L.M., 2008. Separation technologies for the recovery and dehydration of alcohols from fermentation broths. Biofuels, Bioproducts and Biorefining. 2, 553-588.

34. Yen, H.-W., Chen, Z.-H., Yang, I.K., 2012. Use of the composite membrane of poly(ether-block-amide) and carbon nanotubes (CNTs) in a pervaporation system incorporated with fermentation for butanol production by *Clostridium acetobutylicum*. Bioresour. Technol. 109, 105-109.

Chapter 4

Pervaporation of ethanol from lignocellulosic fermentation broth

Abstract

Pervaporation can be applied in ethanol production from lignocellulosic biomass. Hydrophobic pervaporation, using a commercial PDMS membrane, was employed to concentrate the ethanol produced by fermentation of lignocellulosic hydrolysate. To our knowledge, this is the first report describing this. Pervaporation carried out with three different lignocellulosic fermentation broths reduced the membrane performance by 17–20% as compared to a base case containing only 3 wt.% ethanol in water. The membrane fouling caused by these fermentation broths was irreversible. Solutions containing model lignocellulosic components were tested during pervaporation at the same conditions. A total flux decrease of 12–15%, as compared to the base case, was observed for each component except for furfural. Catechol was found to be most fouling component whereas furfural permeated through the membrane and increased the total flux. The membrane selectivity increased in the presence of fermentation broth but remained unchanged for all selected components.

Keywords: Lignocellulosic biomass, fermentation broth, pervaporation, membrane fouling, membrane flux.

4.1. Introduction

Bioethanol is used as renewable transportation fuel (Mustafa, 2011). However, the bioethanol production process can still be improved a lot. Different alternatives, based on process design and process integration, have been suggested by researchers (Brethauer and Wyman, 2010; Cardona and Sánchez, 2007b; Huang et al., 2008).

The cost and availability of the feedstock are crucial. The feedstock cost contributes 65–70% to the total ethanol production costs (Balat and Balat, 2009; Kazi et al., 2010). The current feedstocks used for bioethanol production are derivatives from food crops such as corn grain and sugar cane. However, these raw materials are insufficiently available to meet the increasing demand for fuels and their use raises major nutritional and ethical issues (Brethauer and Wyman, 2010; Mustafa, 2011). These facts lead to the quest for cheaper, abundant and non–food competitive feedstocks for bioethanol production. Lignocellulosic biomass, being renewable and abundant in nature, is an attractive option for the production of biofuel and is being explored by many researchers (Delgenes et al., 1996; Larsson et al., 2000; Mustafa, 2011). It mainly consists of all kinds of waste including agriculture residues, municipal solid waste, forest residues and paper waste. The use of lignocellulosic biomass will not only affect feedstock pretreatment and fermentation process of the ethanol production but also the downstream processing.

Ethanol recovery from fermentation broth is traditionally done by distillation. But for dilute ethanol streams (less than 5 wt.%), the high energy requirements in distillation (Madson and Lococo, 2000) has forced the study of more energy efficient technologies. Among these techniques, pervaporation has been studied by many researchers (Vane, 2008). To recover low concentrations of ethanol from fermentation, pervaporation may be economically more feasible than distillation (O'Brien et al., 2000b; Vane, 2005b). It is known that the achievable ethanol concentration in lignocellulosic fermentations is usually below 5 wt.% (Olsson and Hahn-Hägerdal, 1996). Therefore, we will explore in this paper pervaporation for ethanol recovery from lignocellulosic fermentation broth.

The steps involved in bioethanol production process from lignocellulosic feedstock include biomass pretreatment, cellulose

73

hydrolysis, fermentation and ethanol separation and purification. A block diagram for lignocellulosic ethanol fermentation process with pervaporation as an ethanol recovery step along with distillation is shown in Figure 4.1 (modified from Cardona and Sánchez (2007b)).
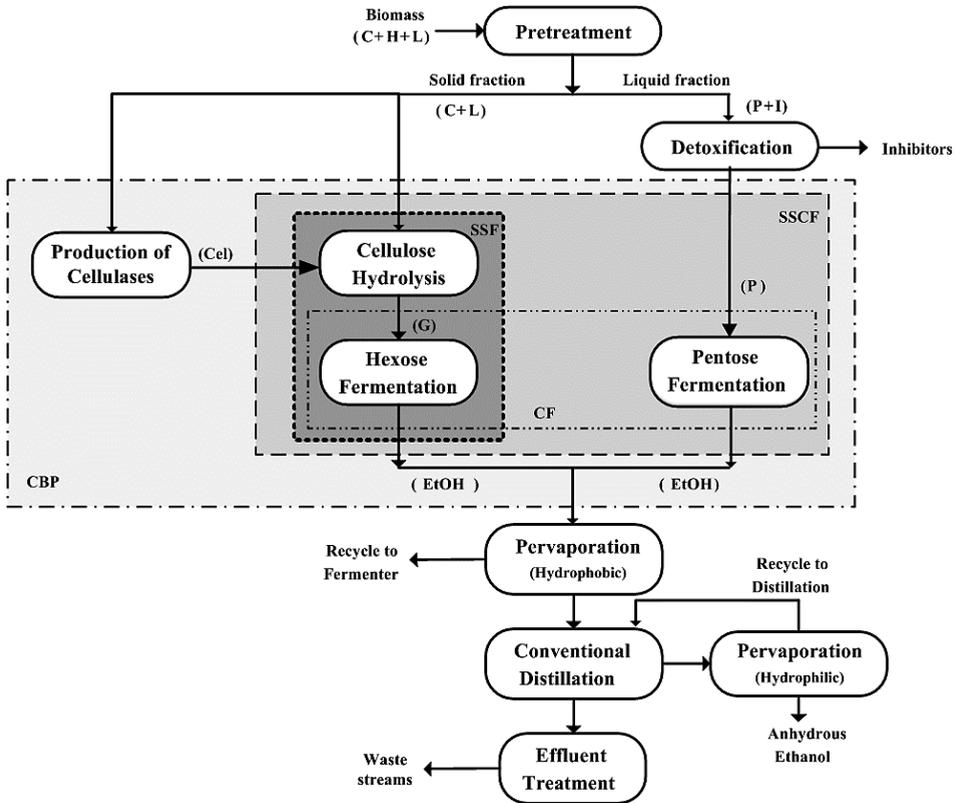
Figure 4.1. Potential application of pervaporation in ethanol production process from lignocellulosic biomass; C-cellulose; H-hemi-cellulose; L-lignin; P-pentose; I-inhibitors; G-glucose; EtOH-ethanol; Cel-cellulases; CF-co-fermentation; SSF-simultaneous saccharification and fermentation; SSCF-simultaneous saccharification and co-fermentation; CBP-consolidated bioprocessing; modified from Cardona and Sánchez (2007b).

The ethanol from fermentation broth can be concentrated, depending on the membrane selectivity, by using hydrophobic pervaporation before feeding it to distillation. This should reduce the energy load on the distillation. Similarly, the remaining 5 wt.% of water from the top product of distillation can be removed by hydrophilic

pervaporation to achieve fuel grade (anhydrous) ethanol (>99.5 wt.%). Here we focus on the ethanol recovery from lignocellulosic fermentation broth by hydrophobic pervaporation.

The breakdown of lignocellulosic biomass by pretreatment and the fermentation of the resulting sugars leads to a variety of by–products (Almeida et al., 2007; Klinke et al., 2004). The nature and concentration of the pretreatment by–products depends on the lignocellulosic feedstock type and pretreatment method (Klinke et al., 2004; Zha et al., 2012). These by–products are mainly divided into carboxylic acids, furans and phenolics (Almeida et al., 2007; Palmqvist and Hahn-Hägerdal, 2000a; Palmqvist and Hahn-Hägerdal, 2000b) and may threat the pervaporation membrane performance. These components were selected from the literature and are listed in Table 4.1 with their respective concentrations. Concentration ranges mentioned here (Table 4.1) are inhibitory to the yeast cells.

Table 4.1. Cell inhibitory concentration of lignocellulosic compounds derived from literature.

Compound	Conc. (g·L^{-1})	Micro–organism
Furfural	0.5[a]	*S. cerevisiae* CBS 1200[†]
5–HMF[#]	~ 1[a]	*S. cerevisiae* CBS 1200[†]
4–Hydroxybenzaldehyde	0.75[a]	*S. cerevisiae* CBS 1200[†]
Vanillin	0.5[a]	*S. cerevisiae* CBS 1200[†]
Syringaldehyde	~ 0.75[a]	*S. cerevisiae* CBS 1200[†]
Catechol	1[b]	*S. cerevisiae* Baker's yeast[‡]
Acetate	10 [a]	*S. cerevisiae* CBS 1200[†]

[a] = The concentration of compounds given here causes ~50% growth reduction.
[b] = The stated concentration causes ~20% growth reduction.
[#] = 5-htdroxymethylfurural.
[†] = Reference : Delgenes et al., 1996.
[‡] = Reference : Larsson et al., 2000.

Thus, the aim of this research is to test if pervaporation can be done for lignocellulosic ethanol and to investigate effects of lignocellulosic biomass fermentation by–products on membrane performance for the recovery of ethanol by using pervaporation. PDMS membrane, being commonly used in lab practice and widely applied

commercially, was tested here. This study evaluates the effects of real fermentation broths and selected model components on pervaporative membrane performance. The effects of feedstock used and pretreatment method applied, on the membrane properties was also explored.

4.2. Materials and Methods

4.2.1 Membrane

Pervaporation experiments were performed using a commercially available PDMS (polydimethylsiloxane) membrane obtained from Pervatech BV (Enter, The Netherlands). The membranes used were from lots 030705–1109S PV (membrane 1, 2, 3, 4, 5, 6) and 030705–1001S PV (membrane 7).

4.2.2 Lignocellulosic fermentation broths

Three different types of lignocellulosic fermentation broths, listed in Table 4.2, were prepared.

4.2.2.1 Preparing lignocellulosic biomass hydrolysates

Barley straw and willow wood were purchased from Oostwaardshoeve, The Netherlands. They were pre–dried at 80 °C for 5 h when received, and stored at room temperature in air–tight bags. Before using, the biomass was ground to pieces with average length of 3 mm and dried again for at least 16 h.

Barley straw hydrolysate was prepared according to the concentrated acid and mild alkaline methods, while willow wood chips hydrolysate was prepared according to the mild alkaline method. The details of these methods are described in Zha et al. (2012). For concentrated acid method, the dried biomass was impregnated in 72% H_2SO_4 at room temperature for 24–48 h, followed by 2 steps of hydrolysis with 40% and 15% H_2SO_4, at 60 °C and 95 °C, respectively. For mild alkaline method, the dried biomass was impregnated with 3% $Ca(OH)_2$ at 80 °C for 3–5 days, followed by enzymatic hydrolysis with Accellerase 1500 (Genencor).

4.2.2.2 Hydrolysate batch fermentation

The strain used was *Saccharomyces cerevisiae* CEN.PK113–7D (CBS 8340). To prepare a pre–culture, glycerol stock of the strain was inoculated into a shake flask with 100 mL mineral medium (Van Hoek et al., 1998), and cultivated at 30 °C, 200 rpm, for 20 h. An inoculum was prepared by harvesting the cells from a 50 mL preculture and re–suspending the cells in 50 mL hydrolysate. Together with inoculum, 2 mL Tween 80–ergosterol stock solution was added to the fermenter. The Tween 80–ergosterol stock contained 5 $g \cdot L^{-1}$ ergosterol and 210 $g \cdot L^{-1}$ Tween 80 in 95% aqueous ethanol. Barley straw and willow wood chips hydrolysates were fermented in 2 L New Brunswick fermenters, with working volume of 1 L. After sterilization at 121 °C, the fermenter was connected to the console and filled with 950 mL filter–sterilized hydrolysate. The fermentation temperature was set at 30 °C, pH at 5.0 by adding 2 $mol \cdot L^{-1}$ KOH or 1 $mol \cdot L^{-1}$ H_2SO_4, dissolved oxygen at 0 by continuous flushing 0.5 $L \cdot min^{-1}$ N_2. The fermentation was monitored by continuously measuring the CO_2 percentage in the off–gas. The fermentation was considered finished when the CO_2 percentage value remained 0 for 10 h. The optical density, glucose and ethanol concentrations of the fermentation samples were determined using ROCHE Cobas Mira Plus. The details of these measurements are described in Zha et al. (2012).

4.2.2.3 Conditioning of fermentation broth

Conditioning of the fermentation broths was done according to Offeman and Ludvik (2011). The broth vessels were stored at -20 °C. Before carrying out the pervaporation experiment, the broth was thawed, centrifuged (MULTISTAGE 1 S–R, Heraeus Instruments, Germany) at 4 °C and at 4700 rpm for 10 min to remove yeast cells and solids. The supernatant was decanted and re–centrifuged at 4 °C and at 4700 rpm for 45 min, then filtered using membrane filter paper (Supor®– 450, 47 mm, 0.45 μm, PALL, USA) to remove low density solids. The filtrate was sampled and analyzed for ethanol content by gas chromatography (GC). Ethanol was added to achieve 3 wt.% in the broth, and the pervaporation experiments were performed.

4.2.3 Ethanol concentration analysis

Ethanol concentrations in the feed and in permeate were determined by using a refractometer (CONVEX, CETI, Belgium). During calibration at 21 °C, a linear relation was observed between refractive index and ethanol concentration in the range of 2.5–30 wt.%. The amount of ethanol added to the feed was used in selectivity and flux calculations. Some of these feed and permeate samples were analysed by GC (Interscience; HP–INNOWAX column 30 m × 0.25 mm, column at 70 °C; injection temperature 200 °C; detector 250 °C, detector: FID, carrier gas: Helium, and injection volume: 0.5 μL) to confirm the ethanol concentrations derived from the refractometer, and then used for calculations. The ethanol concentrations obtained from the refractometer were within 6% from the concentrations measured by GC.

4.2.4 Lignocellulosic fermentation broth and permeate analysis

Selected model components (Table 4.1) were analyzed by High Performance Liquid Chromatography (HPLC) (Waters 2695 system). A Zorbax 3.5 μm SB–C18 column (4.6 × 75 mm) and diode array detector set at 254 nm were used. A linear gradient of acetonitrile in KH_2PO_4–buffer (50 mM, pH 2, 1% $v·v^{-1}$ acetonitrile), as the eluent, was applied increasing from 0% to 25% in 10 min at a flow of 1.2 mL·min^{-1}.

Table 4.2. Lignocellulosic fermentation broths. The ethanol concentrations provided (without brackets) are measured after conditioning of the fermentation broth whereas those given in brackets () are measured directly after fermentation. The ethanol mass yields were calculated on the basis of the ethanol concentration given in brackets and the initial glucose concentration. The final glucose concentration was close to zero.

Broth type	Biomass	Pretreatment method	Initial glucose conc. (g·L^{-1})	Ethanol conc. (g·L^{-1})	Ethanol mass yield (%)
F–9	Barley straw	Concentrated acid	67.5	21.7 (31.1)	46.0
F–12	Willow wood chips	Mild alkaline	23.5	8.7 (11.1)	47.2
F–13	Barley straw	Mild alkaline	42.6	13.3 (18.5)	43.5

4.2.5 Pervaporation experiment

A custom made flat–sheet pervaporation unit was used with an effective membrane cross-sectional area of 50 cm². Feed solution (1 kg) was prepared in a 1 L glass bottle and maintained at 30 °C. The feed was circulated over the membrane through Norprene® tubing (Masterflex 06404–18, Saint Gobain, France) at a flow rate of 905 g·min⁻¹ by using a peristaltic pump (Masterflex console drive) so as to have a Reynolds No. of 5700 (turbulent flow). A constant vacuum of 10 mbar on the permeate side was maintained by a vacuum pump (SC920, KNF, Germany) and permeate was collected alternatively in two parallel glass flasks kept in cryostats at -14 °C (RMS 6, LAUDA, Germany) and -20 °C (RE 307, LAUDA, Germany).

The membrane was equilibrated, before performing the pervaporation experiment, by circulating 3 wt.% ethanol–water solution for at least 12 h. The base case experiments were carried out using 3 wt.% of ethanol in water. The pervaporation experiments were carried out using the different fermentation broths with ethanol concentration make–up to 3 wt.%. After the pervaporation experiments, the system was washed with water for 30 min followed by cleaning with 70% (v·v⁻¹) ethanol in water for at least 3 h. Then the membrane was again equilibrated overnight with 3 wt.% ethanol–water solution. The permeation using 3 wt.% ethanol was performed after this cleaning step to check whether the membrane properties had been restored.

Similarly, the pervaporation experiments with model fermentation broth components were carried out with 1 g·L⁻¹ of individual components in 3 wt.% ethanol–water solution.

Permeate samples were collected after each 60–120 min and the mass amount of total permeate W_p was determined by weighing the flasks. The total flux through the membrane J_{Total} was calculated using Equation (4.1):

$$J_{Total} = \frac{W_p}{A_m \cdot t} \tag{4.1}$$

where A_m represents the effective membrane area (m²) and t indicates the permeate collection time (h). The total flux reported here was the average from 3 h and 5 h samples.

The mass fraction of water w_i^p in permeate was calculated from the mass fraction of ethanol in permeate measured using the refractometer and the assumption that no other compounds were present. The partial fluxes of individual components J_i were evaluated using Equation (4.2):

$$J_i = J_{Total} \cdot w_i^p \tag{4.2}$$

The separation performances of the membranes were compared on the basis of the selectivity α_{EtOH,H_2O}. As feed and retentate compositions will be virtually identical at our conditions, we can apply Equation (4.3) to calculate membrane selectivity.

$$\alpha_{EtOH,H_2O} = \frac{(w_{EtOH}/w_{H_2O})^p}{(w_{EtOH}/w_{H_2O})^f} \tag{4.3}$$

where w_{EtOH} and w_{H_2O} represent the mass fractions of ethanol and water, and superscripts p and f denote the permeate and feed side, respectively. At the conditions used, retentate and feed composition were virtually identical.

4.3. Results and discussion

4.3.1 Pervaporation with lignocellulosic fermentation broth

Three types of fermentation broths, based on different feedstocks and pretreatment methods, are listed in Table 4.2. It can be seen that different pretreatment methods lead to different fermentation performance, even when the biomass type was the same, in this case barley straw (Figure 4.2 A–C). As far as the glucose concentration was concerned, it seems that concentrated acid was a better method than mild alkaline, especially when wood was used as feedstock. However, by comparing the fermentation results of the three hydrolysates, it was noticed that the concentrated acid method gave a longer lag-phase, though the overall ethanol yields were similar (Table 4.2). The ethanol concentration in barley straw–concentrated acid fermentation reached 30 g·L^{-1} after around 30 h, which was the highest among the three fermentations.
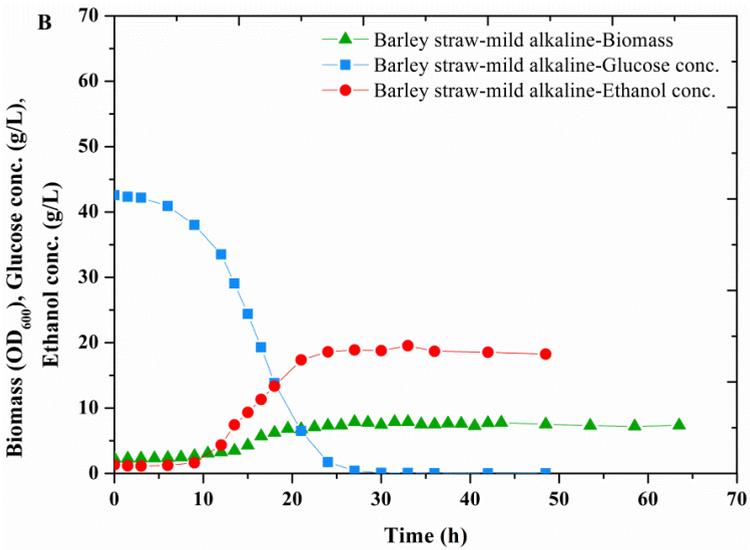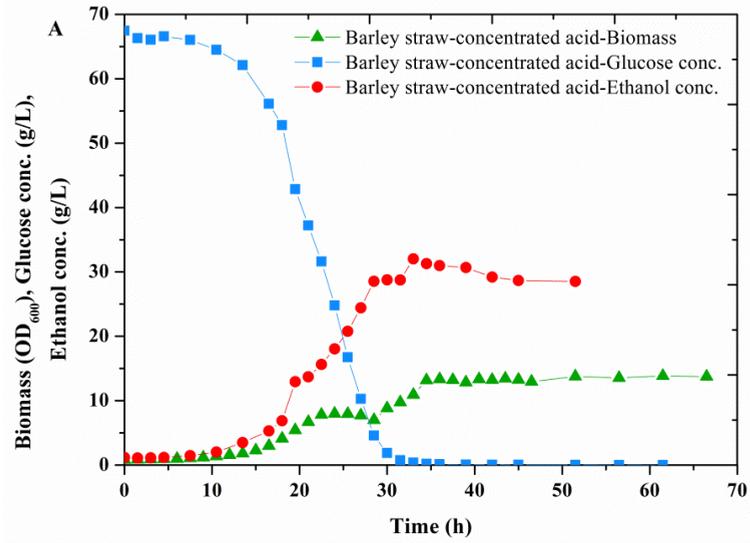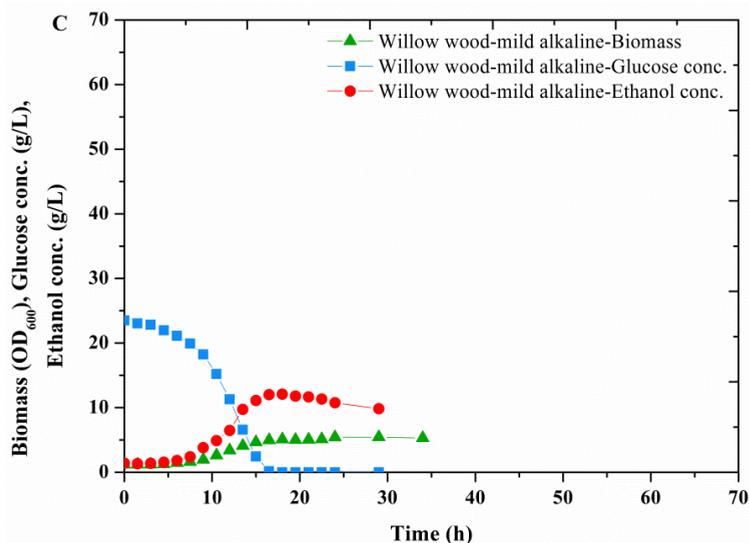
Figure 4.2. Biomass (OD$_{600}$), Glucose (g·L^{-1}) and Ethanol (g·L^{-1}) concentration profiles for fermentation of different lignocellulosic hydrolysate: A-Barley straw pretreated with concentrated acid; B-Barley straw pretreated by mild alkaline method and C-Willow wood chips pretreated by mild alkaline method.

It can be seen from Table 4.2, that the ethanol concentration varies with feedstock and pretreatment method. So, for the ease of comparison, the ethanol concentration was made up to 3 wt.% in each broth before carrying out a pervaporation experiment. At the actual ethanol concentration in the broth, being lower than the make–up concentration, the results would be different.

The pervaporation experiments were carried out with individual broths. The recovery of ethanol from lignocellulosic fermentation broth was achieved successfully for first time in literature and the results obtained are given in Table 4.3.

A variation in total flux was observed for each fresh membrane due to the fact that the PDMS membranes used were not identical. A total flux decrease of 19%, 20% and 17%, compared to the fresh membrane flux using 3 wt.% ethanol was found using F–9, F–12 and F–13 broth types, respectively. The water flux suffered more than the ethanol flux in all cases. Thus, the membrane selectivities achieved using broths were higher than in the respective base cases using 3 wt.% ethanol. The base case experiments performed after membrane cleaning partly restored the water flux but not the ethanol flux. For broth F–13,

the ethanol flux decreased even further. Consequently, washing with 70% (v·v^{-1}) ethanol was not effective.

In another experiment performed with F–13 broth, the membrane was cleaned with isopropanol in addition to the regular washing step (described in Section 4.2.5). A total flux decrease of 20%, compared to the base case, was observed (results not shown). A base case experiment after this membrane cleaning showed a total flux increase by 14% compared to that obtained with membrane fouled by F–13 broth. Thus, the cleaning with isopropanol improved the membrane performance as compared to that achieved upon cleaning by 70% (v·v^{-1}) ethanol, but complete regeneration of the membrane was not attained. Hence we can conclude that for all the fermentation broths tested (Table 4.3) and with the cleaning methods used here, the membrane fouling was irreversible.

4.3.2 Pervaporation with model fermentation components
4.3.2.1 Identification and selection of model lignocellulosic components

The common components present in lignocellulosic hydrolysate and fermentation broth can be divided into carbohydrates (unconverted sugars), cellular polymers released due to cell lysis, pretreatment/hydrolysis by–products, excreted metabolites and antifoam used during fermentation. The carbohydrates should be converted into fermentation products such as ethanol in this case. Pretreatment/hydrolysis by–products can be further divided into carboxylic acids, furanics and phenolics. The weak acids are acetic acid and formic acid; the main furanics are furfural and 5–hydroxymethylfurfural (5–HMF) whereas phenolics contain a wide range of compounds. The effects of unconverted sugars (glucose, xylose), cellular polymers and weak acids (acetic acid, formic acid) on the membrane performance have been already investigated (Chovau et al., 2011a; Gaykawad et al., 2012). Thus, only furanics and phenolic compounds were tested here.

Table 4.3. Pervaporation results with lignocellulosic fermentation broth using PDMS membrane: temperature 30 °C. The fluxes listed are the average values and errors shown here are the standard deviations, both calculated over the period of the experiment.

Membrane no.	Membrane condition	Feed containing 3 wt.% ethanol	Total flux $(g \cdot m^{-2} \cdot h^{-1})$	Partial fluxes EtOH flux $(g \cdot m^{-2} \cdot h^{-1})$	Water flux $(g \cdot m^{-2} \cdot h^{-1})$	Selectivity
1	Fresh	Water	704 ± 11	75 ± 2	628 ± 9	3.9 ± 0.1
	Used	F–9	567 ± 1	65 ± 1	502 ± 0	4.2 ± 0.1
	Used and washed	Water	622 ± 7	67 ± 1	555 ± 6	3.9 ± 0.1
2	Fresh	Water	624 ± 0	75 ± 0	549 ± 0	4.4 ± 0.0
	Used	F–12	498 ± 3	64 ± 1	434 ± 4	4.8 ± 0.1
	Used and washed	Water	545 ± 13	60 ± 1	485 ± 14	4.0 ± 0.2
3	Fresh	Water	646 ± 4	64 ± 1	581 ± 3	3.6 ± 0.1
	Used	F–13	533 ± 13	69 ± 2	464 ± 11	4.8 ± 0.0
	Used and washed	Water	504 ± 4	39 ± 0	465 ± 0	2.7 ± 0.0

The presence of these components (Table 4.3) in tested fermentation broths was confirmed by HPLC analysis and their approximate concentrations are given in Table 4.4. These concentrations are much lower than values given in literature, except for acetic acid. This is possibly due to the different feedstocks and pretreatment methods used. It should also be noticed that the concentrations of these compounds shown in literature are in hydrolysates (before fermentation), while the values measured in this study are in fermentation broth. It is known that during fermentation process, compounds such as furfural and vanillin are converted (Delgenes et al., 1996), which could be the reason for the concentration differences shown in Table 4.4. Also, a difference between ethanol concentration directly after fermentation and after conditioning of fermentation broth (Table 4.2) due to freezing, thawing, centrifugation and transportation involved (mentioned in Section 4.2.2) suggests that these factors might also be responsible for an additional difference between the concentrations of the selected components in the pervaporation feed and hydrolysate.

Table 4.4. Model lignocellulosic component's concentrations.

Compound	Conc. in hydrolysate (g·L^{-1})		Approximate conc. (g·L^{-1}) in fermentation broths[g]		
	Willow wood[f]	Barley straw[f]	F–9	F–12	F–13
Furfural	0.5[a]	2.88[c]	0.002	0.01	0.002
5–HMF	0.14[a]	0.996[c]	0.004	0.008	0.014
4–Hydroxy benzaldehyde	0.01[b]	[d]	0.002	0.006	0.018
Vanillin	0.43[b]	0.106[c]	0.002	0.004	0.026
Syringaldehyde	[d]	[d]	[e]	0.042	1.236
Catechol	[d]	[d]	0.720	0.05	0.054
Acetic acid	2.2[a]	[d]	2.04	5.43	4.75

[a] = Acid hydrolysis pretreatment;
[b] = Dilute acid pretreatment;
[c] = Acid steam pretreatment;
[d] = not available;
[e] = not detected;
[f] = Zha et al. (2012).
[g] = this study.

4.3.2.2 Pervaporation with selected lignocellulosic components

The concentration of components in the hydrolysate varies with the feedstock and pretreatment method used and can be seen in Table 4.4. No general composition of the hydrolysate can be found in literature. The lignocellulosic components concentration used in this study is based on the inhibitory concentration of the selected components found in the literature (Table 4.1), being a value that should not be exceeded as a result of pretreatment.

For the ease of experiment and comparison, experiments were carried out with 1 g·L^{-1} of each component in 3 wt.% ethanol–water solution. The effects of individual components on membrane performance are shown in Table 4.5 and are discussed below.

4.3.2.2.1 5–HMF

The pervaporation carried out with 5–HMF decreased the water flux by 7% as compared to the base case. The ethanol flux remained within the standard deviation and so did the membrane selectivity.

4.2.2.2.2 Furfural

In presence of the furfural, the total flux increased by 9% compared to the base case. The furfural increased the ethanol flux through the membrane by 20%. This increased ethanol flux results in a higher selectivity because the water flux increased only slightly (by 7%).

The furfural permeated through the PDMS membrane and the permeate concentration obtained was 4.3 g·L^{-1} (data not shown). This gives a furfural flux of 3.2 g·m^{-2}·h^{-1} (Table 4.5) and membrane selectivity for furfural/water of 6.8. Application of pervaporation for furfural separation can be found in the literature. Ghosh et al. (2010) used modified polyurethaneurea (PUU) membranes for separation of furfural from aqueous solution and obtained a flux of 41.5 g·m^{-2}·h^{-1} and a furfural separation factor of 284. In a similar study, Sagehashi et al. (2007) used pervaporation for the separation of phenol and furfural from superheated steam pyrolysis derived aqueous biomass solution. The maximum furfural flux, 2.2 g·m^{-2}·h^{-1}, using PDMS membrane, was obtained at 120 °C whereas the maximum enrichment factor, approximately 65, was achieved at 60 °C. Thus, pervaporation can be

potentially applied in ethanol fermentation process and at the same time for furfural removal from fermentation.

4.3.2.2.3 Vanillin

In the presence of vanillin the total flux decreased by 14% compared to the base case (Table 4.5). The water and ethanol fluxes decreased by the same percentage and the ethanol selectivity remained unchanged.

The separation of vanillin from fermentation media by pervaporation has been reported recently by Brazinha et al. (2011). The effects of porous support and downstream pressure on vanillin recovery were evaluated for a POMS–PEI membrane. It was observed that the permeated vanillin solidified immediately due to its high melting point. A similar phenomenon has been stated by Böddeker et al. (1997) using a PEBA membrane for vanillin recovery from fermentation broth.

In our experiments, we used a PDMS membrane and a lower feed vanillin concentration (1 g·L^{-1}) compared to the aforementioned studies. Permeation of vanillin was not detected and would not have been overlooked in our case.

4.3.2.2.4 4–Hydroxybenzaldehyde

Pervaporation carried out with 4–hydroxybenzaldehyde reduced the total flux by 12% and the same percentage decrease was found for the water flux (Table 4.5).

Pervaporation of benzaldehyde from fermentation broth was performed by Lamer et al. (1996). They observed two fold decrease in flux with actual fermentation broth, as compared to a model medium, using PDMS/(PAN+PE) composite membrane. On the other hand, using homogeneous PDMS membrane the flux was improved.

In our study, after cleaning/washing, the membrane properties were regained in this case. During the pervaporation and regeneration experiments, only the water flux decreased and increased, respectively, while the ethanol flux remained unaffected (Table 4.5). From these results, we can conclude that the membrane fouling by 4–hydroxybenzaldehyde was reversible.

Table 4.5. Performance parameters obtained for pervaporation with model lignocellulosic fermentation broth compounds using PDMS membrane: temperature 30 °C; Solute concentrations were 1 g·L^{-1} in 3 wt.% aqueous ethanol. The fluxes listed are the average values and errors shown here are the standard deviations, both calculated over the period of the experiment.

Membrane no.	Solute in 3 wt.% ethanol feed	Experiment Title	Total flux (g·m^{-2}h^{-1})	Partial fluxes		Selectivity EtOH/Water	Flux (g·m^{-2}·h^{-1}) of lignocellulosic component
				EtOH flux (g·m^{-2}·h^{-1})	Water flux (g·m^{-2}·h^{-1})		
7	None	Base case	685 ± 8	89 ± 3	596 ± 8	4.9 ± 0.2	0
	5–HMF	PV exp.	638 ± 16	81 ± 8	557 ± 15	4.7 ± 0.5	0
	furfural	PV exp.	747 ± 20	107 ± 6	637 ± 18	5.4 ± 0.3	3 ± 0
	vanillin	PV exp.	588 ± 4	74 ± 3	514 ± 4	4.7 ± 0.2	0
4	None	Base case	635 ± 1	67 ± 1	568 ± 1	3.8 ± 0.0	0
	4–hydroxy benzaldehyde	PV exp.	561 ± 6	62 ± 2	499 ± 7	4.0 ± 0.2	0
	None	After washing	652 ± 6	64 ± 1	588 ± 6	3.5 ± 0.1	0
5	None	Base case	584 ± 15	57 ± 2	527 ± 16	3.5 ± 0.2	0
	catechol	PV exp.	497 ± 70	51 ± 6	446 ± 65	3.7 ± 0.1	0
6	None	Base case	577 ± 9	51 ± 2	526 ± 11	3.1 ± 0.2	0
	syringaldehyde	PV exp.	503 ± 2	46 ± 1	457 ± 2	3.3 ± 0.0	0
	None	After washing	593 ± 7	57 ± 1	536 ± 8	3.3 ± 0.1	0

4.3.2.2.5 Catechol and syringaldehyde

Catechol decreased the total flux gradually. Almost 22% of initial flux decline was observed within 6 h after the beginning of the pervaporation experiment (data not shown). The results given in Table 4.5, for catechol, are average fluxes calculated over the samples taken at 5 and 6 h of pervaporation experiment and therefore the standard deviation for the total flux is very high. The water flux suffered more than the ethanol flux and decreased by the same percentage as the total flux. The membrane fouling was irreversible instead of applied cleaning methods.

For syringaldehyde, the total flux decreased by 13% compared to the base case. The water flux was affected by the same percentage whereas the ethanol flux decreased slightly less as compared to the base case. The membrane properties were regained back after washing with 70% (v·v^{-1}) ethanol. Hence fouling caused by syringaldehyde was reversible.

In both the cases the membrane selectivity remained unchanged.

4.3.3 General discussion

For all tested components, except furfural, a total flux decrease of 12–15% as compared to the base case was observed. The percentage decrease in the flux by actual fermentation broth is comparable to the decrease in the flux caused by model components. This might be coincidental, as the concentration of tested components was much higher than in literature. The sum of decrease in the flux caused by individual components was much higher than that found with fermentation broths. This might be due to the concentration difference between the components that present in the broth and that in synthetic feed. Moreover, in the fermentation broth, there are many components present in addition to the ones tested here and these might also influence the permeation. Also, the effects achieved were with individual components and their combined effect, as in fermentation broth, was not evaluated.

Higher selectivities compared to base case were observed in presence of all the fermentation broths. This effect might be due to the presence of large number of hydrophobic components in broth resulting in larger reduction in water flux than in ethanol flux. Also, the

experiments with synthetic components were performed without the addition of matrix of hydrolysate and fermentation medium components. So, the effect of these components in combination with broth components on membrane performance still needs to be explored. Selectivity was found to remain unchanged in presence of all model components except furfural.

The actual fermentation broth contains many more components as confirmed by unidentified peaks in HPLC analysis of F–9 fermentation broth (data not shown). Hence, the tested model components are only representative and are not sufficient to compare the results achieved with fermentation broth. The fouling caused by fermentation broth might be due to the synergistic effect of different components present in the broth.

The fouling of the membrane might be caused by adsorption of these components on the membrane surface. Hydrophobic interaction of the fermentation and model components with membrane might be responsible for the adsorption. On the basis of their log P value (octanol–water) (www.chemspider.com), the model components can be arranged like

5–HMF < ethanol < furfural < catechol <4–hydroxybenzaldehyde < vanillin <syringaldehyde

It was surprising to observe that catechol, which is in the centre of this comparison, was the most fouling component. Hence, beside the above proposed theory, there might be another mechanism responsible for membrane fouling caused by catechol.

Catechol, when exposed to oxygen, oxidises to benzoquinone, which might be the actual component responsible for membrane fouling in the catechol experiment. However, Camera–Roda and Santarelli (2007) showed that benzoquinone permeates through GFT 1060, GFT 1070 and POMS/PEI membranes and also had a high separation factor. We detected no benzoquinone permeation. The formation of different products formed from catechol, such as described in literature by Schweigert et al. (2001), might explain the membrane performance in the catechol experiment.

To determine the inherent reasons for membrane performance reduction and membrane fouling, an in–depth study will be necessary of the adsorption mechanism, relationship between adsorbed components

and membrane structure, and change in membrane morphology due to lignocellulosic components. Analytical techniques such as SEM and FT–IR can be applied for this.

4.3.4 Recommendations to avoid fouling

The decrease in the membrane flux caused by fermentation broth and model components should be minimized and avoided for long term operation of pervaporation in the production process. This can be achieved by development of effective membrane cleaning techniques using better solvents than those tested in this study (ethanol and isopropanol). Cleaning of the membranes by using chemicals that do not alter membrane properties, can also be applied.

Another approach to deal with fouling is to opt for different process configurations. This could include stripping of the ethanol by steam or gas followed by vapour permeation for ethanol recovery instead of the pervaporation. This process option avoids the circulation of fermentation broth through the membrane unit thereby avoiding membrane fouling. But this process option needs more investigation to be industrially applicable.

The most effective way to reduce membrane fouling is to minimize by–product concentrations in the hydrolysate and in broth by optimizing the pretreatment and fermentation step. The detoxification of the hydrolysate using physical, chemical and biological methods can be done so as to avoid inhibitory products in the fermenter (Chandel et al., 2011; Parawira and Tekere, 2011).

4.4. Conclusions

Pervaporation of lignocellulosic ethanol is reported for the first time in this study. Membrane fouling, causing a flux decrease by 17–20% compared to the base case, using fermentation broths was observed. The adsorption of the fermentation by–products on membrane surface might be responsible for this irreversible flux reduction. The effects of different feedstock used and pretreatment method applied, on the membrane properties cannot be distinguished due to presence of several unknown components in the broth. Besides furfural, all model lignocellulosic components decreased the total flux by 12–15% as

compared to the base case. Furfural increases the total flux and it permeates through the membrane.

Acknowledgement

References:

1. Almeida, J.R.M., Modig, T., Petersson, A., Hahn-Hagerdal, B., Liden, G., Gorwa-Grauslund, M.F., 2007. Increased tolerance and conversion of inhibitors in lignocellulosic hydrolysates by *Saccharomyces cerevisiae*. J. Chem. Tech. Biotechnol. 82, 340 - 349.

2. Balat, M., Balat, H., 2009. Recent trends in global production and utilization of bio-ethanol fuel. Appl. Energ. 86, 2273-2282.

3. Böddeker, K.W., Gatfield, I.L., Jähnig, J., Schorm, C., 1997. Pervaporation at the vapor pressure limit: Vanillin. J. Membr. Sci. 137, 155-158.

4. Brazinha, C., Barbosa, D.S., Crespo, J.G., 2011. Sustainable recovery of pure natural vanillin from fermentation media in a single pervaporation step. Green Chem. 13, 2197-2203.

5. Brethauer, S., Wyman, C.E., 2010. Review: Continuous hydrolysis and fermentation for cellulosic ethanol production. Bioresour. Technol. 101, 4862-4874.

6. Camera-Roda, G., Santarelli, F., 2007. Intensification of Water Detoxification by Integrating Photocatalysis and Pervaporation. J. Sol. Energy Eng. 129, 68-73.

7. Cardona, C.A., Sánchez, Ó.J., 2007. Fuel ethanol production: Process design trends and integration opportunities. Bioresour. Technol. 98, 2415-2457.

8. Chandel, A.K., Silva, S.S.d., Singh, O.V., 2011. Detoxification of Lignocellulosic Hydrolysates for Improved Bioethanol Production, in: Bernardes, M.A.d.S. (Ed.), Biofuel Production – Recent Developments and Prospects, InTech, Janeza Trdine 9, 51000 Rijeka, Croatia, pp. 225-247.

9. Chovau, S., Gaykawad, S., Straathof, A.J.J., Van der Bruggen, B., 2011. Influence of fermentation by-products on the purification of ethanol from water using pervaporation. Bioresour. Technol. 102, 1669-1674.

10. Delgenes, J.P., Moletta, R., Navarro, J.M., 1996. Effects of lignocellulose degradation products on ethanol fermentations of glucose and xylose by *Saccharomyces cerevisiae, Zymomonas mobilis, Pichia stipitis*, and *Candida shehatae*. Enzyme Microb. Technol. 19, 220-225.

11. Gaykawad, S.S., van der Wielen, L.A.M., Straathof, A.J.J., 2012. Effects of yeast-originating polymeric compounds on ethanol pervaporation. Bioresour. Technol. 116, 9-14.

12. Ghosh, U.K., Pradhan, N.C., Adhikari, B., 2010. Pervaporative separation of furfural from aqueous solution using modified polyurethaneurea membrane. Desalination. 252, 1-7.

13. Huang, H.-J., Ramaswamy, S., Tschirner, U.W., Ramarao, B.V., 2008. A review of separation technologies in current and future biorefineries. Sep. Purif. Technol. 62, 1-21.

14. Kazi, F.K., Fortman, J.A., Anex, R.P., Hsu, D.D., Aden, A., Dutta, A., Kothandaraman, G., 2010. Techno-economic comparison of process technologies for biochemical ethanol production from corn stover. Fuel. 89, Supplement 1, S20-S28.

15. Klinke, H.B., Thomsen, A.B., Ahring, B.K., 2004. Inhibition of ethanol-producing yeast and bacteria by degradation products produced during pre-treatment of biomass. Appl. Microbiol. Biotechnol. 66, 10-26.

16. Lamer, T., Spinnler, H.E., Souchon, I., Voilley, A., 1996. Extraction of benzaldehyde from fermentation broth by pervaporation. Process Biochem. 31, 533-542.

17. Larsson, S., Quintana-Sáinz, A., Reimann, A., Nilvebrant, N.-O., Jönsson, L., 2000. Influence of lignocellulose-derived aromatic compounds on oxygen-limited growth and ethanolic fermentation by *Saccharomyces cerevisiae*. Appl. Biochem. Biotechnol. 84-86, 617-632.

18. Madson, P., Lococo, D., 2000. Recovery of volatile products from dilute high-fouling process streams. Appl. Biochem. Biotechnol. 84-86, 1049-1061.

19. Mustafa, B., 2011. Production of bioethanol from lignocellulosic materials via the biochemical pathway: A review. Energy Convers. Managem. 52, 858-875.

20. O'Brien, D.J., Roth, L.H., McAloon, A.J., 2000. Ethanol production by continuous fermentation–pervaporation: a preliminary economic analysis. J. Membr. Sci. 166, 105-111.

21. Offeman, R.D., Ludvik, C.N., 2011. Poisoning of mixed matrix membranes by fermentation components in pervaporation of ethanol. J. Membr. Sci. 367, 288-295.

22. Olsson, L., Hahn-Hägerdal, B., 1996. Fermentation of lignocellulosic hydrolysates for ethanol production. Enzyme Microb. Technol. 18, 312-331.

23. Palmqvist, E., Hahn-Hägerdal, B., 2000a. Fermentation of lignocellulosic hydrolysates. I: inhibition and detoxification. Bioresour. Technol. 74, 17-24.

24. Palmqvist, E., Hahn-Hägerdal, B., 2000b. Fermentation of lignocellulosic hydrolysates. II: inhibitors and mechanisms of inhibition. Bioresour. Technol. 74, 25-33.

25. Parawira, W., Tekere, M., 2011. Biotechnological strategies to overcome inhibitors in lignocellulose hydrolysates for ethanol production: review. Crit. Rev. Biotechnol. 31, 20-31.

26. Sagehashi, M., Nomura, T., Shishido, H., Sakoda, A., 2007. Separation of phenols and furfural by pervaporation and reverse osmosis membranes from biomass – superheated steam pyrolysis-derived aqueous solution. Bioresour. Technol. 98, 2018-2026.

27. Schweigert, N., Zehnder, A.J.B., Eggen, R.I.L., 2001. Chemical properties of catechols and their molecular modes of toxic action in cells, from microorganisms to mammals. Environ. Microbiol. 3, 81-91.

28. Van Hoek, P., Van Dijken, J.P., Pronk, J.T., 1998. Effect of Specific Growth Rate on Fermentative Capacity of Baker's Yeast. Appl. Environ. Microbiol. 64, 4226-4233.

29. Vane, L.M., 2005. A review of pervaporation for product recovery from biomass fermentation processes. J. Chem. Technol. Biotechnol. 80, 603-629.

30. Vane, L.M., 2008. Separation technologies for the recovery and dehydration of alcohols from fermentation broths. Biofuel. Bioprod. Bior. 2, 553-588.

31. Zha, Y., Muilwijk, B., Coulier, L., Punt, P.J., 2012. Inhibitory compounds in lignocellulosic biomass hydrolysates during hydrolysate fermentation processes. J. Bioproces. Biotechniq. 2:112, doi: 10.4172/2155-9821.1000112.

Chapter 5

Vapour permeation for ethanol recovery from fermentation off–gas

Abstract

In ethanol fermentations, about 2% of the ethanol leaves the fermenter with the off–gas. Conventionally, this is recovered by absorption in water. As alternative, vapour permeation was investigated conceptually for ethanol recovery from fermentation off–gas. A preliminary techno–economic evaluation of this system using hydrophobic membrane was carried out. The results were compared with conventional absorption. For the assumed membrane, concentrated ethanol (~ 66 mass%) might be achieved using vapour permeation whereas absorption achieves 2 mass%, and needs much more distillation to achieve ~ 93 mass%.

The ethanol recovery costs for base case absorption and for hydrophobic vapour permeation were calculated to be 0.217 and 1.366 US $\$\cdot kg^{-1}$, respectively. The ethanol recovery cost decreases with increase in membrane permeability in hydrophobic vapour permeation but the base case cost was not achieved. In the vapour permeation process, membrane cost dominates at lower membrane permeabilities whereas at the permeabilities 3 times higher than original, the costs for vacuum on permeate side of membrane governs the ethanol recovery cost.

Keywords: Fermentation, absorption, vapour permeation, economic evaluation.

5.1. Introduction

Bioethanol is potentially more sustainable than fossil fuels and is currently used as a fuel or fuel additive. This application leads to increasing demand for bioethanol. To compete with the fossil fuels, the bioethanol production should be cost effective. This can be achieved by increasing the process yield and productivity, and by using cheaper feedstock. Moreover, the process will require efficient and effective separation technologies (He et al., 2012).

Distillation is the most applied industrial process for bioethanol separation. But for dilute ethanol feed streams (ethanol concentration < 5 wt.%), distillation is relatively energy intensive (Madson and Lococo, 2000). For ethanol recovery from such a dilute stream, pervaporation, a membrane separation process, is one of the options that could be more economical than distillation (O'Brien et al., 2000a; Vane, 2005a). Pervaporation has additional advantages over distillation and has been investigated by many researchers (Groot et al., 1992b; O'Brien et al., 2000a; Vane, 2005a).

During an integrated experiment of a two–stage fermentation coupled with pervaporation, we observed severe fouling of the pervaporation membrane (unpublished data). The potential fouling candidates, present in the fermentation broth, have been identified and their effects on the membrane performance have been evaluated (Chovau et al., 2011a; Gaykawad et al., 2012; Gaykawad et al., 2013). To regain the membrane properties fouled membrane was washed with 70% (v·v^{-1}) ethanol and isopropanol. However, complete regeneration of the membrane was not attained.

One of the approaches to deal with fouling is to opt for another membrane process such as vapour permeation (VP). Here, the feed is vapour and not liquid (as in pervaporation). The separation is achieved by degrees to which components are dissolved and diffuse through the membrane (Bolto et al., 2012). Vapour–gas permeation is used industrially for recovering high value solvents, liquefied petroleum gas, for methane enrichment (removing CO_2), air purification and also for removal of volatile organic compounds (Baker et al., 1998; Jonquières et al., 2002; Rebollar-Pérez et al., 2012). Vapour permeation is also widely studied and commercially applied for dehydration (water removal) from

organic solvent vapours such as ethanol using hydrophilic membranes (Bolto et al., 2012).

One might envisage a process option including stripping of the ethanol from fermentation broth by CO_2 or another gas, followed by vapour permeation for ethanol recovery. This process option avoids the circulation of fermentation broth through the membrane unit thereby avoiding membrane fouling and additionally utilizes the fermentation by–product, CO_2, which otherwise is mostly vented–off from the process. Ethanol stripping from fermentation broth by CO_2 and recovery by different separation techniques, such as adsorption, rectification and condensation, has been successfully demonstrated (Hashi et al., 2010; Pham et al., 1989; Taylor et al., 1995). To our knowledge, this is the first report proposing the above mentioned process option. It might be applied industrially but needs more investigation due to possibility of many process configurations. Also, the availability of a membrane suitable for separation is a prerequisite.

However, before considering the combination of stripping and vapour permeation, we focus on vapour permeation to recover ethanol merely from off–gas in a conventional fermentation set–up. The bioethanol yield is increased by recovering ethanol from fermentation off–gas. Another reason for this recovery is the legal limit for ethanol emission from a bioethanol plant, which can be 40 t·year^{-1} for example. The ethanol recovery from fermentation off–gas is conventionally done by water absorption. In US–based bioethanol production processes, this recovered stream (absorber bottom outlet), being very dilute in ethanol, is recycled to an up–stream process unit such as slurry mix tank for use in corn hydrolysis (Kwiatkowski et al., 2006). The ethanol present in this stream later enters the fermentation but does not disturb it. In the Brazilian ethanol production process (Figure 5.1), no water recycle is needed as cane juice, rich in water, is used as feedstock. Also, the Brazilian process uses yeast recycling and is sensitive to volatile inhibitors that are recovered together with ethanol upon absorption. Thus, the dilute ethanol stream from the absorber is combined with the much larger and more concentrated ethanol stream originating from fermentation, and fed to the beer column (Dias et al., 2011). The mixing of outlet streams of absorption and fermentation conceals that relatively much energy is required for recovering ethanol from the vapour stream.

Vapour permeation might be used instead of absorption, for ethanol recovery from off–gas.

Thus the focus of this study is to investigate the feasibility of vapour permeation for ethanol recovery from fermentation off–gas. Vapour permeation using hydrophobic membrane will be evaluated. A techno–economic evaluation of the proposed system will be carried out and will be compared to absorption. The comparison between the conventional and proposed process will mainly be based on the ethanol concentration in the outlet of the recovery units (absorption/vapour permeation), on its effect on distillation energy consumption, and the on overall process economics.

5.2. Process description: Base case and vapour permeation case

5.2.1 Base case

The conventional corn dry–grind ethanol process described in literature was considered as the base case. In this process, the ethanol from fermentation off–gas was recovered by absorption and the dilute ethanol stream was recycled back. The process shown in Figure 5.1, is modification of a published case (Kwiatkowski et al., 2006).
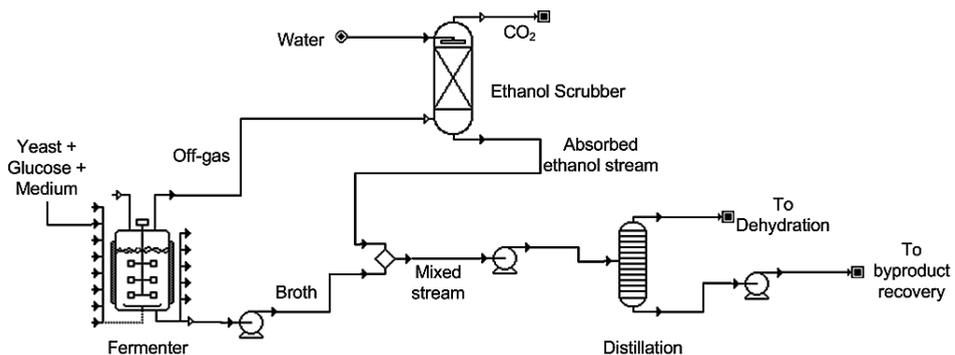
Figure 5.1. Base case for ethanol recovery from off–gas by conventional absorption with recovered ethanol fed to distillation (Process by (Dias et al., 2011) modified from (Kwiatkowski et al., 2006)).

The modification is that the absorbed ethanol is sent downstream instead of upstream, to simplify comparison of this base case with the

vapour permeation case. Thus, the recovery of the ethanol from fermentation off–gas was carried out by ethanol absorption in water. The recovered ethanol (bottom outlet) was mixed with the fermentation broth stream and then fed to the distillation. The washed CO_2 from the top of the absorber was vented to the atmosphere. The key data considered are given in Table 5.1.

Table 5.1. Base case data taken from literature (Kwiatkowski et al., 2006).

Parameter	Value	Unit
Ethanol production capacity	119×10^6	$kg \cdot year^{-1}$
Plant operation time	330	$days \cdot year^{-1}$
Ethanol emission limit	40	$t \cdot year^{-1}$
Fermentation temperature	305.15	K
Fermentation pressure	0.1	MPa
Ethanol mass fraction in fermenter	0.108	

5.2.2 Vapour permeation case

The proposed vapour permeation process is shown in Figure 5.2.
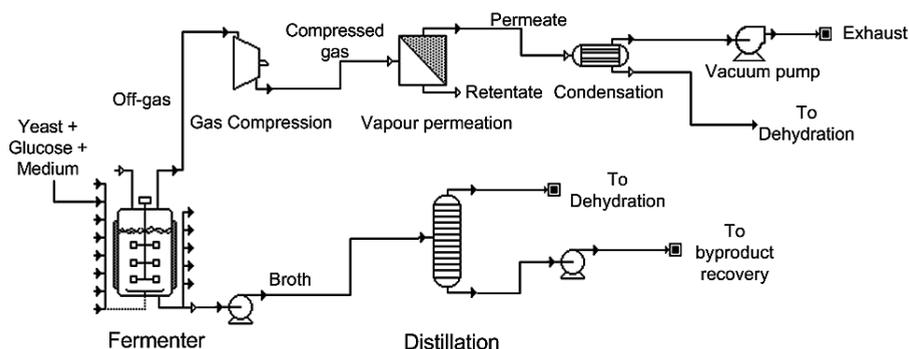
Figure 5.2. Proposed process for ethanol recovery from fermentation off–gas by vapour permeation with recovered ethanol fed to distillation.

Using a centrifugal compressor, the fermentation off–gas was compressed from 0.1 MPa to 0.15 MPa pressure, which was taken as reasonable value. Then, it was fed to the vapour permeation unit. A hollow fibre membrane module, consisting of hydrophobic PIM–1 membrane (Adymkanov et al., 2008; Budd et al., 2005), was assumed

for vapour permeation. The permeate pressure was assumed to be maintained at 0.002 MPa by using a roots vacuum pump. The permeate was then liquefied in a condenser using chilled water as a coolant. The condensed stream, rich in ethanol, was fed to the distillation or directly to the ethanol dehydration unit, depending on the ethanol composition of the stream. The retentate stream, largely containing CO_2 and traces of ethanol, satisfying the legal ethanol emission limit, was vented to the atmosphere, similar to the base case.

Thus, in both cases, the fermentation is identical and does not need to be designed. Also, the ethanol dehydration does not need to be designed, assuming that in both cases all ethanol vapour from the off–gas is converted to 93 mass% ethanol, suitable for dehydration.

5.3. Design Methods

5.3.1 Base case

The mass balances for the absorption were derived from the simulation of the base case process in SuperPro Designer® software (Intelligen Inc., Scotch Plains, NJ, USA) (Kwiatkowski et al., 2006). The results thus obtained were further used for economic evaluation.

5.3.2 Vapour permeation case
5.3.2.1 Compressor

An adiabatic centrifugal compressor was assumed in the proposed configuration. It was assumed that the stream flow rate and its composition remain the same upon compression. The stream outlet temperature (T_2) to compress the off–gas from the inlet temperature (T_1) of 303.15 K and the feed pressure (p_1) of 0.1 MPa to the outlet pressure (p_2) of 0.15 MPa was calculated using Equation (5.1) (Sinnott, 2005),

$$\left(\frac{T_2}{T_1}\right) = \left(\frac{p_2}{p_1}\right)^{\frac{(K-1)}{K}} \tag{5.1}$$

where K indicates the capacity ratio, given by,

$$K = \frac{C_P}{C_V} \tag{5.2}$$

Here C_P and C_V are specific heat capacities at constant pressure and constant volume, respectively, and were taken for CO_2 at standard conditions since this is the major component of the off–gas.

For simplicity, the energy needed for the required compression was calculated using Equation (5.3) which gives the adiabatic heat (H_{AD}) (Sinnott, 2005),

$$H_{AD} = \frac{C^f \cdot R \cdot T_1 \cdot K}{(K-1)} \cdot \left(\left(\frac{p_2}{p_1} \right)^{\frac{(K-1)}{K}} - 1 \right)$$ (5.3)

C^f (= 0.99) is the compressibility factor and R is the gas constant. The total power required for compression (P_{comp}) was calculated using Equation (5.4). F_{comp} is compressor feed flow rate and η_{comp} is mechanical efficiency of the compressor. The compressor efficiency was assumed to be 75%.

$$P_{comp} = \frac{F_{comp} \cdot H_{AD}}{\eta_{comp}}$$ (5.4)

5.3.2.2 Vapour permeation

Permeate and retentate flows and compositions, flux through the membrane, and membrane area required for ethanol recovery were determined by solving the mass balance equations across the membrane as indicated below.

The summation of mole or mass fraction of components on permeate side (Y_i) and retentate side (Z_i) is given by,

$$\sum_i Y_i = 1; \qquad \sum_i Z_i = 1$$ (5.5)

The feed and permeate side component balances for the vapour permeation unit are denoted by Equation (5.6) and (5.7),

$$F_m \cdot X_i = R_m \cdot Z_i + J_i \cdot A_m$$ (5.6)

$$J_i \cdot A_m = Y_i \cdot P_m$$ (5.7)

where F_m, R_m and P_m are membrane feed, retentate and permeate molar or mass flows. X_i is mole or mass fraction of component i in the feed with i = CO_2, ethanol or water. A_m is the membrane area required for the separation and J_i is the component molar or mass flux through the membrane and was calculated using Equation (5.8) (Sommer and Melin, 2005),

$$J_i = \frac{P_i^e}{l}\left(p^F \cdot X_i - p^P \cdot Y_i\right)$$
(5.8)

P_i^e indicates the component permeability through the membrane, p^F and p^P are pressures at feed and permeate side and l is the membrane thickness. The calculation of component mass fluxes were carried out by converting molar based membrane permeabilities to mass based using molar masses.

A plug flow model was assumed consisting of a series of mixed sections, with 20 mass% permeation of the ethanol in feed of each section. The retentate obtained in a previous section was then considered as feed for a next.

The mass balance and flux equations, mentioned earlier, with an additional equation of

$$R \cdot Z_e = 0.8 \times (F \cdot X_e)$$
(5.9)

were solved by iteration till the legal ethanol emission limit was achieved and the membrane area needed for each section was determined. This led to 20 consecutive sections. During these calculations, the pressure drop over the membrane fibre length was considered to be negligible (discussed in section 5.5.1).

The overall permeate flow was obtained by summing the permeate flows of all sections, and the overall permeate composition was obtained by averaging according to Equation (5.10) (Figure 5.3). For simplicity, the reversibility term in the flux calculation for CO_2 was neglected.

$$\text{Average permeate composition} = Y_{i,j} = \frac{\sum_{j=1}^{l} P_j \cdot Y_{i,j}}{\sum_{j=1}^{l} P_j} \qquad (5.10)$$
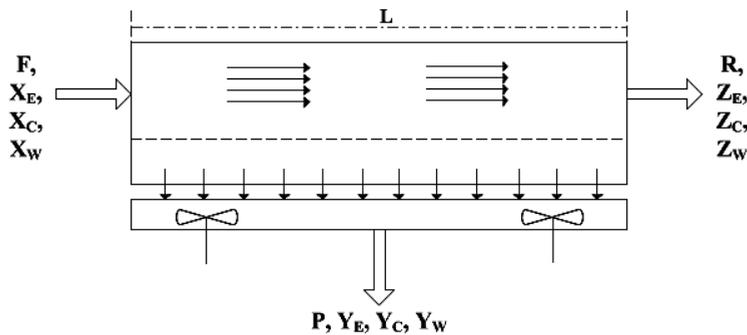
Figure 5.3. Modeling of hollow fibre membrane module.

PIM–1 membrane was considered for hydrophobic vapour permeation. This membrane was selected on the basis of availability of membrane parameters. The ethanol and water permeabilities for PIM–1 membrane were determined during ethanol–water pervaporation whereas for CO_2 it was determined during gas permeation at 303.15 K. The ethanol and water permeabilities at higher temperature (332.15 K) were calculated using the literature data for 10 wt.% ethanol–water solution and their corresponding equilibrium vapour pressures at this temperature. The resulted PIM–1 membrane parameters were further used for mass balance calculations and are listed in Table (5.2) (Adymkanov et al., 2008; Budd et al., 2005).

Table 5.2. Vapour permeation membrane properties for 10 wt.% ethanol–water solution calculated at 332.15 K on the basis of literature data (Adymkanov et al., 2008; Budd et al., 2005).

Membrane	Permeability (kg·m·m^{-2}·h^{-1}·Pa^{-1})			Membrane thickness (m)
	Ethanol	CO_2	Water	
PIM–1	1.56×10^{-9}	6.12×10^{-11}	1.69×10^{-9}	40×10^{-6}

Hollow fibre membrane modules were assumed for vapour permeation. The pressure drop (Δp) across a membrane fibre was calculated from the Hagen–Poiseuille equation.

$$\Delta p = \frac{128 \cdot \mu \cdot L \cdot F_m^v}{\pi \cdot d^4} \tag{5.11}$$

Here μ is the kinematic viscosity of the gas (based on CO_2), L is the length of the membrane, F_m^v is the feed volume flow rate and d is the inner membrane fibre diameter.

5.3.2.3 Condenser

A shell and tube type condenser, operating under the vacuum, with counter–current flow of vapour and coolant was assumed. The hot vapour flows through the shell side under vacuum whereas the coolant, the chilling water, flows through the condenser tubes.

The sensible heat flow removed ($Q_{R,V}$) by the coolant (chilled water) in the condenser was calculated using an energy balance (Equation 5.12) (Sinnott, 2005).

$$Q_{R,V} = m_i \cdot C_{P,i} \cdot (T_{out} - T_{in}) \tag{5.12}$$

m_i is molar flow of components in the hot vapour whereas T_{out} and T_{in} are outlet and inlet temperatures of hot and cold vapour, respectively. As the coolant temperature was above the boiling point of CO_2 and the solubility of CO_2 in water–ethanol solution was considered to be negligible, it was assumed that only ethanol and water were condensed while CO_2 was emitted to the atmosphere. The heat flows of condensation ($Q_{C,i}$) for ethanol and water were calculated from their heat of vaporisation ($\Delta H_{V,i}$) using Equation (5.13).

$$Q_{C,i} = m_i \cdot \Delta H_{V,i} \tag{5.13}$$

The total heat flow removed (Q_T) is the sum of sensible heat flow ($Q_{R,V}$) and heat flow of condensation ($Q_{C,i}$). The heat transfer area required (A_T) was determined using Equation (5.14), and assuming the overall heat transfer coefficient (U) of 300 W·m^{-2}·K^{-1} (1997).

$$A_T = \frac{Q_T}{U \cdot \Delta T_{LM}} \tag{5.14}$$

The log mean temperature difference (ΔT_{LM}) was calculated by using Equation (5.15).

$$\Delta T_{LM} = \frac{\left(T_{hot,in} - T_{cold,out}\right) - \left(T_{hot,out} - T_{cold,in}\right)}{\ln\left[\dfrac{\left(T_{hot,in} - T_{cold,out}\right)}{\left(T_{hot,out} - T_{cold,in}\right)}\right]} \tag{5.15}$$

The parameters used during calculations are given in Table 5.3.

Table 5.3. Parameters used in condenser calculations.

Components	C_P	$\Delta H_{V,i}$	Temperature[a] (K)	
	(kJ·kg⁻¹·K⁻¹)	(kJ·kg⁻¹)	Inlet	Outlet
Vapour			332.15	283.15
Ethanol	1.44	837.17		
CO_2	0.85	--		
H_2O	2.16	2443.89		
Liquid			278.15	291.15
H_2O	4.20	--		

[a] = Inlet and outlet temperatures for hot vapour and coolant (chilled water).

5.3.2.4 Vacuum pump

The power required for the vacuum pump (P_{vac}) to maintain the desired vacuum on the permeate side of a membrane was calculated using Equation (5.16) .

$$P_{vac} = \frac{S_0 \cdot \Delta p}{\eta_{mech}} \tag{5.16}$$

Here S_0 indicates pumping speed of a vacuum pump without counter pressure, η_{mech} is the mechanical efficiency of the vacuum pump and Δp is the pressure difference between outlet and inlet side of the vacuum pump.

5.3.2.5 Distillation energy calculation

The distillation energy needed to achieve 93 mass% of ethanol from 2 mass% and 66 mass% of ethanol in feed for base case and vapour permeation case respectively, was evaluated based on literature

data (Kwiatkowski et al., 2006; Vane, 2008). A graph of ethanol recovery energy (MJ.kg^{-1}–ethanol) against feed ethanol concentration (mass%) was used (Vane, 2008). Annual distillation energy required was then calculated based on the annual ethanol production from this recovered stream.

5.3.3 Process Economics
5.3.3.1 Purchased Equipment Cost (PEC)

All the cost calculations were done in US dollars ($). The equipment cost for the base case were taken from the literature (Kwiatkowski et al., 2006) whereas for the vapour permeation case the equipment costs, except the membrane costs, were determined from a website. As the ethanol recovered stream flow from absorption and vapour permeation was small compared to fermenter outlet flow to distillation, the distillation equipment costs mentioned in the literature cannot be directly used. The distillation equipment cost for both cases were calculated by taking the mass flow ratio of aqueous stream from the absorption or vapour permeation to aqueous stream from the fermenter and multiplying this with the distillation equipment costs given in literature. The resulted mass flow ratio of aqueous streams for absorption was 0.167 and for vapour permeation was 0.0049. The distillation equipment cost from literature includes the cost of a beer column and a rectification column (Kwiatkowski et al., 2006). The base year for equipment costs for base case and vapour permeation case were 2008 and 2007, respectively, whereas the base year for membrane cost was 2000. The adjustment of the prices from base year to 2011 was carried out using Equation (5.17).

$$Cost_{2011} = Cost_{Base\ year} \cdot \left(\frac{CEPCI_{2011}}{CEPCI_{Base\ year}} \right) \qquad (5.17)$$

CEPCI are the Chemical Engineering Plant Cost Indexes. The indexes for years 2000, 2007, 2008 and 2011 were 394.1, 525.4, 575.4 and 585.7, respectively .

The cost of the vapour permeation unit was based on the total membrane area needed. A membrane capital cost of 200 $·m^{-2} (including modules) with replacement cost of 100 $·m^{-2} and with a membrane life of 5 years was assumed without any price correction to

2011 (O'Brien et al., 2000a). A centrifugal compressor made of carbon steel and with maximum compression capacity of 0.8 MPa was selected for costing. A condenser with carbon steel shell under vacuum and stainless steel (SS316) fixed U–shaped tubes was chosen.

5.3.3.2 Fixed capital investment

The fixed capital investment for the base case and vapour permeation case was estimated by using typical factors for fluid processes (Sinnott, 2005). These factors are given in Table 5.4.

Table 5.4. Typical factors for estimating fixed capital investment (Sinnott, 2005).

Item	Costs
Direct plant costs (DPC)	
Purchased equipment cost (PEC)	Table 5.9
Equipment erection/installation	40% of PEC
Piping	70% of PEC
Instrumentation	20% of PEC
Electrical	10% of PEC
Buildings, process	15% of PEC
Site development	5% of PEC
Indirect plant costs (IPC)	
Design and Engineering	30% of DPC
Contractor's fee	5% of DPC
Contingency	10% of DPC
Fixed capital investment (FCI)	DPC + IPC

5.3.3.3 Variable costs

Variable costs constitute of raw material, utility and shipping costs. In our study, within the battery limit considered, raw material was not necessary in either case. Only utility costs, different for both cases, were considered.

5.3.3.4 Total recovery costs

The annual recovery cost or total recovery cost was calculated based on the variable costs, fixed cost and general expenses. The factors used for this calculation are listed in Table 5.5.

Table 5.5. Estimation of total recovery costs (Sinnott, 2005).

Item	Costs
Variable costs (VC)	Table 10
Fixed costs(FC)	
Maintenance	5% of FCI
Operating labour (OL)	5% of FCI
Laboratory costs	20% of OL
Supervision	20% of OL
Plant overheads	50% of OL
Capital charges	10% of FCI
Insurance	1% of FCI
Local taxes	2% of FCI
Royalties	1% of FCI
Direct recovery costs (DRC)	VC + FC
General expenses	25% of DRC
Annual recovery cost	DRC + General expenses

5.4. Results

Here the results consisting of mass and energy flows for both process options are presented.

5.4.1 Base case

The fermentation off–gas stream size; its composition and the absorber outlet stream specification are listed in Table 5.6.

A calculation of off–gas composition based on vapour liquid equilibria of a pure ethanol–water mixture, showed lower ethanol content in vapour phase as compared to that in assumed fermenter off–gas (Table 5.6) (Kwiatkowski et al., 2006). This contradiction can be explained by the increase volatility of ethanol due to other solutes (Roychoudhury et al., 1986). For the ease of calculations and comparison, the composition stated in Table 5.6 was kept.

Table 5.6. Simulation results for base case adopted from literature (Kwiatkowski et al., 2006).

Parameter	Value	Unit
Fermenter off-gas		
Flow rate	14675	kg·h^{-1}
Mass fraction		
Ethanol	2.7	%
CO_2	95.84	%
Water	1.46	%
Absorber specifications		
Water inlet flow rate	19863	kg·h^{-1}
Water temperature	286.15	K
Recovered ethanol stream		
Flow rate	20399	kg·h^{-1}
Mass fraction		
Ethanol	1.94	%
CO_2	0.069	%
Water	97.99	%

5.4.2 Vapour permeation case

5.4.2.1 Off–gas compression

The fermenter off–gas composition was the same as in the base case. The compression power required to increase the feed pressure from 0.1 MPa to 0.15 MPa was 134 kW. The resulting compressed stream was at 332.15 K.

5.4.2.2 Vapour permeation

The stream compressed to 0.15 MPa and at 332.15 K was fed to the hollow fibre tubes. Permeation of the components occurs, based on their membrane properties, and the permeate was collected under vacuum (0.002 MPa pressure) at the shell side of the module (Figure 5.3).

During the calculations, using membrane permeabilities given in Table 5.2, the legal ethanol emission limit could not be achieved. This was due to the presence of less water than ethanol in the feed, whereas membrane permeabilities of water and ethanol were almost the same. These conditions led to faster removal of water than of ethanol. To avoid this, the ethanol permeability was assumed to be twice the value given

in Table 5.2. The results achieved for membrane area, flow rates and their compositions are given in Table 5.7.

The membrane area required for vapour permeation depends on the membrane properties and the multiplication factor used in Equation (5.9) (0.8), which determines the extent of the ethanol removal. The multiplication factor in Equation (5.9) was assumed for these calculations so as to have enough iteration to give plug flow effect and it can be varied.

Table 5.7. Vapour permeation mass balance results calculated using plug flow model at feed temperature = 332.15 K.

Membrane	Area		Flow rate	Composition (mass%)		
	(m^2)		(kg·h^{-1})	Ethanol	CO$_2$	Water
PIM–1	7010[a]	Feed	14675	2.70	95.84	1.46
		Retentate	12510	0.03	99.86	0.11
		Permeate	2165[a]	18.10[b]	72.61[b]	9.29[b]

[a] = the sum of values obtained for individual sections over the length of membrane fibre.

[b] = the average compositions obtained over the length of membrane fibre.

5.4.2.3 Condenser

The permeate stream from vapour permeation was condensed using chilled water. Ethanol rich condensate (66.08 mass%) was achieved as only ethanol and water were assumed to condense. The condenser specifications and the results are given in Table 5.8.

Table 5.8. Condenser specifications and results.

Parameter	Value	Unit
Coolant flow	17117	kg·h^{-1}
Condenser flow rate[a]		
Inlet	2165	kg·h^{-1}
Outlet	593	kg·h^{-1}
Heat removed from vapour	259.60	kW
Heat transfer area	50.39	m^2
Condensate composition		(mass fraction) %
Ethanol	66.08	
Water	33.92	

[a] = Condenser hot vapour inlet and condensate outlet flow rate.

5.4.2.4 Vacuum pump

The vacuum of 0.002 MPa on the permeate side of the membrane was achieved by using a roots vacuum pump . The capacity and energy requirement of the vacuum pump were determined on the basis of permeate volume flow of uncondensed gas (here CO_2). Permeate mass flow was converted to volume flow using the molar density of CO_2 calculated at 283.15 K and 0.002 MPa and it resulted in 42055 $m^3 \cdot h^{-1}$. The maximum pumping speed used for a vacuum pump without back pressure was 17,850 $m^3 \cdot h^{-1}$. The mechanical efficiency of the pump was assumed to be 85% and the power required for a vacuum pump, calculated using Equation (5.16), was 583 kW. To meet the required permeate volume flow, three vacuum pumps were considered and the results obtained for single pump were multiplied by factor 3.

5.4.3. Process Economics

5.4.3.1 Purchased Equipment Cost (PEC)

The purchased equipment costs for the process units are given in Table 5.9. All indicated prices of equipment contribute significantly. The equipment costs of vapour permeation and condenser are affected by the required membrane and heat transfer area, respectively.

Because no price was available for a roots vacuum pump, a large, cast iron 1–stage blower was assumed as vacuum pump for the equipment costing and the calculation was based on permeate flow of uncondensed gas (42055 $m^3 \cdot h^{-1}$ = 24,752 $ft^3 \cdot min^{-1}$). Two vacuum pumps of maximum flow capacity of 22000 $ft^3 \cdot min^{-1}$ were considered. The distillation equipment cost was calculated as discussed in section 5.3.3.1 and the results are given in Table 5.9. This table shows that the membrane unit costs dominate.

Table 5.9. Purchased equipment costs for base case and vapour permeation case.

Equipment	Capacity/	Base year costs	Base year	2011 cost
	Specification	($)		($)
Base case				
Absorber	13.41 m^3	97,000	2008	98,736
Distillation[b]		144,96	2008	147,550
Vapour Permeation				
Compressor	P = 134.09 kW	80,300	2007	89,516
Membrane Unit	A_m = 7010 m^2	200[a]	2000	1,402,000
Condenser	A_T = 50.39 m^2	62,800	2007	70,008
Vacuum pump	--	159,200	2007	177,471
Distillation[b]		4,192	2008	4,285

[a] = per m^2.

[b] = The cost for the base year was calculated by taking the mass flow ratio of aqueous stream from the absorption or vapour permeation to aqueous stream from the fermenter and multiplying this with the distillation equipment costs given in literature (Kwiatkowski et al., 2006). The resulting mass flow ratio of aqueous streams was 0.167 for absorption and 0.0049 for vapour permeation. The distillation equipment cost from literature includes the cost of a beer column and a rectification column.

5.4.3.2 Fixed capital investment

The fixed capital investment for both the cases was calculated based on the parameters given in Table 4 (section 5.3.3.2). The resulting fixed costs are given in Table 5.11.

5.4.3.3 Variable costs

Variable costs were calculated on annual basis as shown in Table 5.10. (Kwiatkowski et al., 2006; Sinnott, 2005).

In the base case, the ethanol concentration achieved in absorber outlet stream was 1.94 (mass%) whereas in the hydrophobic vapour permeation case the concentration attained was 66.08 (mass%). To compare the two processes, the ethanol concentration in both cases should be the same and was assumed to be at 93% (mass%). To achieve this, the recovered stream from the absorber and permeate condensate stream from vapour permeation were sent to the distillation. The annual distillation energy, needed to achieve the required ethanol concentration, was determined as described in section 5.3.2.5. The total

energy cost was evaluated based on the steam cost (Kwiatkowski et al., 2006). Distillation equipment cost was calculated as explained in section 5.3.3.1. The total energy cost required to get 93% (mass%) of ethanol was added as variable cost to both cases (Table 5.10). Comparing the utility costs for both cases, distillation and vacuum pump were found to be most significant contributor for base case and VP case respectively.

Table 5.10. Utility costs for base case and vapour permeation case (Kwiatkowski et al., 2006; Sinnott, 2005).

Utility	Units	Consumption		Rate	Cost ($.year^{-1})
Base case					
Cooling Water	Absorber	19863	kg·h^{-1}	0.07 $·t^{-1}	11,012
Steam	Distillation	47013912 MJ		5.69×10^{-3} $·MJ^{-1}	267,509
Vapour permeation case					
Electricity	Compressor	134.09	kW	0.0682 $·kWh^{-1}	72,428
	Vacuum pump	1749	kW		944,712
Chilled water	Condenser	17117	kg·h^{-1}	0.08 $·t^{-1}	10,845
Steam	Distillation	9310831 MJ		5.69×10^{-3} $·MJ^{-1}	52979

5.4.3.4 Total recovery costs

The annual recovery costs for the hydrophobic vapour permeation case was split in two parts, namely cost of the vapour permeation unit and cost of the rest. This was done because maintenance and membrane replacement for vapour permeation were calculated based on membrane area required at a rate of 100 $·m^{-2} and was included in the fixed costs. Thus for both parts, purchased equipment costs, fixed capital investments and fixed cost were calculated separately. The results are given in Table 5.11.

Table 5.11. Annual recovery costs.

Cost type	Source	Base case ($)	Vapour permeation (VP) case ($)		
			VP unit	Rest	Total
Purchased equipment cost	Table 5.9	246,287	1,402,000	341,280	1,743,280
Fixed capital investment	Table 5.4	928,503	5,285,540	1,286,626	6,572,166
Fixed costs	Table 5.5	264,623	1,943,102	366,688	2,309,790
Annual recovery cost	Table 5.5	678,930			4,238,442

5.4.3.5 Ethanol recovery cost

The ethanol recovery cost was calculated for two schemes using total annual recovery cost and annual ethanol production. The results obtained (Table 5.11 and 5.12) indicate that the membrane process is more expensive than the conventional absorption–distillation process. Membrane and vacuum costs dominate the overall costs in the membrane process. The ethanol recovery cost obtained with hydrophobic vapour permeation was almost 6 times of that achieved with the base case.

Note that the literature reports cost of ethanol recovery from fermentation broth of 0.05–0.15 $·kg^{-1} including cell removal (Straathof, 2011). However, this involves distilling relatively concentrated ethanol. Recovering ethanol from off–gas will be more expensive.

Table 5.12. Ethanol recovery cost for base case and vapour permeation case.

Process scheme	Feed pressure (MPa)	Membrane properties	Ethanol recovery cost ($·kg^{-1})
Base case	0.1	not applicable	0.217
Vapour permeation case	0.15	Permeabilities in Table 5.2.	1.366

5.5. Sensitivity analysis

5.1 Effect of better membrane properties

The effect of an increase in membrane permeability in vapour permeation on the membrane cost, compression cost, condensation cost, and ethanol recovery cost was evaluated.

The membrane permeabilities mentioned in Table 5.2 were multiplied by factors ranging from 10 to 50 and the calculations for membrane area and ethanol recovery cost were repeated. During these calculations, the ethanol permeability was additionally multiplied by a factor 2 as discussed in section 5.4.2.2. The increase in membrane permeability results in a faster separation which causes decrease in membrane area required for separation and hence reduces the membrane cost (Figure 5.4). The vacuum and compression cost, which comprise of equipment cost and utility cost, remained unchanged as membrane permeability does not affect these costs.

The overall effect of variation in membrane permeability can be seen on ethanol recovery cost. The ethanol recovery cost follows a similar trend as membrane cost and decreases with increasing membrane permeability. At the initial membrane permeabilities, ethanol recovery cost was affected more by membrane cost than by other costs. However, the ethanol recovery cost for base case (0.217 $\cdot kg^{-1}$) was not achieved even at 50 times higher membrane permeability than originally. This was due to the fact that, at permeabilities 3 times higher than original, the vacuum cost becomes higher than the membrane cost and hence dominates the ethanol recovery cost. This leads to a minimum in ethanol recovery cost of 0.599 $\cdot kg^{-1}$ at 50 times membrane permeability, still 3 times higher than the base case cost (0.217 $\cdot kg^{-1}$).

The higher vacuum cost was due to a larger flow of uncondensed gas (CO_2) through the vacuum pump which increases the energy requirement for maintaining the desired vacuum. The cost calculations were also performed based on ethanol–water permeate flow only, thus assuming a CO_2–impermeable membrane. The resulting ethanol recovery cost at 50 times higher permeability was 0.310 $\cdot kg^{-1}$, which is still higher than the base case cost. The vacuum calculations were checked using the data presented by Peters and Timmerhaus (Peters

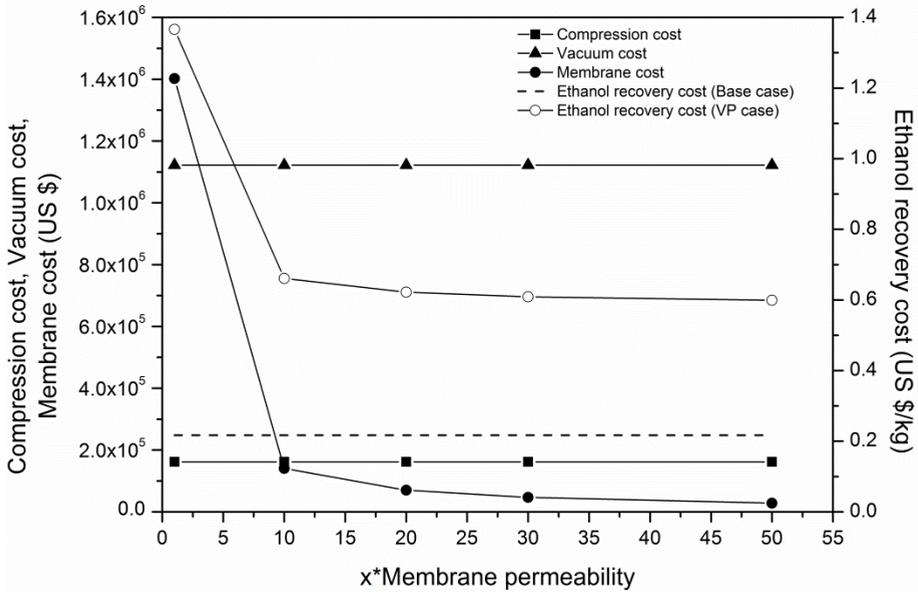and Timmerhaus, 1991), and the results obtained were found to be in the same range of those presented here.

Figure 5.4. Effect of increase in membrane permeability on ethanol recovery cost.

The role of membrane thickness as additional variable in decreasing the ethanol recovery cost was identified (Equation 5.8). Instead of increasing the membrane permeability, the membrane thickness can also be reduced. This can result in higher fluxes through the membrane thereby decreasing the membrane area needed for the desired separation and hence the ethanol cost.

It was checked if a pressure drop might occur over the length of the membrane in the hollow fibre vapour permeation module. Based on required membrane area (Table 5.7), the number of fibres was 656,200 when using single fibre dimensions of 1.6 m × 2 mm (length × inner diameter). The pressure variation in the hollow fibre membrane module can be caused due to friction of gas with the membrane surface and by the permeation of the gas. The change in the pressure, at the outlet of the fibre, due to the friction was calculated using the Hagen–Poiseuille equation. It was found that the pressure loss due to friction was negligible.

5.5.2 Different membrane type – Hydrophilic membrane

A similar analysis as that for hydrophobic vapour permeation, was performed using a hydrophilic membrane, such as alginate based (separation layer: alginate, membrane support: PVDF, chitosan; total flux = 0.172 kg·m^{-2}·h^{-1} and $\alpha_{water/ethanol}$ = 90 at 323.15 K) (Huang et al., 2000). In this case, it was assumed that dehydration of fermenter off–gas was carried out and the permeate mainly containing water and ethanol (satisfying the legal emission limit) was vented. The retentate, after condensation, will produce an ethanol rich stream with ethanol composition of 95 mass%.

During hydrophilic vapour permeation calculations, it was tried to apply the legal ethanol emission limit on the permeate side (permeate ethanol flow = 5 kg·h^{-1}). The results achieved using this condition indicated that this constraint was not held and not even with unrealistic large values for the membrane area required. Therefore, this ethanol emission constraint should not be applied immediately at the permeate side of the vapour permeation because even for a very good membrane too much ethanol will permeate when most of the water needs to permeate. Besides, the ethanol lost with uncondensed CO_2 in the retentate should also be taken into account while applying the emission limit.

Thus, a more complex process option, such as recycling of the permeate stream to a stripping column for heat recovery, permeate stream condensation, etc. may be necessary to meet the ethanol emission limit when using a hydrophilic membrane (Huang et al., 2010; Vane, 2008). Evaluation of such process option will require a separate study and this is considered to be out of scope of the present research.

5.6. Conclusions

Vapour permeation using hydrophobic membrane for ethanol recovery from fermentation off–gas was proposed and techno–economic comparison was carried out against conventional absorption process. In the vapour permeation case, the ethanol concentration obtained in the recovered stream was 66.08 mass% and was very high compared to the concentration in the absorber outlet (bottom) stream (1.94 mass%).

Consequently, the mass flow rate of the dilute absorber stream was very high.

The energy cost needed to distil the absorber outlet stream and condensed permeate stream of vapour permeation to achieve 93 mass% ethanol was added and ethanol recovery cost was calculated for both process options. The recovery cost obtained indicates that the membrane process is much more expensive than the conventional absorption–distillation process. Besides the membrane costs, vacuum costs dominate the overall costs in the membrane process.

The sensitivity analysis carried out by varying membrane properties in hydrophobic vapour permeation showed that the ethanol recovery cost decreases with increase in membrane permeability but the base case cost was not achieved. In the vapour permeation process, at membrane permeability higher than 3 times original permeability, the vacuum cost becomes larger than the membrane cost.

Nomenclature:

A_m = Membrane area (m²)

A_T = Total heat transfer area in condenser (m²)

C^f = Compressibility factor

C_P = Specific heat capacity at constant pressure (J·mol⁻¹·K⁻¹)

C_V = Specific heat capacity at constant volume (J·mol⁻¹·K⁻¹)

d = Inner membrane fibre diameter (m)

F_{comp} = Compressor feed flow rate (mol·h⁻¹)

F_m = Feed flow rate to VP (mol·h⁻¹)

F_m^v = Feed volume flow (m³·s⁻¹)

H_{AD} = Adiabatic heat (J·mol⁻¹)

$H_{V,i}$ = Heat of vaporization (J·mol⁻¹)

J_i = Flux of component i through the membrane (mol·m⁻²·h⁻¹)

K = Capacity ratio

L = Membrane fibre length (m)

l = Membrane thickness (m)

m_i = Molar flow of component i (mol·h⁻¹)

P_{comp}	= Power required for compression (W)
P_i^e	= Permeability of component i (mol·m·m^{-2}·h^{-1}·Pa^{-1})
p^F	= Feed pressure in VP (Pa)
P_m	= Permeate flow in VP (mol·h^{-1})
p^P	= Permeate pressure in VP (Pa)
P_{vac}	= Power requirement for vacuum pump (W)
$Q_{C,i}$	= Heat flow of condensation (J·h^{-1})
$Q_{R,V}$	= Heat flow removed from hot vapour (J·h^{-1})
Q_T	= Total heat flow removed by condenser (J·h^{-1})
R	= Gas constant (= 8.312 J·mol^{-1}·K^{-1})
R_m	= Retentate flow in VP (mol·h^{-1})
S_0	= Pumping speed of vacuum pump without counter pressure (m^3·s^{-1})
T	= Temperature (K)
$T_{cold,in}$, $T_{cold,out}$	= Temperature of cold stream inlet and outlet respectively (K)
$T_{hot,in}$, $T_{hot,out}$	= Temperature of hot stream inlet and outlet respectively (K)
U	= Heat transfer coefficient (W·m^{-2}·K^{-1})
μ	= Dynamic viscosity of gas (CO_2) (Pa·s)
η_{comp}	= Mechanical efficiency of compressor (fraction)
η_{mech}	= Mechanical efficiency of vacuum pump (fraction)

Sub-/Super-script:

i	= Components (Ethanol, CO_2 and water)
c	= CO_2
e	= Ethanol
w	= Water
Δ	= Difference
Σ	= Sum
1	= Inlet side;
2	= Outlet side.

References:

1. He Y, Bagley DM, Leung KT, Liss SN, Liao B-Q. Recent advances in membrane technologies for biorefining and bioenergy production. Biotechnol Adv 2012;30:817.
2. Madson P, Lococo D. Recovery of volatile products from dilute high-fouling process streams. Appl Biochem Biotechnol 2000;84-86:1049.
3. O'Brien DJ, Roth LH, McAloon AJ. Ethanol production by continuous fermentation–pervaporation: a preliminary economic analysis. J Membr Sci 2000;166:105.
4. Vane LM. A review of pervaporation for product recovery from biomass fermentation processes. J Chem Technol Biotechnol 2005;80:603.
5. Groot WJ, Kraayenbrink MR, Waldram RH, van der Lans RGJM, Luyben KCAM. Ethanol production in an integrated process of fermentation and ethanol recovery by pervaporation. Bioprocess Biosystems Eng 1992;8:99.
6. Chovau S, Gaykawad S, Straathof AJJ, Van der Bruggen B. Influence of fermentation by-products on the purification of ethanol from water using pervaporation. Bioresour Technol 2011;102:1669.
7. Gaykawad SS, van der Wielen LAM, Straathof AJJ. Effects of yeast-originating polymeric compounds on ethanol pervaporation. Bioresour Technol 2012;116:9.
8. Gaykawad SS, Zha Y, Punt PJ, van Groenestijn JW, van der Wielen LAM, Straathof AJJ. Pervaporation of ethanol from lignocellulosic fermentation broth. Bioresour Technol 2013;129:469.
9. Bolto B, Hoang M, Xie Z. A review of water recovery by vapour permeation through membranes. Water Res 2012;46:259.
10. Baker RW, Wijmans JG, Kaschemekat JH. The design of membrane vapor–gas separation systems. J Membr Sci 1998;151:55.
11. Jonquières A, Clément R, Lochon P, Néel J, Dresch M, Chrétien B. Industrial state-of-the-art of pervaporation and vapour permeation in the western countries. J Membr Sci 2002;206:87.
12. Rebollar-Pérez G, Carretier E, Lesage N, Moulin P. Vapour permeation of VOC emitted from petroleum activities: Application for low concentrations. J Ind Eng Chem 2012;18:1339.
13. Taylor F, Kurantz MJ, Goldberg N, Craig JC. Continuous Fermentation and Stripping of Ethanol. Biotechnol Prog 1995;11:693.
14. Hashi M, Tezel FH, Thibault J. Ethanol Recovery from Fermentation Broth via Carbon Dioxide Stripping and Adsorption†. Energy & Fuels 2010;24:4628.
15. Pham CB, Motoki M, Matsumura M, Kataoka H. Simultaneous ethanol fermentation and stripping process coupled with rectification. J Ferment Bioeng 1989;68:25.
16. http://www.epa.gov/region07/priorities/agriculture/pdf/ethanol_plants_manual.pdf.

17. Kwiatkowski JR, McAloon AJ, Taylor F, Johnston DB. Modeling the process and costs of fuel ethanol production by the corn dry-grind process. Ind Crop Prod 2006;23:288.

18. Dias MOS, Cunha MP, Jesus CDF, Rocha GJM, Pradella JGC, Rossell CEV, et al. Second generation ethanol in Brazil: Can it compete with electricity production? Bioresour Technol 2011;102:8964.

19. Budd PM, Msayib KJ, Tattershall CE, Ghanem BS, Reynolds KJ, McKeown NB, et al. Gas separation membranes from polymers of intrinsic microporosity. J Membr Sci 2005;251:263.

20. Adymkanov SV, Yampol'skii YP, Polyakov AM, Budd PM, Reynolds KJ, McKeown NB, et al. Pervaporation of alcohols through highly permeable PIM-1 polymer films. Polym Sci Ser A 2008;50:444.

21. Sinnott RK. Coulson & Richardson's Chemical Engineering: Chemical Engineering Design Vol. 6. 4th ed: Elsevier Butterworth-Heinemann; 2005.

22. Sommer S, Melin T. Influence of operation parameters on the separation of mixtures by pervaporation and vapor permeation with inorganic membranes. Part 1: Dehydration of solvents. Chem Eng Sci 2005;60:4509.

23. Perry's Chemical Engineer's Handbook. 1997;7th Edition.

24. http://www.pfeiffer-vacuum.com/know-how/vacuum-generation/roots-vacuum-pumps/application-notes/technology.action?chapter=tec2.6.2.

25. Vane LM. Separation technologies for the recovery and dehydration of alcohols from fermentation broths. Biofuel Bioprod Bior 2008;2:553.

26. http://www.matche.com/EquipCost/index.htm.

27. www.che.com/pci.

28. Roychoudhury PK, Ghose TK, Ghosh P, Chotani GK. Vapor liquid equilibrium behavior of aqueous ethanol solution during vacuum coupled simultaneous saccharification and fermentation. Biotechnol Bioeng 1986;28:972.

29. www.eia.gov.

30. Straathof AJJ. The Proportion of Downstream Costs in Fermentative Production Processes. In: Editor-in-Chief: Moo-Young M, editor. Comprehensive Biotechnology (Second Edition). Burlington: Academic Press; 2011, p. 811.

31. Peters MS, Timmerhaus KD. Plant Design and Economics for Chemical Engineers. 1991.

32. Huang RYM, Pal R, Moon GY. Pervaporation dehydration of aqueous ethanol and isopropanol mixtures through alginate/chitosan two ply composite membranes supported by poly(vinylidene fluoride) porous membrane. J Membr Sci 2000;167:275.

33. Huang Y, Ly J, Nguyen D, Baker RW. Ethanol Dehydration Using Hydrophobic and Hydrophilic Polymer Membranes. Ind Eng Chem Res 2010;49:12067.

Chapter 6

Outlook

In an attempt to improve the ethanol productivity and minimize the production cost, the integration of ethanol fermentation and pervaporation (PV) was explored. In–situ ethanol removal by hydrophobic pervaporation from continuous two–stage fermentation was performed successfully. Effects of fermentation broth and its components on membrane performance during ethanol recovery by pervaporation were investigated. Vapour permeation, as an alternative to pervaporation, was proposed and evaluated techno–economically for ethanol recovery from fermentation off–gas. In general, the work presented in this thesis provides the know-how of hydrophobic pervaporation for ethanol recovery during fermentation.

Continuous two–stage fermentation integrated with pervaporation was employed to achieve high cell density in fermenter 2 and high ethanol productivity. Here pervaporation served dual functions as an ethanol recovery unit and cell retention system. However, the higher cell densities and productivities, as reported in literature, were not achieved experimentally. Some of the potential reasons for this are discussed here. The pervaporation unit used was smaller, which resulted in a very small ethanol–water permeate stream and most of the cells and ethanol were lost through the bleed. The formation of ethanol by the Crabtree effect in the 1st fermenter and cell growth in the 2nd fermenter were observed which led to undesirable utilization of substrate. Additionally, irreversible fouling of PDMS membrane was observed. These effects can be minimized by using a larger pervaporation system and by applying a cell retention system such as microfiltration (MF) in the process. Various process configurations can be proposed and the choice of the system should be based on detailed modelling. To do so, the determination of kinetic parameters for *S. cerevisiae* at fermentation conditions is highly recommended. The necessity of using a recycle flow from fermenter 2 to fermenter 1 to maintain cell viability in fermenter 2 should also be determined experimentally. Evaluation of model based optimized settings for integrated system is strongly suggested before experimentation.

Pervaporative membrane fouling was observed during integrated experiment and also by lignocellulosic fermentation broth and its components. It should be minimized and avoided for long term operation of pervaporation in the production process. Membrane

washing by hot water, 70% (v·v⁻¹) ethanol and isopropanol was not effective and initial membrane properties were not regained. To avoid membrane fouling, it is recommended to develop and apply effective membrane cleaning techniques using better solvents that do not alter membrane properties. To avoid the formation of inhibitory components from lignocellulosic biomass, modification of pretreatment and hydrolysis steps is proposed. Different biological and non–biological detoxification strategies for lignocellulosic hydrolysate are mentioned by Chandel and coworkers (2011). These methods can be employed to lower the concentration of inhibitory components in hydrolysate which can help to minimize the membrane fouling. Besides these strategies, pervaporation can also be used for recovery of some of the inhibiting components. The results obtained during this study indicated that pervaporation can be used successfully for the separation of furfural from fermentation broth. Another hydrolysate component that can be separated by pervaporation is vanillin. To determine the inherent reasons for membrane performance reduction and membrane fouling, an in–depth study is recommended of fouling mechanism due to lignocellulosic components. Analytical techniques such as SEM and FT–IR can be applied for this.

Techno–economic feasibility of vapour permeation, as an alternative to pervaporation, for ethanol recovery from fermentation off–gas was evaluated in this research. It was observed that besides the membrane costs, vacuum costs dominate the overall costs in the vapour permeation process, which was more expensive than a conventional ethanol absorption process. A novel process option including stripping of the ethanol from fermentation broth by CO_2 followed by vapour permeation for ethanol recovery is also proposed. It has the advantages of avoiding membrane fouling by preventing circulation of fermentation broth through the membrane unit and additionally utilizing the fermentation by–product, CO_2, which otherwise is mostly vented–off from the process. However, the prerequisite for this process to be successful is the development of novel membranes with better properties for separation of ethanol from a mixture of CO_2, ethanol and water vapour. Also, it needs more investigation due to possibility of many process configurations.

The recovery of ethanol by hydrophobic pervaporation cannot compete with existing mature technologies due to lower membrane performance (membrane flux and selectivity) and higher membrane costs. The recovery of pure ethanol cannot be achieved by hydrophobic pervaporation as the separation of water takes place along with ethanol. This is due to smaller size of water molecule compared to ethanol and by partitioning of water into the polymer matrix solely due to sorption entropy (Schäfer et al., 2005). Thus while developing hydrophobic membranes (PDMS), to improve the membrane properties, the focus should be to enhance the hydrophobic nature of the membrane material rather than enhancing the organophilic nature of the membrane (Watson and Baron, 1996). However, with current membrane properties, hydrophobic pervaporation can be used to concentrate the feed stream prior to distillation and make distillation less energy intensive.

The application of hydrophilic pervaporation, instead of hydrophobic pervaporation, is suggested for ethanol recovery. The more developed hydrophilic membranes with better membrane properties can be used for water removal from fermentation broth. But a detailed study is necessary to investigate the feasibility of hydrophilic pervaporation due to possibility of various process configurations and fouling components. The requirement of membrane area may be large due to handling of large feed stream.

References:

1. Chandel, A.K., Silva, S.S.d., Singh, O.V., 2011. Detoxification of Lignocellulosic Hydrolysates for Improved Bioethanol Production, in: Bernardes, M.A.d.S. (Ed.), Biofuel Production – Recent Developments and Prospects, InTech, Janeza Trdine 9, 51000 Rijeka, Croatia, pp. 225-247.
2. Schäfer, T., Heintz, A., Crespo, J.G., 2005. Sorption of aroma compounds in poly(octylmethylsiloxane) (POMS). J Membr Sci. 254, 259-265.
3. Watson, J.M., Baron, M.G., 1996. The behaviour of water in poly(dimethylsiloxane). J Membr Sci. 110, 47-57.

List of publications

Journal articles:

1. <u>S.S. Gaykawad</u>, Ying Zha, P.J. Punt, J.W. van Groenestijn, L.A.M. van der Wielen, A.J.J. Straathof, (2013), 'Pervaporation of ethanol from lignocellulosic fermentation broth', *Bioresource Technology,* (129), 469-476.

2. <u>S.S. Gaykawad</u>, L.A.M. van der Wielen, A.J.J. Straathof, (2012), 'Effects of yeast-originating polymeric compounds on ethanol pervaporation', *Bioresource Technology*, (116), 9–14.

3. Chovau S., <u>Gaykawad S.S</u>, Straathof A.J.J., Van der Bruggen B., (2011), 'Influence of fermentation by-products on the purification of ethanol from water using pervaporation', *Bioresource Technology*, (102), 1669-1674.

4. F. Ozde Utkur, <u>Sushil Gaykawad</u>, Bruno Buhler, Andreas Schmid, (2011), 'Regioselective aromatic hydroxylation of quinaldine by water using quinaldine 4-oxidase in recombinant *Pseudomonas putida*', *Journal of Industrial Microbiology and Biotechnology*, (38), 1067-1077.

5. <u>S.S. Gaykawad</u>, D.N. Rütze, L.A.M. van der Wielen, A.J.J. Straathof, (2013), 'Vapor permeation for ethanol recovery from fermentation off-gas', *Submitted for publication.*

Book chapter:

S. Chovau, <u>S.S Gaykawad</u>, A.J.J. Straathof, B. van der Bruggen, (2011), 'Comparison of membrane performance of PDMS-based membranes during ethanol/water pervaporation and fermentation broth pervaporation', Modern Applications in Membrane Science and Technology, Chapter 5, pp 51-59,
Chapter DOI: 10.1021/bk-2011-1078.ch005, ACS Symposium Series, Vol. 1078. ISBN13: 9780841226180. eISBN: 9780841226203

Oral presentation:

<u>S.S. Gaykawad</u>, L.A.M. van der Wielen and A.J.J. Straathof, (2012), 'Integrated ethanol fermentation and pervaporation', *RRB8 conference*, 4-6 June 2012, Toulouse, France.

Poster presentation:

1. S.S. Gaykawad, L.A.M. van der Wielen and A.J.J. Straathof, (2013), Investigating the effects of lignocellulosic fermentation broth and fermentation by-products on membrane performance during ethanol recovery by pervaporation, 21-25 April, *ECCE-9/ECAB-2*, Den Haag, The Netherlands.

2. S.S. Gaykawad, L.A.M. van der Wielen and A.J.J. Straathof, (2012), Effects of cellular polymers on membrane performance in pervaporation integrated with fermentation, *DNM project workshop*, 15-18 May 2012, Cetraro, Italy.

3. S.S. Gaykawad, L.A.M. van der Wielen and A.J.J. Straathof, (2011), Continuous staged ethanol fermentation coupled with pervaporation, *ECCE-8 and ECAB-1*, 25-29 August 2011, Berlin, Germany.

4. S.S. Gaykawad, L.A.M. van der Wielen and A.J.J. Straathof, (2011), Effects of cellular polymers on membrane performance in pervaporation integrated with fermentation *NPS-11*, 24-26 October 2011, Papendal, Arnheim, The Netherlands.

5. S.S. Gaykawad, L.A.M. van der Wielen and A.J.J. Straathof, (2010), Integrated ethanol fermentation and pervaporation- Basic modelling, *RRB6 conference*, 7-9 June 2010, Dusseldorf, Germany.

6. S. Chovau, B. Van der Bruggen, A. J. J. Straathof, S. Gaykawad, (2010), Bio-ethanol production using a hybrid pervaporation-distillation system: Influence of fermentation by-products on membrane performance, *Gordon Research Conference on Membranes: Materials & Processes*, July 25-30, 2010, New London, NH, USA.

7. Bruno Bühler, F.Özde Bayraktar, Sushil Gaykawad, Andreas Schmid, (2008), Application of Molybdenum-Containing Dehydrogenases for Carbon Oxyfunctionalization. *Gordon Research Conference*. Biocatalysis. July 6-11, Smithfield, RI, USA.

8. F.Özde Bayraktar, Sushil Gaykawad, Andreas Schmid, Bruno Bühler, (2008), Application of quinaldine 4-oxidase (Qox) containing recombinant *P. putida* as a biocatalyst in hydroxylation reactions, *7th European Symposium on Biochemical Engineering Science (ESBES 7)*, September 7-10, Faro, Portugal.

Curriculum vitae

Sushil S. Gaykawad was born on 24th March 1979 at Chalisgaon, Maharashtra, India. He completed his secondary education from Jawahar Navodaya Vidyalaya, Bhusawal and higher secondary education from Arts, Science and Commerce college, Chalisgaon, India. During 1996 to 2000 he was studying Chemical Engineering at North Maharashtra University, Jalgaon, India and acquired Bachelor of Technology degree in 2000. He worked as Production Engineer at Sabero Organics Gujarat Ltd, Gujarat, India from 2001 till 2003. During this tenure, he was responsible for production related activities and ISO documentation of multipurpose plant. He pursued his Master's in Chemical Engineering at Technische Universität Dortmund, Germany from 2005 till 2008. During his master's thesis, he developed two-liquid phase biotransformation process for the production of 4-hydroxy quinaldine. In 2009, he started as a PhD student at Biotechnology Department of TU Delft under the supervision of Prof.dr.ir. L.A.M. van der Wielen and Dr.ir. A.J.J. Straathof. During this research he was investigating the implications of process modification and integration on the bioethanol process development. The results of this study are presented in this thesis. Currently, he is working as Postdoctoral researcher at Cell System Engineering group of Biotechnology Department at TU Delft.

Acknowledgements

The successful completion of this research was made possible through the invaluable contribution and support of many individuals and I am greatly indebted to all of them.

I am extremely grateful to my promotor Prof. Luuk van der Wielen for providing me the opportunity to carry out this PhD research. Thank you Luuk for your valuable guidance and scholarly inputs which helped to make this research more refined.

I owe my deepest gratitude to my co-promotor Dr. Adrie Straathof for his profound supervision during this research. Thank you for giving me ample freedom and encouragement to perform this research. I feel extremely honoured to have you as a supervisor who cared so much about my work. Your sharing of knowledge and ideas, critical analysis of the results and constructive criticism has helped me to become better researcher. Adrie thanks for showing faith in me and for all your support on professional and personal level.

I am extremely thankful to Dr. Maria Cuellar for her generous support, ever readiness to resolve my queries and her interest in my research. Maria it was pleasure working with you during T&S course. I am also very grateful to you for allowing me to use ultra-filtration unit and your help during integrated experiments performed using this system.

Special thanks to Prof. Sef Heijnen for his time to discuss the experimental results. The meetings with you were very insightful and helped me to understand the fermentation process better.

During this research, I have been benefited by assistance of technical teams. I would like to express my greatest appreciation to Stef, Mervin and Cor for their help during sample analysis. Max thank you for GC analysis of the samples and also for Dutch translation of my thesis summary and propositions. I greatly appreciate Rob and Dirk who ensure smooth running of my fermentation experiments.

This research would not have been complete without the pervaporation unit which was in-house built by Nico and his team from Chemical Engineering department (former DCT). I am highly indebted to

them for their unrelenting willingness to modify the pervaporation system until it was properly functional. I am also thankful to Arno and his team from our department for their ever readiness to timely help even for very trivial maintenance related issues.

This research was funded by European Union under the project titled DoubleNanoMem. I am extremely grateful to all the members involved in this project. Among these, I am particularly thankful to Dr. John Jansen for well receiving me in this team and for his proficient coordination of the project. The testing of the membranes, produced in the consortium, in my experimental setup was an integral part of my research and I am highly obliged to Prof. Budd, Dr. Mason for sending me the PIM membranes and Dr. Figoli and John for furnishing me with the SBS membranes. I am also thankful to Prof. Van der Bruggen and Dr. Simon Chovau for rewarding collaborative work. Simon, thank you for providing every information related to pervaporation and resolving my queries related to membrane applications. Special thanks to Dr. Friess, Dr. Nicolay Belovna and Prof. Yampolskii for informative and fruitful discussions and to Michele for making each project meeting enjoyable, specially the last one.

I am extremely grateful to all the committee members Prof. Noorman, Prof. Wichmann, Prof. Punt, Prof. Boom, Dr. Jansen and Prof. Osseweijer for accepting to be a part of my defense committee and for their valuable comments and suggestions on my thesis.

During my research, I have been surrounded by wonderful people who provided the best atmosphere to do PhD in. With deep sense of gratitude, I would like to thank all my colleagues at BPE: Marcel, Çağri, Esteban, Beckley, Kedar, Sreekanth, Corjan, Rosario, Camilo, David, Alex, Arjan, Susana, and Erik for their constant support, time, scientific inputs and discussions. I formed a special bond with Camilo as we started our PhD at a same time and share many good moments. I am also thankful to Corjan for his inputs and efforts in making lignocellulosic fermentation broth available to me. Thank you Arjan for helping me to take cover page picture. These thanks also extended to colleagues from CSE group: Amit, Hilal, Lodewijk, Elaheh, Katelijne, Ana Luisa, Walter, Aljoscha, Peter, Camilo (thanks for helping me with photoshop), Hugo, Jinrui, Cristina and Mihir who helped me in one or other way during my research. Being a part of rapid sampling team was

truly learning experience and I enjoyed it a lot. You all will always remain dear to me.

I would also like to express my gratitude to Sjaak. Jos, Hans, Herman, Ginie, Rob, Astrid, Apilena, Jannie and Kees for providing the necessary facilities when needed. I am especially indebted to Kawieta for her generous support and assistance in administrative work and constant encouragement on personal level.

I sincerely appreciate the productive contribution of different students in my research work. I am thankful to Dennis for carrying out his master's thesis on my research topic. This appreciation extends to Sumit, Manas, Shreyas and Tomas who carried out their master's design group project on integration of pervaporation in bioethanol process. I am also thankful to Zha Ying for providing lignocellulosic fermentation broth and sharing her fermentation results which led to fine collaborative work.

The days I spent in Delft were made more eventful and enjoyable by my friends Amit, Kedar, Samir Kulkarni, Deepak, Sreekanth, Sameer Patwardhan, Somanath, Sudam, Amol, Amit Patil, Nishant, Abhay and Ishwar. I also relish the company of my friends Bhaskar, Krishna, Venkatesh and Lalit. I am especially grateful to Amit, who has been my friend since the day I stepped-in in Europe, for his consistent support and encouragement in the times when I needed it most. In him I found a friend on whom I can always count on. Thanks also for your critical inputs which helped me to improve. I also grateful to Ria for accommodating me in her house as tenant and allowing me to watch closely the Dutch ways of living. Profuse thanks to my friends in back home Abhijit Chandode, Yashawant Bhalerao and Dr. Rahul Salunkhe for their encouragement. Thank you all for wonderful memories.

My social life in the Delft has been kept busy by my family friends Shruti-Samir Kulkarni, Swati-Amit Deshmukh, Rupali-Amol Khalate, Vaishali-Ishwar Bajaj, Nita-Deepak Patil, Supriya-Sachin Singare, Sayali-Nishant Lawand, Snehal-Shishir Sabale and Bharati-Yogeshwar Patil. Profuse thanks to all of you for your timely support. I will always cherish the memories with you.

I can hardly express my gratitude for unconditional love, support and inspiration I received from my father, my elder sister-Swati, my brother in law-Milind and my brother-Samir. During this period, Mom

passed away after prolonged sickness and it was very hard to accept it for all of us. But, its only because of your encouragement, strong determination and arduous efforts during mom's sickness that keeps me going on. It was not possible to achieve all this without you. I owe you too much and I would like to be remain indebted for whole of my life. I would also like to express my sincere gratitude to my other family members and in-laws for their support and confidence in me.

Finally, I am would like to acknowledge my wife-Jaimala, for her patience, undying love and support during these years. Thank you for extending the strength and motivation to finish this thesis. I cannot have a better better-half than you!

Sushil S. Gaykawad
June 2014, Delft.